PERFORMANCE ANALYSIS AND MULTI OBJECTIVE OPTIMIZATION OF MULTI STAGE VAPOUR COMPRESSION REFRIGERATION SYSTEMS

A Thesis submitted to Delhi Technological University, Delhi in fulfilment of the requirement for the award of the degree of

DOCTOR OF PHILOSOPHY

in

MECHANICAL ENGINEERING

By

KAUSHALENDRA KUMAR SINGH
(2K17/PhD/ME/20)

Under the Supervision of

Prof. (Dr.) Rajesh Kumar
(Supervisor)
Department of Mechanical Engineering,
Delhi Technological University, Delhi

Prof. (Dr.) Anjana Gupta
(Co-Supervisor)
Department of Applied Mathematics,
Delhi Technological University, Delhi

DEPARTMENT OF MECHANICAL, PRODUCTION, INDUSTRIAL AND AUTOMOBILE ENGINEERING

DELHI TECHNOLOGICAL UNIVERSITY,

DELHI – 110042 (INDIA)

SEPTEMBER, 2021

Dedicated to

My Parents

Shri Rajendra Singh

& Smt. Shashikala Singh

DECLARATION

I hereby declare that the thesis entitled **"Performance Analysis and Multi Objective Optimization of Multi Stage Vapour Compression Refrigeration Systems"** submitted by me, for the award of the degree of ***Doctor of Philosophy*** to **Delhi Technological University (Formerly Delhi College of Engineering)** is a record of bona fide work carried out by me under the guidance of **Prof. Rajesh Kumar** (Department of Mechanical Engineering, DTU) and **Prof. Anjana Gupta** (Department of Applied Mathematics, DTU)**.**

I further declare that the work reported in this thesis has not been submitted and will not be submitted, either in part or in full, for the award of any other degree or diploma in this University or any other Institute or University.

Kaushalendra Kumar Singh
Enrollment No.: 2K17/PHDME/20
Department of Mechanical Engineering
Delhi Technological University
Bawana Road, Delhi- 110042

Place: New Delhi
Date: September, 2021.

CERTIFICATE

This is to certify that the thesis entitled **"Performance Analysis and Multi Objective Optimization of Multi Stage Vapour Compression Refrigeration Systems"** submitted by **Mr. Kaushalendra Kumar Singh** to Delhi Technological University, Delhi, for the award of the Degree of **"Doctor of Philosophy"** in Mechanical Engineering is a bona fide record of research work carried out by him. Kaushalendra Kumar Singh has worked under our supervision and has fulfilled the requirements for the submission of this thesis, which to my knowledge has reached requisite standards.

The results contents in this thesis are original and have not been submitted to any other Institution or University for the award of any degree or diploma.

Prof. Rajesh Kumar
(Supervisor)
Professor,
Department Of Mechanical Engineering,
Delhi Technological University,
Delhi-110042

Prof. Anjana Gupta
(Co-Supervisor)
Professor,
Department Of Applied Mathematics,
Delhi Technological University,
Delhi-110042

ACKNOWLEDGEMENTS

I would like to express my gratitude to Prof. Yogesh Singh, Vice chancellor, Delhi Technological University, Delhi for providing me the opportunity to carry out this work in this prestigious institute. I would like to pay my sincere thanks to Prof. S.K. Garg, HOD and DRC Chairman, Department of Mechanical Engineering, for his support to finish this work.

With immense pleasure, I would like to express my greatest gratitude to my supervisor Prof. Rajesh Kumar, Department of Mechanical Engineering, DTU and my co-supervisor Prof. Anjana Gupta, Department of Applied Mathematics, DTU for their proficient guidance, intelligent approach, constructive critique, whole hearted and ever available help, which has been the primary impetus behind the research. Without their wise advice and able guidance, it would have been impossible to complete the thesis in this manner.

I wish to record my thanks and gratitude to my all Internal and External SRC experts, Prof. M. M. Hasan (JMI, Delhi), Prof. (Emeritus) Suresh Chandra (IIT, Delhi), Prof. Raminder Kaur (DTU, Delhi) and Prof. Raj Kumar Singh (DTU, Delhi) for their valuable guidance, critical and constructive discussion during this work.

I would like to thank to the wonderful friends in my life who were always on the stand-by to bring me to positivity, hope and smiles when things didn't seem favouring and it seemed a far-fetched journey. I am greatly indebted to my parents Mr. Rajendra Singh and Smt. Shashikala Singh, my elder brother and Sister in law Mr. Shivendra Singh and Smt. Archana Singh for their love and blessings to see me scaling greater heights in life. I wish to register special credits to my beloved wife Dr. Geetanjali Singh who remained fellow companion in all the ups and downs of this journey. I thank her for the

care and attention which was much needed during the hard work required to pursue my PhD work. Last but not the least I am thankful to my nephews Utpal & Utkarsh and my little daughter Vaibhavi for the ignorance they endured because of me being continuously involved in the work. Their single smile could remove all the tiredness of my work.

Above all, I would thank Almighty for blessing such an affectionate & efficient people playing great asset for me.

(KAUSHALENDRA KUMAR SINGH)

ABSTRACT

Finding optimum operating conditions for maximum performance, minimum cost and energy consumption using environment-friendly refrigerants is now-a-days an important objective to be reached in the area of refrigeration. Energy, exergy, economic and exergoeconomic analyses play vital role in selection of refrigeration systems and suitable refrigerant. Multi-objective optimization paves the way to achieve optimal thermodynamic performances with reasonable cost. This thesis explores the thermo-economic behaviour of basic and hybrid multi-stage refrigeration systems through analysis and multi-objective optimization approach. The systems under analysis are: A two-stage refrigeration system with flash intercooler cum indirect sub-cooler, A cascade refrigeration system and A hybrid cascade refrigeration system which is a combination of two-stage and cascade system. Keeping in view the environmental hazards caused by refrigerants, only natural refrigerants have been included in the study.

First multi-objective optimization of an ammonia based two-stage vapour compression refrigeration system incorporated with a flash intercooler cum indirect sub-cooler has been done. The study is carried out via thermo-economic optimization of the system in order to maximize the exergetic efficiency and minimize the total capital cost of the system. Evaporator temperature, condenser temperature, subcooling parameter and de-superheating parameter are considered as the four design variables of optimization problem. Multi-objective Genetic Algorithm (MOGA) is employed to carry out the optimization using MATLAB. TOPSIS decision making technique has been used to find unique solutions for five different weights of exergetic efficiency and total cost. The results reveal that exergetic efficiency and total capital cost of the system are

41.76% and 223717.6 USD respectively at thermo-economic optimal operating conditions.

Thereafter a comparative analysis based on multi-objective optimization of a cascade refrigeration system using NH_3-CO_2 and NH_3-N_2O refrigerant pairs has been done. Exergetic effciciency and overall cost rate has been taken as the two conflicting objective functions and evaporator temperature, condenser temperature, LTC condenser temperature and cascade heat exchanger temperature difference are the four design variables. The optimization work has been carried out using genetic algorithm which results in non-dominated optimal solution represented in the form of pareto-optimal curve and TOPSIS method is used to select a unique solution. The results show that NH_3-N_2O is a better alternative as compared to NH_3-CO_2 refrigerant pair from multi-objective optimization point of view. The corresponding optimal operating conditions has also been suggested for both the refrigerant pairs.

The above work is followed by comparative energy, exergy and economic analysis of natural refrigerant couples working in a cascade refrigeration system incorporated with a flash tank in its higher temperature cycle and a flash intercooler with indirect sub-cooler in its lower temperature cycle (Hybrid Cascade Refrigeration System). The analysis is conducted using seventeen refrigerant couples namely R717, R290, R600a, R744, R744a, R170, R1150 and R1270. A comparison based on COP, exergy efficiency, system cost rates, and exergy destruction rate, to identify the best alternative refrigerant couple, is performed. Thermodynamic optimization has also been carried out with evaporator temperature, condenser temperature, LTC condenser temperature, cascade temperature difference, de-superheating and subcooling parameter of LTC intercooler, as six design variables. To evaluate the economic accountability of refrigerant couples a simple payback analysis has been done at the thermodynamic

optimal conditions of system. Results of analysis and optimization show that R717-R290 is the best refrigerant couple for this system from thermodynamic as well as economic point of views. The maximum COP and exergy efficiency obtained are 1.917 and 39.14% respectively and the corresponding total annualized system cost is 836395 $/yr for R717-R290 refrigerant couple. From the study is can be concluded that R717-R290 (ammonia-propane), R290-R1270 (propane-propylene) and R600a-R290 (isobutane-propane) are the best refrigerant pairs from thermo-economic point of view. Therefore an exergoeconomic analysis is done on a Hybrid Cascade Refrigeration System (HCRS) using the three natural refrigerant pairs- ammonia-propane, propane-propylene and isobutane-propane. Thermodynamic optimization of system is carried out with exergy efficiency as the objective function and evaporator temperature, condenser temperature, subcooling parameter, de-superheating parameter, LTC condenser temperature and cascade temperature difference as the six design variables. Overall system cost rate, component-wise exergy destruction rates, exergy efficiencies and exergo-economic factors are investigated for the three refrigerant pairs at thermodynamic optimal operating conditions. The study concludes that ammonia-propane is the best performing refrigerant pair from exergetic and economic point of view with an exergy efficiency of 39.14% and total cost rate of 836395 $/yr. Propane-propylene and Isobutane-propane give moderate and worst thermo-economic results with 38.03% and 37.06%`of exergy efficiency and 1178000 $/yr and 2189000 $/yr of total system cost rate respectively. The exergo-economic factor is maximum in flash tank and minimum in EV II for all the three refrigerant pairs.

Lastly a thermo-economic optimization and comparative analysis of HCRS using different natural refrigerant pairs is performed. Thermo-economic optimization is carried out to maximize the exergetic efficiency and minimize the overall cost rate. The

optimization model involves six design variables which include subcooling and de-superheating parameters, LTC evaporation and condensation temperatures, HTC condenser temperature and cascade temperature difference. The comparative analysis of twenty-two natural refrigerant pairs based on results of thermodynamic and economic optimizations reveal that R717-R290 is most efficient pair and R290-R1150 is least efficient refrigerant pair thermodynamically whereas R717-R1270 is the best and R600a-R290 is the worst pair economically. Seven potential refrigerant pairs are chosen via thermodynamic and economic optimization results and they are further compared based on their performances obtained through multi-objective optimization (maximization of exergetic efficiency and minimization of total cost rate). Multi-Objective Genetic Algorithm (MOGA) is used for optimization which results in seventy nondominated Pareto optimal solutions where TOPSIS method is used to select a unique solution for each refrigerant pair. A comparison of refrigerant pairs using these unique solutions shows that R717-R1270 is the best refrigerant pair for the cascade system under consideration. It is also found that R717-R1270 results in 7.77% rise in COP and 5.32 % reduction in overall cost when compared with NH_3-CO_2 refrigerant pair working under identical operating conditions

List of Publications

1. **Kaushalendra Kumar Singh**, Rajesh Kumar, Anjana Gupta. Comparative energy, exergy and economic analysis of a cascade refrigeration system incorporated with flash tank (HTC) and a flash intercooler with indirect subcooler (LTC) using natural refrigerant couples, Sustainable Energy Technologies and Assessments, Vol. 39, pp. 100716, 2020. **(*Published*) (Elsevier; SCIE indexed, Impact factor: 5.353, Quartile - Q1);** DOI: https://doi.org/10.1016/j.seta.2020.100716

2. **Kaushalendra Kumar Singh**, Rajesh Kumar, Anjana Gupta. Multi-objective optimization of thermodynamic and economic performances of natural refrigerants for cascade refrigeration, Arabian Journal for Science and Engineering. **(*Published*) (Springer Nature; SCIE indexed, Impact factor: 2.334, Quartile – Q2);** DOI: https://doi.org/10.1007/s13369-021-05924-w

3. **Kaushalendra Kumar Singh**, Rajesh Kumar, Anjana Gupta. (*In Press*), Comparative Exergetic, Economic and Exergoeconomic analysis of a hybrid cascade refrigeration system using ammonia-propane, propane-propylene and isobutane-propane refrigerant pairs, International Journal of Exergy. **(*In Press*) (Inderscience publications; SCIE indexed, impact factor: 1.383, Quartile - Q2)**

4. **Kaushalendra Kumar Singh**, Rajesh Kumar, Anjana Gupta. Comparative economic and exergoeconomic analysis of a hybrid cascade refrigeration system using ammonia-propane, propane-propylene and isobutane-propane refrigerant pairs**,** *Poceedings:* 12th International Exergy, Energy and Environment Symposium; 2020 Dec 20-24; Doha Qatar. **(*presented in International Conference*)**

5. **Kaushalendra Kumar Singh**, Rajesh Kumar, Anjana Gupta. Multi-objective optimization of an ammonia based multi-stage vapour compression refrigeration system with flash intercooler cum sub-cooler. *Paper presented at*: 3rd International conference on Computational and Experimental Methods in Mechanical Engineering; 2021 Feb 11-13; Greater Noida, India. **(*presented in International Conference*)**

6. **Kaushalendra Kumar Singh**, Rajesh Kumar, Anjana Gupta. Multi-objective optimization of cascade refrigeration system using NH_3-CO_2 and NH_3-N_2O refrigerant pairs. *Paper presented at*: 3rd International conference on Computational and Experimental Methods in Mechanical Engineering; 2021 Feb 11-13; Greater Noida, India. (*presented in International Conference*)

Table of Contents

List of Figures

List of Tables

List of Abbreviations and Nomenclature

Abbreviations

A	area (m^2)
a	subcooling parameter
b	de-superheating parameter
$\dot{C}$	cost rate ($/year)
CFC	chlorofluorocarbon
CHX	cascade heat exchanger
COP	coefficient of performance
CRF	capital recovery factor
$\dot{E}x$	exergy flow rate (kW)
F	correction factor
$FIIS$	flash intercooler with indirect sub-cooler
GWP	global warming potential
G	total capital investment in cold storage in complete life time
h	specific enthalpy (kJ/kg)
$HCFC$	hydrochlorofluorocarbon
HTC	high temperature cycle
i	annual interest rate
LTC	lower temperature cycle
$\dot{m}$	mass flow rate (kg/s)
n	system lifetime (years)
N	annual operational hours (h)
ODP	ozone depletion potential
p	pressure (kPa)
$\dot{Q}$	heat flow rate (kW)
$\dot{R}$	Annual earnings from fish cold storage ($/yr)
s	specific entropy (kJ/kg K)
t	payback period
T	temperature (^{0}C)
ΔT_{lm}	logarithmic mean temperature difference (K)
U	overall heat transfer coefficient (kW/m^2K)
$\dot{V}$	volume flow rate (m^3/s)

$\dot{W}$	work input (kW)
Z	capital cost ($)
$\dot{Z}$	capital cost rate ($/year)

Greek Symbols

α_{el}	cost of electricity ($/kWh)
ϕ	maintenance factor
η	energy efficiency
ψ	exergy efficiency
λ	pressure ratio
Δ	difference

Subscripts

0	ambient state
AC	air change
ca	cold air
cas	cascade
$cond$	condenser
$comp$	compressor
d	destruction
e	exit
el	electrical
env	environmental
$EV\ I$	expansion valve I
$EV\ II$	expansion valve II
$EV\ III$	expansion valve III
FL	fish loading
FT	flash tank
FI	flash intercooler with indirect sub-cooler
$Fan\ I$	fan I
$Fan\ II$	fan II
$HTC\ comp$	high temperature cycle compressor
i	inlet
ins	insulation

k	kth component
$LTC\ comp\ I$	lower temperature cycle compressor I
$TC\ comp\ II$	lower temperature cycle compressor II
m	mechanical
OL	other loads
op	operational
s	isentropic
sup	superheat

Superscripts

Q	heat transfer
W	work Transfer

Chapter 1

Introduction and Literature Review

1.1 Motivation

Economic and environmental sustainability are one of the most important requirements of any sustainable development model. Refrigeration industry plays an important role in both of these issues because of being a remarkable stakeholder in energy consumption and emission of substances causing global warming. In India, refrigerators and air conditioners have the highest aspirational value of all consumer durables, with the exception of televisions and now the smart phones. This accounts for the high growth rate of this industry. The refrigerator market has been growing at a rate of about 15% per year, while the consumer durables industry as a whole has grown at almost 8%. The size of the refrigerator market is estimated to be 3.5- 4 million units approximately, valued at Rs 50 billion. The domestic penetration rate of refrigerators is about 9%. The penetration of refrigerators is considerably higher in urban areas, which account for 75% of the demand, with rural areas constituting the other 25%. The demand is also higher in the northern and western parts of the country than in the east. The south also has high demand as the warmer weather of the south requires a refrigerator running throughout the year **[1]**. Also with the wake in packaged/frozen food industry, chemical and process industry, medical preservatory, and comfort air conditioning, low temperature refrigeration applications have gained importance like never before. Therefore, design of energy efficient and environment-friendly refrigeration systems has become the prime objective to be reached for the researchers working in this area. Improving energy efficiency, achieving ultralow temperature cooling, controlling the capital and operational cost and reducing the environmental

hazards caused by refrigerants are some of the major challenges to be worked upon. Efforts are being made to overcome these challenges through comprehensive energy, exergy and economic analyses, optimization of different refrigeration systems using smart search algorithms, introducing novel hybrid energy efficient systems, development of environment benign synthetic refrigerants and application of natural refrigerants. The work embodied in this thesis is an endeavour to attempt these methods on multi-stage vapour compression refrigeration systems with a theoretical approach.

1.2 Multi-stage vapour compression Refrigeration system

The idea of multi stage compression, has unanimously been accepted for very low temperature applications because of deteriorating performance of single stage compression systems with increase in temperature gap between the evaporator and condenser temperatures. For a fixed evaporator temperature, as the condenser temperature increases the throttling loss in the expansion valve increases and at the same time the compressor work also increases. Both of these phenomenon deteriorate the cycle performance. This is insignificant for the applications where the gap between evaporator and condenser temperatures (Temperature Lift) is low, but there are some important applications where the temperature lift is very high. For example in frozen food industries the required evaporator temperature can be as low as -40 ^{0}C while in chemical industries a temperature of -150 ^{0}C may be required for the liquefaction of gases. In such systems the performance of a single stage refrigeration system degrades to an unacceptable level. In such applications multistage refrigeration systems are of utmost importance.

1.2.1 Basic Multi-Stage System

Single stage compression refrigeration systems are basic systems in vapour compression refrigeration systems. But they fail to serve low and ultra-low temperature requirements of commercial and industrial refrigeration applications. Because in such applications, the required pressure lift is high and operating temperature range is also wide which limits the use of a single refrigerant. The problem of high pressure lift is solved by employing multi-stage compression using multi-stage refrigeration systems. The limitation on operating temperature limits is delt with employing two different refrigerants operating in two separate single stage refrigeration systems coupled with each other through a cascade heat exchanger and the system is called a cascade refrigeration system. Hence Cascade and Multi-stage refrigeration systems are one of the major contributors in the area of low and ultra-low temperature refrigeration applications.

1.2.2 Hybrid Multi-stage system

Amalgamation of basic multi-stage refrigeration systems to form novel hybrid systems is a smart approach to achieve the high cooling load and better system performance but it is justifiable only when the plant load is sufficiently high to overcome the capital and running cost of the hybrid systems. Vapour compression absorption system, combined power and refrigeration system, Solar powered cascade absorption refrigeration system are some examples of hybrid multi-stage refrigeration system which have been developed to cater the demands of such applications. In the present study, hybridization approach has been implemented to combine a two stage compression system and cascade refrigeration system forming a hybrid cascade refrigeration system (HCRS) with an objective to get better thermodynamic performance as compared to two-stage and cascade refrigeration system. The system can be employed to serve the low and ultralow temperature cooling requirements more effectively than that of individual

constituent systems. Further a thermo-economic analysis, exergoeconomic analysis and multi-objective optimization is done to investigate the feasibility of the system.

1.3 Refrigerants

Some decades ago, CFC and HCFC refrigerants were being developed to cater the demands of high thermodynamic performances of refrigeration systems, but they reasoned the significant detrimental environmental impacts like depletion of the stratospheric ozone layer and global warming. CFCs were found to be responsible for depleting the stratospheric ozone layer and consequently banned under Montreal Protocol (1987). Later on, HCFCs, alternatives to CFCs, were also identified as hazardous to ozone layer & possessing high global warming potential and were scheduled the phase-out by 2020-2030 under Kyoto protocol (1997). Time-bound permission and interim solution to use HFC (up to 2040), also alternatives to CFCs, was also given under Kyoto Protocol. As the deadline is approaching, the search of environment-friendly alternative refrigerants has become a challenge for the researchers working in this area. This has initiated the search of alternative environment-friendly refrigerants. Efforts are being made in two directions, one is to keep developing low GWP and zero ODP synthetic refrigerants like R1234yf and R1234ze, etc. and other is to go for natural refrigerants like R744, R717, and others. Natural refrigerants are good choices because of their inherent properties of having zero ODP and negligible GWP. They include ammonia, CO_2, N_2O and hydrocarbons etc. which eventuate in nature's chemical and biological cycle without human intervention. Ammonia possessing zero ODP and GWP shows excellent miscibility with water and largely used in the food and beverage industry. CO_2 being abundantly available in the air has zero ODP and one GWP and shows higher COP than HFC based systems in

supermarket applications. The hydrocarbons like ethane and ethylene have extremely low boiling points of -88.84 ^{0}C and -104^{0}C respectively and hence they are used for ultra-low temperature refrigeration applications (-80^{0}C). Propane and propylene are effective alternatives of R12 and R22 synthetic refrigerants respectively. Although some natural refrigerants are doing well but still most of them do not meet the potential of synthetic refrigerants to appear as environment-friendly alternative solutions. The problem of relatively low performance can be worked upon through two major endeavours. One is to optimize the existing systems using smart search algorithms like Artificial Neural Network (ANN). Another approach is to employ these refrigerants under suitable operating conditions in more efficient hybrid systems like vapour compression absorption and hybrid cascade refrigeration systems rather than the basic systems in order to get better performance. Here a comprehensive comparative analysis of natural refrigerants has been done through thermo-economic analysis, exergoeconomic analysis and multi-objective optimization approach.

1.4 Analyses and optimization approach

The Analyses of different multi-stage refrigeration systems include energy analysis, exergy analysis, environmental analysis, economic analysis and exergoeconomic analysis. The thermodynamic performance of refrigeration systems depends upon system configuration, values of input parameters, environmental conditions and refrigerants being used. New system configurations are obtained by combining different systems to form a more efficient hybrid systems. But improving the thermodynamic performances by amalgamation of different systems often lead to excessive increase in system's capital and operating cost. Therefore it is important to perform a parallel economic analysis along with the thermodynamic one. A thermo-

economic comparative analysis of different refrigeration systems using different natural refrigerants is a smart approach to seek environment benign, thermodynamically efficient and economically reasonable systems. Another important technique to improve system performance is the multi-objective optimization. Multi-objective optimization method is an efficient approach for optimizing the problems dealing with conflicting objectives. This technique is commonly used to determines the optimal operational parameters in order to maximize the thermodynamic efficiencies and minimize the cost of refrigeration systems. In recent studies, use of smart search algorithms like artificial neural network (ANN) are frequently used to carry out multi-objective optimization. Genetic algorithm and Nondominated shorting genetic algorithm – II (NSGA -II) are used here for performing multi-objective optimization. These are some of the elitist algorithms which find the best optimal solution by imitating the process of natural selection and survival of the fittest (Darwinism).

To fulfil the current need of identifying potential eco-friendly refrigerants, it is required to carry out thermo-economic performance analysis and multi-objective optimization on different multi-stage refrigeration systems and their hybrid versions using various natural refrigerants. Therefore in the present work, the results of performance analysis and multi-objective optimization of two-stage system and cascade refrigeration system along with multi-objective optimization has been explored. Both the analyses and optimization problems are developed in a thermo-economic frame work. Thereafter a hybrid system has been formed which combines two-stage and cascade systems and the similar analysis is done on it. Keeping in view the environmental impact of refrigerants, only natural refrigerants has been included as working fluids for different systems. The aim of study is to explore the thermo-economic behaviour of natural refrigerants in

basic and hybrid multi-stage systems and identify the most suitable natural refrigerant/refrigerant pair for low-temperature refrigeration applications.

1.5 Literature Survey

A good number of experimental and theoretical studies regarding thermodynamic analysis, economic analysis, and optimization of multi stage refrigeration systems have been done so far. Some of the noticeable works are summarised here.

1.5.1 Thermodynamic Analysis

Thermodynamic analysis includes the investigation of effects of different system operating parameter on thermodynamic performances like COP, Exergy efficiency, exergy destruction, work input, cooling load etc. In this regard, **Ratts and Brown [2]** used the entropy generation method to analyse a cascade cycle working on R134a by expressing the second law equations in terms of specific heat and temperature ratio and found an optimum intermediate temperature such that the entropy generation was minimum. **Bingming et al. [3]** experimentally analysed the CO_2-NH_3 cascade refrigeration system and concluded that the COP increases with an increase in evaporator temperature, a decrease in condenser temperature, and almost independent of the degree of superheat. **Park et al. [4]** studied a cascade refrigeration system using R134a-R410A refrigerant couple and found the optimum intermediate temperature for the maximum COP of the system. The major design parameters they considered for the analysis were R134a condensing temperature, R410A evaporating temperature and the temperature difference between the cascade heat exchanger. **Lee et al. [5]** determined an optimum cascade condensing temperature for the maximum COP and minimum exergy destruction. **Bhattacharya et al.[6]** studied a natural refrigerant based cascade refrigeration system with N_2O-CO_2 as the refrigerant couple. N_2O was used in low

temperature cycle and CO_2 was used in high temperature cycle. Optimization of intermediate pressure for maximum COP for various design and operating parameters were presented. In another study, **Bhattacharya et al. [7]** studied two-stage internally reversible cascade cycles to find the intermediate temperature resulting in maximum cooling load. **Getu and Bansal [8]** analysed a CO_2-NH_3 cascade system to optimize its evaporation temperature and NH_3 to CO_2 mass flow ratio to maximize its COP. **Zubair et al. [9]** analysed a two-stage refrigeration cycle through the First and Second law of thermodynamics and obtained an intermediate pressure required for having maximum COP. **Dopazo et al.[10-11]** determined CO_2 condensing temperature through practical and theoretical analyses of CO_2-NH_3 cascade system in two different studies. **Torella et al. [12]** presented a general methodology based on subcooling parameter and de-superheating parameters derived from the inter-stage conditions of the refrigerant, for the analysis of a two-stage refrigeration system.

1.5.2 Economic Analysis

Thermodynamic analyses mainly deals with improving the thermodynamic performances which could lead to excessive cost. Therefore a parallel economic analysis is also of equal importance. With this interest, **Rezayan and Behbahaninia [13]** presented cost functions for different components of a cascade refrigeration system and investigated the economic performance of the a CO_2-NH_3 cascade system. **Bakeem et al. [14]** carried out a parallel thermodynamic and economic analysis and optimization of a two-stage refrigeration system with flash intercooler and indirect subcooler using eight different refrigerants, and found that ammonia was the refrigerant from both thermodynamic as well as economic aspects. **Mosaffa et al. [15]** carried out a comparative thermodynamic and economic analyses of two different configurations of cascade refrigeration system using flash tank and flash intercooler and found that a

cascade refrigeration system with flash intercooler in LTC and flash tank in HTC was better system from thermodynamic as well as economic point of view. **Shishov et al. [16]** performed payback analysis along with the economic analysis on irreversible refrigeration cycle and they found that the payback period comes down to less than one year when the temperature difference in condenser is 15 K.

1.5.3 Exergoeconomic Analysis

An exergy aided economic analysis, also known as exergo-economics is a significant tool to analyse and optimize the thermo-economic performance of systems. The concept of exergo-economics is based on the principle of cost balance and has been used in many studies for getting a better system design under thermo-economic framework. **Vicent and Heun[17]** investigated domestic refrigeration system from exergo-economic point of view and concluded that compressor is the most important component which decides the system performance and economics. **Asgari et al.[18]** performed multi-objective optimization on a auto-cascade refrigeration system with mass flow rates and the operating temperature as four design variables and avoidable exergy destruction and cost rates as the two objective function and reported a performance improvement from the concept of exergo-economics. **Nemati et al.[19]** performed a comparative analysis of two-stage trans-critical refrigeration system with ejector expansion using nitrous oxide, CO_2 and ethane using the concept of exergo-economics and found that nitrous oxide corresponded to minimum product unit cost. **Erol et al.[20]** carried out exergo-economic analysis on an ice rink refrigeration cycle with exergy destruction rate, investment cost rate and cost rate of exergy destruction as the main investigation parameters. **Asgharian et al.[21]** investigated the effect of nanofluid as heat transfer fluid in a solar refrigeration system through exergy and exergo-economic analysis and reported a decrease in cost and increase in COP and

exergy efficiency of the system. **Sharifi et al.[22]** carried out exergo-economic analysis on a natural gas driven combined power and refrigeration system for minimization of exergy destruction cost investment cost.

1.5.4 Multi-objective optimization

Multi-objective optimization is an efficient approach for solving optimization problems including more than one objectives which are generally conflicting in nature. **Knowles et al.[23]** introduced an evolution scheme for multi objective problems, called the pareto archived evolution strategy (PAES). They argued that, PAES might represent the simplest possible non-trivial algorithm capable of generating diverse solutions in the pareto optimal set. The algorithm was identified as being a (1+1) evolution strategy, using local search from a population of one but using a reference archive of previously found solutions in order to identify the approximate dominance ranking of the current and candidate solution vectors. **Deb K et al. [24]** presented an elitist multi-objective genetic algorithm (NSGA II) which is a fast non-dominated sorting approach with O(MN/sup 2/) computational complexity (where m is the number of objective functions and n is the population size). Also, a selection operator was presented that created a mating pool by combining the parent and offspring populations and selecting the best N solutions (with respect to fitness and spread). Since, thermodynamic and economic performances are commonly conflicting in nature, the results do not agree with each other and end up giving disputed solutions. Therefore multi-objective optimization plays an important role and helps providing optimized values of thermodynamic as well as economic performances which are in a good agreement with each other. In this regard, **Aminyaveri et al. [25]** performed a multi-objective optimization using evolutionary NSGA-II algorithm on a similar system with exergetic efficiency and total system cost as the two conflicting objective functions. **Eini et al. [26]** performed a

three-dimensional multi-objective optimization with risk function caused by leakage of NH_3 and propane in CO_2-NH_3 and CO_2-propane refrigerant pairs respectively used in cascade refrigeration systems. **Nasruddin et al.[27]** performed multi-objective optimization on cascade refrigeration system using refrigerant C_3H_8 in HTC and mixture of C_2H_6/CO_2 in LTC to minimize total annual cost as well as the total exergy destruction of the system. **Yarmohammadi et al. [28]** carried out experimental evaluations and multiobjective optimization to find optimum combinations of pressure drop and heat transfer coefficient during evaporation of R404a inside corrugated tubes of the evaporator and found that the corrugated tubes enhance both the parameters simultaneously. **Roy and Mandal [29]** performed thermoeconomic analysis and multiobjective optimization on the cascade refrigeration system using four refrigerant pairs and found that R41-R161 and R170-R161 are better than R41-R404a refrigerant pair.

1.5.5 Selection of refrigerants

Selection of refrigerants is one of the issues which has been given high importance in recent years. Due to environmental impacts caused by HCFC and HFC refrigerants, natural refrigerants have gained special attention because of their inherent properties of zero ODP and negligible GWP values. **Sarkar et al. [30]** presented a study on eight natural refrigerants to identify the best suitable pair for cascade refrigeration system giving maximum cooling COP as well as the volumetric cooling capacity. They found that the NH_3/Propylene pair is best for cooling COP and the Propylene/CO_2 pair is best for volumetric cooling capacity. **Parmar et al. [31]** compared the thermodynamic performances of the cascade refrigeration cycle by using six synthetic and natural refrigerants with R744 in LTC and found that highest COP corresponds to R717-R744 refrigerant couple. **Sarbu et al. [32]** worked on natural refrigerants and concluded that

R744 is the most promising natural refrigerant for heat pump, and air conditioning applications because of excellent properties of no toxicity, no flammability, zero ODP and negligible GWP. **Paradeshi et al.[33]** experimentally investigated the possibility of R290 being a drop in substitute of R22 in a direct expansion solar assisted heat pump system and reported an increase in exergy efficiency of the system with R290 compared to R22. **Kilicarslan and Hosoz [34]** compared different refrigerant pairs in a cascade refrigeration system based on COP and total irreversibility and reported that R717-R23 is the best choice. **Sun et al.[35]** evaluated the thermodynamic performance of low GWP refrigerant pairs in the cascade system and found that R41 is an effective replacement of R23 as HTC refrigerant when paired with R404a. **Sun et al.[36]** carried out a comparative study on twenty-eight low GWP refrigerant pairs working in the cascade system and reported that R41-R161 is the most suitable low GWP refrigerant pair from both the energy and exergy point of views. In another study **Sun et al.[37]** investigated the performance of low GWP refrigerants in a three-stage cascade refrigeration system which involved a low, medium and high-temperature cycles, and they recommended to use R1150 in the low-temperature cycle, R170 in a medium temperature cycle and R717 in the high-temperature cycle. **Shovon et al.[38]** performed a thermodynamic comparative analysis on a solar ejector system using six environmental benign refrigerants and found that R717 gives maximum COP as well as the cooling load. **Saleh et al.[39]** worked on process optimization of refrigeration system using different environment friendly refrigerants focussing on minimization of compressor power with the help of Aspen HYSYS software and suggested useful strategies for achieving most efficient and economical system. **Turgut et al.[40]** performed a thermoeconomic comparative analysis on a cascade vapour compression absorption refrigeration system using four low GWP refrigerants on the basis of results

of single and multiobjective optimizations. They found that R717 gives the lowest cost whereas R290 gives the maximum second law efficiency. **Sun et al.[41]** worked on thermo-economic optimization of operational parameters and different configurations of integrating a compression-absorption cascade system with Organic Rankine Cycle. They aimed at minimization of destroyed exergy and annual cost simultaneously with multi-objective optimization technique and found the optimal configuration as well as the operational parameters for the system.

1.6 Origin of research problem

Various studies have been conducted regarding thermodynamic and economic analysis as well as multi-objective optimization of different multi-stage refrigeration systems. Efforts are being made to improve their thermo-economic performances by tuning different system parameters to optimum values using different environment benign refrigerants. Though there are some issues which may be addressed in this regard.

- A thermoeconomic multi objective optimization can be done on a two stage compression system with flash intercooler and indirect sub-cooler, with exergetic efficiency and cost rate, as the two objective functions, evaporator temperature, condenser temperature, subcooling and de-superheating parameter as design parameters and atmospheric conditions and cooling load as design constraints.
- A thermoeconomic multi objective optimization can be done on a cascade refrigeration system using different natural refrigerant pairs considering exergetic efficiency and total cost rate as the two objective functions and evaporator temperature, condenser temperature, cascade temperature difference

and lower temperature cycle (LTC) condenser temperature as four design variables.

- The above two systems can be amalgamated to yield a hybrid cascade refrigeration system incorporated with flash intercooler cum indirect subcooler in its lower temperature cycle (LTC). The thermo-economic analysis and multi objective optimization can be done on the system to find the optimum values of the design parameters – evaporator temperature, condenser temperature, cascade temperature difference, lower temperature cycle - condenser temperature, sub-cooling parameter and de superheating parameter in order to maximize the exergetic efficiency and minimize the total cost rate.
- An exergoeconomic analysis can be done on the hybrid cascade refrigeration system to investigate the exergoeconomic factors for different system components.

1.7 Contribution of Present Research work

Based on the literature reviewed so far, it can be concluded that very less attention is given to thermoeconomic analysis and multi-objective optimization of different multi-stage configurations using natural refrigerants. This thesis explores the thermo-economic behaviour of basic and hybrid multi-stage refrigeration systems through analysis and multi-objective optimization approach. The systems under analysis are: A two-stage refrigeration system with flash intercooler cum indirect subcooler, A cascade refrigeration system and A hybrid cascade refrigeration system which is a combination of two-stage and cascade system. Input parameters studied are evaporator temperature, condenser temperature, cascade condenser temperature, cascade temperature difference, subcooling parameter and de-superheating parameter. Performance

parameters studied are COP, exergetic efficiency, exergy destruction rates, exergoeconomic factor and overall cost rate of the system. Contribution of present thesis has multiple folds which are as follows:

- Multi objective optimization of a two stage refrigeration system incorporated with a flash intercooler cum indirect subcooler.
- Multi objective optimization of a cascade refrigeration system using different refrigerant couples.
- Thermo-economic performance analysis of a hybrid cascade refrigeration system (Combination of cascade refrigeration system and two stage refrigeration system with flash intercooler cum indirect subcooler).
- Multi-objective optimization of hybrid cascade refrigeration system.
- Exergoeconomic analysis of hybrid cascade refrigeration system.

Keeping in view the environmental impact of refrigerants, only natural refrigerants have been included as working fluids to the systems.

1.8 Organisation of Thesis

The work embodied in the thesis is arranged in five chapters. *First chapter* provides the introduction of basic and multi-stage refrigeration systems, their importance, their economic and environmental challenges and different approaches to deal with these challenges. This chapter also includes the literature review section which informs the progression of research works in the field of analysis and optimization of multi-stage refrigeration system. The *Second chapter* presents a thermoeconomic multi-objective optimization of two-stage and cascade refrigeration systems with two conflicting objectives to increase the system exergetic efficiency and minimize the cost. The Third *chapter* presents thermo-economic and exergoeconomic analysis of hybrid cascade

refrigeration system. This chapter also presents a comprehensive comparative analysis of seventeen natural refrigerants through different plots showing variations of COP, exergetic efficiency and total cost rate with different input parameters like evaporator temperature, cascade temperature difference, subcooling and de-superheating parameters. The *Fourth chapter* presents the results of multi-objective optimization of hybrid cascade refrigeration system using different natural refrigerant couples. and *Fifth chapter* concludes the thesis and suggests future scope of the present work.

Chapter 2

Multi-objective optimization of Two-stage and Cascade Refrigeration System

With the rise in demand of cooling systems to fulfil the requirements of refrigeration for chemical industries and frozen food industries, multi-stage refrigeration systems are rapidly gaining the attention of researchers. The reason for using these systems is the requirement of lower temperature which is much needed to preserve the food items and carry out chemical reactions occurring at specified lower temperature. In this study results of multi-objective optimization for an ammonia based two-stage refrigeration system with flash intercooler cum subcooler has been explored considering the exergetic efficiency and total capital cost as the objective functions and evaporator temperature, condenser temperature, subcooling parameter and de-superheating parameter as four design variables.

2.1 System Description:

Fig 2.1(a) shows the schematic diagram of a two-stage refrigeration system with flash intercooler (FIIS) which also serves as an indirect sub-cooler. Ammonia is used as the working fluid in the system. Heat from cold space is absorbed by the refrigerant in evaporator and the saturated vapour refrigerant (1) undergoes first compression (1-2) in compressor I and then fed to the FIIS where it gets intercooled (2-3). A saturated vapour refrigerant stream (3) exiting FIIS goes for the second stage compression (3-4) in compressor II and then rejects the heat to the ambient air in the condenser (4-5). The condensed refrigerant (5) is separated into two streams (5’ and 5’’). One stream (5’’) after expansion (5’’-6) through the expansion valve II (EV II), is used for make-up supply (6) to FIIS. The other stream (5’) passes by FIIS in an enclosed pipe and gets

subcooled (5'-7). This subcooled liquid refrigerant is fed to the evaporator after expansion (7-8) through the expansion valve I for further heat absorption from the space to be cooled. **Fig 2.1(b)** shows the thermodynamic cycle on a p-h diagram. Other important system parameters assumed for simulation work are listed in **Table 2.1**.

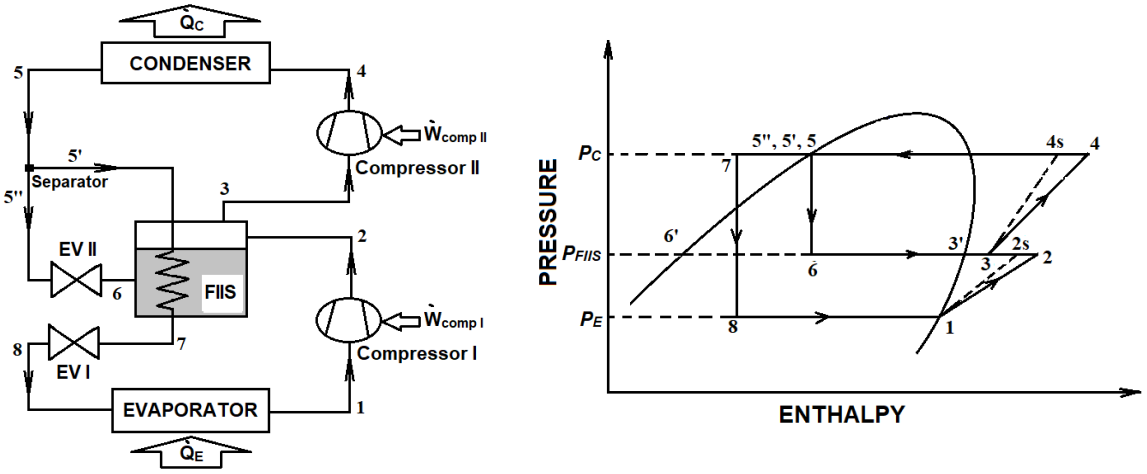

Figure 2.1: (a) Schematic diagram of two-stage refrigeration system with flash intercooler, **(b)** Thermodynamic cycle on p-h diagram

Table 2.1: Basic system parameters assumed for simulation work

Parameter	**Assumed Value**
Cooling Load	1000 kW
Cold Room Temperature	-10 ^{0}C
Temperature of ambient environment	25 ^{0}C
Atmospheric pressure	101.125 kPa
Compressor electrical and mechanical efficiency[a]	91%
Evaporator heat transfer coefficient[a]	1.1 kWm^{-2}K^{-1}
Condenser heat transfer coefficient[b]	0.5 kWm^{-2}K^{-1}
Flash intercooler heat transfer coefficient[b]	1 kWm^{-2}K^{-1}

[a]value are taken from Baakeem et al. (2018)
[b]values are taken from Roy and Mandal (2020)

2.2 System Modelling:

Two-stage compression refrigeration system is modelled on EES software through basic thermodynamic balance equations. The properties of refrigerant at different state points has been fetched by the in-built property functions. A multiple regression

analysis is done to model the expressions of exergetic efficiency and total capital cost using EES **[42]**. These expressions are used to carry out multi-objective optimization of the system using GAMULTIOBJ tool of MATLAB.

2.2.1 Thermodynamic modelling

In thermodynamic analysis *COP* and exergetic efficiency are the main performance parameters which are to be monitored. Component-wise Mass, energy and exergy balance equations are listed in **Table 2.2**.

Where the isentropic efficiency of both the compressors are calculated as **[43]**:

$$\eta_s = 0.85 - 0.046667\left(\frac{P_{discharge}}{P_{suction}}\right) \tag{2.1}$$

Pressure in flash intercooler is expressed as **[14]**:

$$P_{FIIS} = \sqrt{P_E \times P_C} \tag{2.2}$$

De-superheating and Subcooling parameters are defined as **[12]**:

Subcooling Parameters: $a = \frac{h_5 - h_8}{h_5 - h_{6\prime}}$ (2.3)

De-superheating parameter: $b = \frac{h_2 - h_3}{h_2 - h_{3\prime}}$ (2.4)

Table 2.2: Component-wise Mass, energy and exergy balance equations

Component	Mass balance	Energy balance	Exergy balance
Evaporator	$\dot{m}_8 = \dot{m}_1$	$\dot{Q}_E = \dot{m}_1(h_1 - h_8)$	$(\dot{\chi}_d)_E = (\dot{\chi}_8 - \dot{\chi}_1) + \dot{Q}_E(1 - \frac{T_O}{T_{CL}})$
Condenser	$\dot{m}_4 = \dot{m}_5$	$\dot{Q}_C = \dot{m}_4(h_4 - h_5)$	$(\dot{\chi}_d)_C = (\dot{\chi}_4 - \dot{\chi}_5) - \dot{Q}_C(1 - \frac{T_O}{T_C})$
Flash intercooler	$\dot{m}_2 + \dot{m}_6 = \dot{m}_3$ $\dot{m}_{5'} = \dot{m}_7$	$\dot{m}_6 h_6 + \dot{m}_{5'} h_{5'} +$ $\dot{m}_2 h_2 = \dot{m}_3 h_3 + \dot{m}_7 h_7$	$(\dot{\chi}_d)_{FIIS} = (\dot{\chi}_2 + \dot{\chi}_{5'} + \dot{\chi}_6) - (\dot{\chi}_3 + \dot{\chi}_7)$
Compressor I	$\dot{m}_1 = \dot{m}_2$	$\dot{W}_{comp\ I} = \dot{m}_1 \frac{(h_{2s} - h_1)}{\eta_{el}\eta_m\eta_s}$	$(\dot{\chi}_d)_{comp\ I} = (\dot{\chi}_1 - \dot{\chi}_2) + \dot{W}_{comp\ I}$
Compressor II	$\dot{m}_3 = \dot{m}_4$	$\dot{W}_{comp\ II} = \dot{m}_3 \frac{(h_{4s} - h_1)}{\eta_{el}\eta_m\eta_s}$	$(\dot{\chi}_d)_{LTC\ comp\ II} = (\dot{\chi}_3 - \dot{\chi}_4) + \dot{W}_{comp\ II}$
Expansion valve I	$\dot{m}_7 = \dot{m}_8$	$h_7 = h_8$	$(\dot{\chi}_d)_{EV\ I} = (\dot{\chi}_7 - \dot{\chi}_8)$
Expansion valve II	$\dot{m}_{5''} = \dot{m}_6$	$h_{5''} = h_6$	$(\dot{\chi}_d)_{EV\ II} = (\dot{\chi}_{5''} - \dot{\chi}_6)$

Physical exergy of refrigerant stream at a given state point can be expressed as:

$$\dot{\varphi}_k = \dot{m}_{refrigerant}[(h_k - h_0) - T_0(s_k - s_0)] \quad (2.5)$$

$$COP = \frac{\dot{Q}_E}{\dot{W}_{comp\ I} + \dot{W}_{comp\ II}} \quad (2.6)$$

Exergetic efficiency of the system can be written as:

$$\eta_\chi = 1 - \frac{\sum_k \dot{\chi}_{d,k}}{\dot{W}_{comp\ I} + \dot{W}_{comp\ II}} \quad (2.7)$$

Where $\sum_k \dot{\chi}_{d,k}$ is total exergy destruction in the system and can be found by summation of all the exergy destructions of different system components.

2.2.2 Economic Analysis:

In economic analysis total capital cost of the system is studied which is found by the summation of capital costs of different system components.

$$C_{cap} = \sum_k Z_k \quad (2.8)$$

Where Z_k is the capital cost k_{th} component. The functions used for the estimation of capital cost of components are listed in **Table 2.3**.

Where $\dot{W}$ is the compressor power input, $\dot{m}$ is the mass flow rate through the expansion valve and A is are of heat exchanger which can be found by the relation:

$$A = \frac{\dot{Q}}{U \times \text{LMTD}} \quad (2.9)$$

Table 2.3: Capital cost functions for different system components [13]

Component	Capital cost function (Z_k)
Evaporator and Condenser	$1397 \times A_{E\ or\ C}^{0.89}$
Compressor I and II	$10167.5 \times \dot{W}_{comp\ I\ or\ II}^{0.46}$
Flash Intercooler with indirect sub-cooler (FIIS)	$1438.1 \times (A_{FIIS})^{0.65}$
Expansion Valve I and II	$114.5 \times \dot{m}$

2.2.3 Multi-objective optimization:

Multi-objective optimization is a technique to find the best solution to an optimization problem with multiple objectives which are generally conflicting in nature. A general multi-objective optimization problem can be written as **[44]**:

Find $x = (x_i)$, $\forall i = 1, 2, 3 \ldots \ldots N_{vrbl}$ (2.10)

Minimize or maximize $f_i(x)$, $\forall i = 1, 2, 3 \ldots \ldots N_{Obj\ Fcn}$ (2.11)

$g_m(x) = 0$, $\forall m = 1, 2, 3 \ldots \ldots p$ (2.12)

$h_n(x) = 0$, $\forall n = 1, 2, 3 \ldots \ldots q$ (2.13)

Where $N_{vrbl}, N_{obj\ Fcn}, p$ and q are number of design variables, objective functions, equality constraints and inequality constraints.

Here the optimization problem is formulated with exergetic efficiency and system's total capital cost as the two conflicting objective functions and evaporator temperature, condenser temperature, de-superheating parameters and subcooling parameter as four design parameters. A multiple regression analysis is performed to model the expressions for both the objective functions. These expressions are further fed to MATLAB software and the solution is obtained using multi-objective genetic algorithm tool provided with MATLAB. No unique solution is obtained which satisfies both the objective functions as they are conflicting in nature. Rather a number of non-dominated solutions are obtained in such a way that not any one of the objectives can be improved without worsening the other. These solutions are called pareto optimal fronts and are represented through a curve between exergetic efficiency and total capital cost with the help of bullets. As all the solutions on pareto optimal curve are optimal and any one of them may be used for optimal system design, it is a very important task to select one of them as the final solution. This is done through a multi-criteria decision making technique called TOPSIS (Technique for order of preference to by similarity to

ideal solution). The range of design variables considered in the study are presented in **Table 2.4**.

Table 2.4: Range of design variables

Parameter	Upper and Lower Bounds
Evaporator Temperature (T_E)	-45 ^{0}C < T_E < -20 ^{0}C
Condenser Temperature (T_C)	35 ^{0}C < T_C < 55 ^{0}C
Sub-cooling parameter (a)	0 < a < 1
De-superheating parameter (b)	0 < b < 1

2.3 Results and discussions:

2.3.1 Model validation:

The two-stage compression system is simulated on EES software with the help of first and second law of thermodynamics and the simulated model is validated through the results published in reference Bakeem et al. (2018). **Table 2.5** presents the values of COP, Exergetic efficiency and compressor work published in reference (R), present work (P) and the deviation (D) of present values from that of referenced values. The deviation is calculated as

$$D = (\frac{P-R}{R}) \times 100 \quad (2.14)$$

It can be observed that for each refrigerant used in the referenced work, a good agreement is achieved with the corresponding values obtained in present work with a maximum deviation of 2.1%.

Table 2.5: Model validation from the work of Bakeem et al. [14]

Refrigerant	Operating Conditions				COP			Exergetic Efficiency (%)			Total compressor work (Watt)		
	a	b	T_E (^{0}C)	T_C (^{0}C)	P	R	D (%)	P	R	D (%)	P	R	D (%)
R717	1	1	10	40	6.165	6.17	0.08	32.66	32.7	0.12	162.2	160	1.3
R22	1	1	10	40	5.968	5.99	0.36	31.72	31.7	0.06	167	170	1.7
R404A	1	0	10	40	5.567	5.6	0.58	29.49	29.5	0.03	179	180	0.55
R134a	1	0	10	40	6.012	6.01	0.03	31.85	31.9	0.15	166.3	170	2.1

2.3.2 Pareto optimal front

The multiple regression analysis has been done using in-built linear regression tool of EES to formulate the objective functions in terms of subcooling parameter, de-superheating parameter, evaporator temperature and condenser temperature. Modelling of COP, exergetic efficiency and total capital cost of system is done with excellent regression characteristics showing 98.98% to 99.31% of R^2 value as can be observed in **Table 2.6**. COP and Exergetic efficiency are modelled using one degree polynomials whereas the total capital cost of system is modelled with two degree polynomial in order to obtain the best possible fit.

Table 2.6: Regression models and R2 values of different regression models.

Regression Models	R^2 value
$COP = 3.5273 + 0.1205a + 0.1166b + 0.0366T_E - 0.0244T_C$	98.98%
$\psi = 46.9222 + 2.3371a + 2.2385b + 0.7030T_E + 0.12076T_C$	99.37 %
$C_{cap} = 158326.27 - 22772.88a + 3384.63a^2 - 7724.15b - 7145.1b^2 + 1384.56T_E + 82.88{T_E}^2 + 2061.62T_C + 15.20{T_C}^2$	99.31 %

The results of multi-objective optimization are presented with the help of a pareto curve plotted between Total capital cost and exergetic efficiency as shown in **Fig. 2.2**. It can be observed from the pareto curve that both the objective functions are conflicting in nature because as the exergetic efficiency is increased from 41.64% to 44.031% the total capital cost also increases from 220582 USD to 288718 USD. That means an increase of 5.6% in exergetic efficiency demands a hike of 30.89% in total capital cost. All the solutions lie between two points called cost ideal solution (a solution with minimum cost) and the exergetic efficiency ideal solution (a solution with maximum cost) as shown in the **Fig. 2.2**. Since all the solutions on graph are potentially optimal and non-dominated by each other, therefore TOSIS method has been used to select a unique combination of the exergetic efficiency and total system cost. **Table 2.7** presents

the selected unique solution by the TOPSIS method with optimum values of exergetic efficiency, total capital cost, and optimum design parameters.

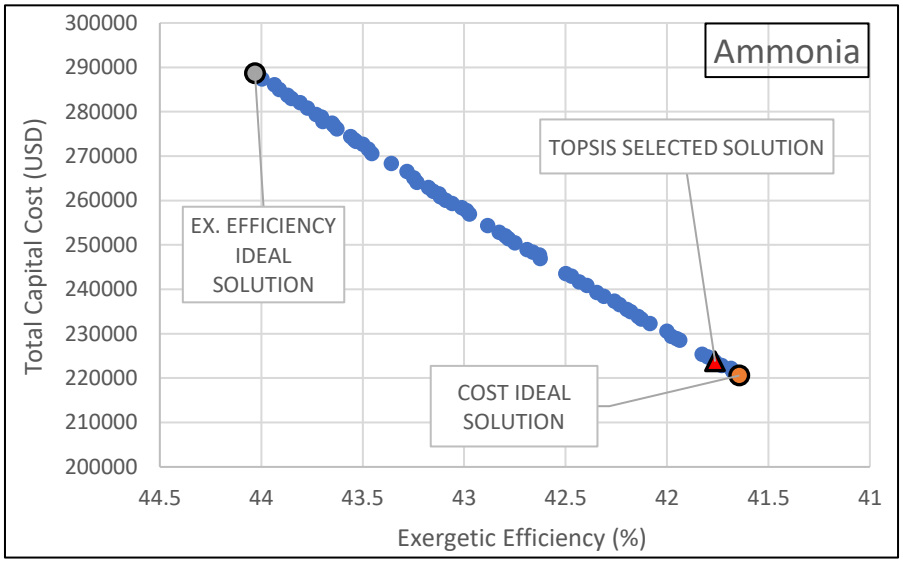

Fig. 2.2: Pareto optimal front showing ideal solutions and TOPSIS selection

Table 2.7: Results of Multi-objective optimization

Optimal values of design variables				Optimum performance parameters	
a	b	T_E(°C)	T_C(°C)	η_χ(%)	$C_{cap}(USD)$
0.998137	0.995787	-20.0182	36.03575	41.76286	223717.6

Table 2.8: Important system parameters at optimal conditions

Thermodynamic State	Specific Enthalpy (kJ kg^{-1})	Specific Entropy (kJ kg^{-1} K^{-1})	Temperature (^{0}C)	Pressure (kPa)
1	1438	5.904	-20.02	189.9
2	1621	6.058	66.85	514.1
3	1469	5.563	5.457	514.1
4	1662	5.712	96.73	1391
5	371.1	1.583	36.04	1391
6	371.1	1.616	4.898	514.1
7	224.2	1.082	5.103	1391
8	224.2	1.111	-20.02	189.9

The thermodynamic properties of refrigerants at different state points at optimal working conditions are as shown in **Table 2.8**. It can be seen that all the values conform to the expected variations in thermodynamic properties of refrigerant with different

processes occurring in the thermodynamic cycle of a two-stage compression refrigeration system.

Fig. 2.3 shows the values of exergy destruction rates occurring in different system components at the thermodynamic optimal operating conditions. It can be observed that the maximum exergy destruction occurs in compressor II with 66.56 kJ/s and minimum destruction is observed in expansion valve I with 2.21 kJ/s. This is because of the fact that the mass flow rate of refrigerant handles by compressor II is higher than that of compressor I.

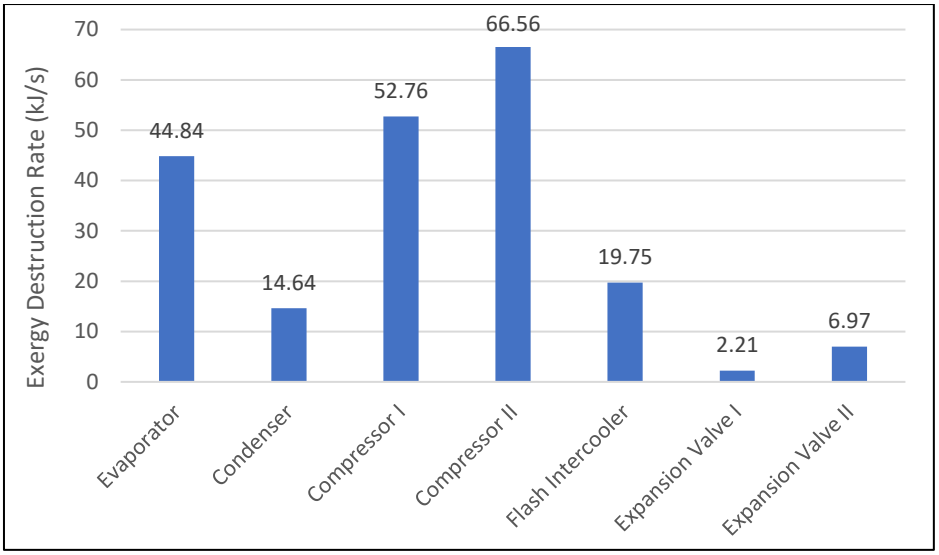

Fig. 2.3: Component-wise exergy destruction rates at optimal operating conditions

Exergy destruction in evaporator is higher than that of the condenser because of higher amount of temperature gap between cold space and evaporator (*i.e* 10 ^{0}C) as compared to the condenser in which the temperature gap is 16 ^{0}C at thermodynamic optimal operating condition. A heat transfer with higher temperature difference causes higher irreversibility and hence a higher destruction of exergy.

A Cascade refrigeration system is an important system which is used in supermarket refrigeration system and chemical processing and gas liquefaction industries. NH_3-CO_2 is a popular natural refrigerant pair used to run the system. Here a comparative analysis

is presented on the basis of multi-objective optimization results of cascade refrigeration system using NH_3-CO_2 and NH_3-N_2O refrigerant pairs.

2.4 System Description:

Fig. 2.4(a) shows the schematic diagram of Casacde refrigeration system. It consists of two single stage compression cycles coupled through cascade heat exchanger (CHX).

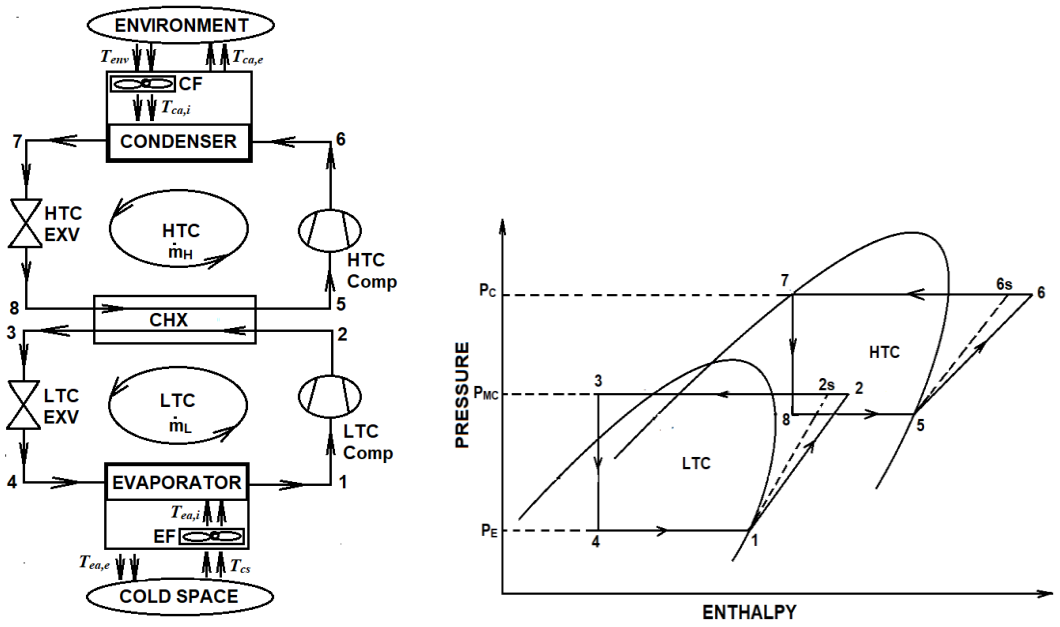

Fig. 2.4: (a) Schematic diagram of Cascade Refrigeration System **(b)** Thermodynamic cycle on p-h diagram

Air from the cold space enters the LTC evaporator (E) through evaporator fan (EF) causing the LTC refrigerant to evapoarate by absorbing heat from the air and then saturated vapour LTC refrigerant enters the LTC compressor (LTC Comp) where it is compressed and after condensation in CHX it again enters the evaporator (E) after being expanded in the LTC expansion valve (LTC EXV). The HTC refrigerant in CHX recieves the heat rejected by LTC refrigerant and fed to the HTC compressor (HTC Comp) where it is compressed to superheated state and after heat rejection to the

environmental air in the condenser (C) the HTC refrigerant undergoes expansion in HTC expansion Valve (HTC EXV) and then again enters the CHX to further absorb the heat from LTC refrigerant. **Fig. 2.4(b)** shows the thermodynamic cycle on a p-h diagram. The properties of refrigerants used and the important operational parameters assumed in the simulation work are presented in **Table 2.9** and **Table 2.10** respectively.

Table 2.9: Basic properties of refrigerants **[25]**

Cycle	Chemical Names of Refrigerants	Refrigerant codes	Critical Pressure (bar)	Critical Temperature (^{0}C)	Specific heat ratio	Triple Point (^{0}C)	Latent heat (kJ kg^{-1})	NBP (^{0}C)
HTC	Ammonia	R717	113	132.3	1.346	-77.7	1370	-33.3
LTC	Carbon Dioxide	R744	73.77	30.98	1.3	-56.6	349.5	-78.4
	Nitrous Oxide	R744a	72.45	36.37	1.7949	-90.8	379.43	-88.4

Table 2.10: Operational parameters assumed in the simulation work

Parameter	Value
Cooling Load, $\dot{Q}_E$	50 kW
Cold space temperature, T_{CS}	-35 ^{0}C
Ambient Temperature, T_0	25 ^{0}C
Ambient pressure, P_0	101.3kPa

2.5 Mathematical Modelling:

In this study the cascade refrigeration system is modelled on EES software using basic energy and exergy balance equations. The thermophysical properties of refrigerants at different state points has been found by built-in properties functions. Economic modelling is done using the equations provided by Rezayan and Bahbaninia, **[13]** and Aminyavari et al., **[25]**.

2.5.1 Thermodynamic Modelling:

Based on first and second laws of thermodynamics balance equations for different system components have been established which are shown in **Table 2.11**. Following assumptions have been taken for adding simplicity to the analysis.

1. Pressure losses are negligible.
2. Refrigerants are at their respective saturated states at the entry and exit points of all heat exchangers.
3. All components essentially follow steady state flow conditions.
4. Mechanical and electrical efficiencies of compressors are 100%.

Table 2.11: Energy and Exergy balance equations.

Component	Energy balance equations	Exergy balance equations
Evaporator	$\dot{Q}_E = \dot{m}_L(h_1 - h_4)$	$\dot{E}x_{d,E} = \left(\dot{E}x_4 - \dot{E}x_1\right) + \dot{Q}_E\left(1 - \frac{T_0}{T_E}\right) + \dot{W}_{EF}$
Condenser	$\dot{Q}_C = \dot{m}_H(h_6 - h_7)$	$\dot{E}x_{d,C} = \left(\dot{E}x_6 - \dot{E}x_7\right) + \dot{Q}_C\left(1 - \frac{T_0}{T_C}\right) + \dot{W}_{CF}$
Cascade Heat Exchanger	$\dot{m}_L(h_2 - h_3) = \dot{m}_H(h_5 - h_8)$	$\dot{E}x_{d,CHX} = \left(\dot{E}x_2 - \dot{E}x_3\right) + \left(\dot{E}x_8 - \dot{E}x_5\right)$
LTC Compressor	$\dot{W}_{LTC\ Comp} = \dot{m}_L(\frac{h_{2s} - h_1}{\eta_s})$	$\dot{E}x_{d,LTC\ Comp} = \dot{E}x_1 - \dot{E}x_2$
HTC Compressor	$\dot{W}_{HTC\ Comp} = \dot{m}_H(\frac{h_{6s} - h_5}{\eta_s})$	$\dot{E}x_{d,HTC\ Comp} = \dot{E}x_6 - \dot{E}x_5$
LTC Expansion Valve	$h_3 - h_4$	$\dot{E}x_{d,LTC\ EXV} = \dot{E}x_3 - \dot{E}x_4$
HTC Expansion Valve	$h_7 - h_8$	$\dot{E}x_{d,HTC\ EXV} = \dot{E}x_7 - \dot{E}x_8$

Isentropic efficiency of compression process in both compressors is given as **[26]**:

$$\eta_s = 1 - (0.04 \times Pressure\ Ratio) \tag{2.15}$$

$$COP = \frac{\dot{Q}_E}{(\dot{W}_{LTC\ Comp} + \dot{W}_{HTC\ Comp})} \tag{2.16}$$

Total exergy destruction can be written as:

$$\dot{E}x_{d,Total} = \sum \dot{E}x_{d,k} \tag{2.17}$$

Exergetic Efficiency can be expressed as:

$$\eta_{Ex} = \frac{\dot{Q}_E\left(\frac{T_0}{T_E} - 1\right)}{(\dot{W}_{LTC\ Comp} + \dot{W}_{HTC\ Comp} + \dot{W}_{EF} + \dot{W}_{CF})} \tag{2.18}$$

2.5.2 Economic Modelling:

In economic modelling, there are three components which constitute the overall cost of the system *i.e.* capital cost, operating cost and environmental cost which is the penalty

cost due to CO_2 emission. Operating cost and environmental costs are calculated on per year basis whereas the capital cost is also converted in per year basis taking into account the annual maintenance cost and annual interest imposed on capital investment. Since the overall cost of system is analysed on per year basis it is expressed in USD year^{-1} and is called overall cost rate.

The overall cost rate of system can be expressed as:

$$\dot{C}_{OA} = \dot{C}_{Op} + \dot{C}_{env} + \sum \dot{Z}_k \tag{2.19}$$

$$\dot{C}_{Op} = \alpha_{el} \times H \times (\dot{W}_{LTC\ Comp} + \dot{W}_{HTC\ Comp} + \dot{W}_{EF} + \dot{W}_{CF}) \tag{2.20}$$

Where α_{el} is the electricity tariff (0.06 USD kWh^{-1}) and H is the annual operational hours (7000 hrs).

$$\dot{C}_{env} = \frac{\mu_{CO_2} \times C_{CO_2} \times (\dot{W}_{LTC\ Comp} + \dot{W}_{HTC\ Comp} + \dot{W}_{EF} + \dot{W}_{CF})}{1000} \tag{2.21}$$

Where μ_{CO_2} is CO_2 emission conversion factor (0.968 kg kwh^{-1}), and C_{CO_2} is the rate of penalty cost (90 USD per ton of CO_2 emission) for CO_2 emission **[26]**.

$$\dot{Z}_k = CRF \times \emptyset \times \sum Z_k \tag{2.22}$$

Where $\emptyset$ is the maintenance factor (1.06) and Z_k is the capital cost of k^{th} component which is estimated using the cost functions given by Rezayan and Bahbaninia, **[13]**. CRF is the capital recovery factor which can be expressed as **[45]**:

$$CRF = \frac{i(1+i)^n}{(1+i)^n - 1} \tag{2.23}$$

Where i and n are annual interest rate (14%) and system life time (15 years).

2.5.3 Multi-objective optimization:

Here genetic algorithm is used for carrying out the multi-objective optimization of system with exergetic efficiency and overall cost rate as the two conflicting objective functions and evaporator temperature *(T_E)*, condenser temperature (T_C), cascade heat exchanger temperature difference (T_{CHX}) and LTC condenser temperature (T_{MC}) as the

four design variables. The objective functions are modelled in terms of four design variables using multiple regression analysis and thereafter these modelled functions are imported on MATLAB workspace to perform multi-objective optimization using its genetic algorithm multi-objective optimization tool. After the iterative search procedure for optimization is completed, a set of seventy non-dominated optimal solutions is obtained in the form of pareto-optimal front. For the selection of a unique optimal solution TOPSIS method is employed with five different values of weights given to the objective functions in order to show the variation of final optimal solution with change in relative importance of the objective functions **[46]**. A solution with equal weights of exergetic efficiency and overall cost rate has been considered as the final solution in this study. The range of design variable considered in formulating the multi-objective optimization problem are presented in **Table 2.12**.

Table 2.12: Range of design variables

Design variables	Range
Evaporator temperature, T_E	-55^{0}C$\leq T_E \leq$ -45 ^{0}C
Condenser temperature, T_C	45 ^{0}C $\leq T_C \leq$ 55 ^{0}C
Cascade condenser temperature, T_{MC}	-9 ^{0}C $\leq T_{MC} \leq$ 1 ^{0}C
Cascade temperature difference, ΔT_{CHX}	2^{0}C $\leq T_{CHX} \leq$ 5 ^{0}C

Results and Discussions:

2.6.1 Model Validation Table:

The simulation model of cascade refrigeration system is validated with data published by Aminyaveri et al. **[25]**. Deviation of the results obtained from present simulation model from that of the reference data lies between -1.706% to 0.14% which shows a good agreement between the present model and reference model as depicted in **Table 2.13**.

2.6.2 Multiple regression analysis:

Table 2.14 presents the results of multiple regression analysis for the two refrigerant pairs. It has been observed from the previous studies that a one degree polynomial fit for exergetic efficiency and COP and two degree polynomial fit for overall cost rate suffice therefore same has been used while modelling the objective functions **[29]**. It can be observed that R^2 values are greater than 95% which shows that all the functions are in good agreement with actual data.

Table 2.13: Validation of the simulation model

	Operating conditions		
	$\dot{Q}_E = 50kW, T_{CS} = -45$℃, $T_E = -48.68$ ℃, $T_C = 40.1$℃, $T_{MC} = -7.06$ ℃, $\Delta T_{CHX} = 2$℃		
	Results		
Parameters	Present Study	Aminyavari et al., **[25]**	% deviation
$\dot{W}_{LC}\ (kW)$	14.79	14.7721	+0.12
$\dot{W}_{HC}(kW)$	18.62	18.6755	-0.29
COP	1.497	1.4949	+0.14
η_{Ex} (%)	45.95	45.89	+0.13
$\dot{C}_{OA}\ (USD\ year^{-1})$	272341	277070	-1.706

Table 2.14: Results of multiple regression analysis

Refrigerant Pair	Results of multiple regression analysis.	R^2 Value
NH_3-CO_2	$\eta_{ex} = 93.4351 + 0.6876T_E - 0.5396T_C + 0.04738T_{MC} - 0.6866\Delta T_{CHX}$	97.61
	$COP = 3.7062 + 0.02727T_E - 0.0214T_C + 0.00188T_{MC} - 0.0272\Delta T_{CHX}$	97.61
	$\dot{C}_{OA} = (13.4017 + 0.34925T_E + 0.003442{T_E}^2 - 0.094401T_C + 0.000817\ {T_C}^2 + 0.023367T_{MC} + 0.0006276{T_{MC}}^2 - 0.02064\Delta T_{CHX} + 0.002074\ {\Delta T_{CHX}}^2) \times 10^5\ USD/YR$	95.75
NH_3-N_2O	$\eta_{ex} = 94.4916 + 0.6688T_E - 0.55956T_C + 0.09456T_{MC} - 0.7117\Delta T_{CHX}$	97.72
	$COP = 3.7481 + 0.02653T_E - 0.0222T_C + 0.00375T_{MC} - 0.0282\Delta T_{CHX}$	97.72
	$\dot{C}_{OA} = (13.254 + 0.34404T_E + 0.003374{T_E}^2 - 0.0934064T_C + 0.000809\ {T_C}^2 + 0.02137T_{MC} + 0.0005703{T_{MC}}^2 - 0.020474\Delta T_{CHX} + 0.0020574\ {\Delta T_{CHX}}^2) \times 10^5\ USD/YR$	96.21

2.6.3 Pareto-optimal curves:

Fig. 2.5 shows the pareto optimal variations for the two refrigerant pairs. A set of seventy non-dominated combination of exergetic efficiency and overall cost rate is represented through bullets on a exergetic efficiency vs overall cost rate plot. It can be observed that as the exergetic efficiency is increased the overall cost rate also increases. This indicates a clear conflict occurring between the two objective functions. **Fig. 2.5(a)** shows the variation of exergetic efficiency with overall cost rate for NH_3-CO_2 refrigerant pair. It can be observed that the exergetic efficiency increases from 25.47% to 36.83% which is an increase of 44.63% whereas the overall cost rate increases from 1.6143×10^5 USD $year^{-1}$ to 2.03×10^5 USD $year^{-1}$ with a hike of 25.75%. In a Similar way, for NH_3-N_2O exergetic efficiency increases by 49.11% from 25.29% to 37.71% at an expense of increase in overall cost rate by 25.07% increasing from 1.5982×10^5 USD $year^{-1}$ to 1.999×10^5 USD $year^{-1}$ as shown in **Fig. 2.5(b)**.

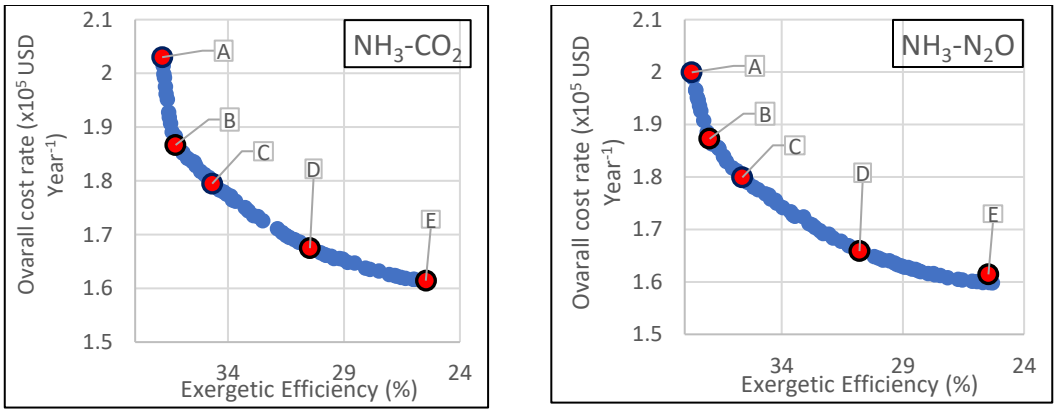

(a) **(b)**

Fig. 2.5: Pareto optimal curves for **(a)** NH_3-CO_2 and **(b)** NH_3-N_2O refrigerant pairs

Since all the points shown on pareto optimal fronts are potentially optimal and any one of them can be used to design an optimal system configuration. It is becomes imperative to choose one best solution. Here TOPSIS decision making technique has been employed for selection of a unique solution. This selection procedure requires

weightages to be assigned to each objective function depending upon their relative importance as felt by the designer according the constraints of cost. Here five such selections for each refrigerant pair has been shown with larger bullets named as A, B, C, D and E which correspond to the weightage of overall cost being 0, 0.25, 0.5, 0.75 and 1 respectively. Since It is a common practice to take the weightage of each objective function as equal (i.e. 0.5 for each), therefore in this study, solution 'C' for each of the two refrigerant pairs is considered as the unique solution of the multi-objective optimization problem.

Considering the weightages of both the objective functions as 0.5, unique solution for each of the two refrigerant pairs has been selected using TOPSIS decision making method. The optimal exergetic efficiency and overall cost rates along with the optimal values of all the four design variables for both the refrigerant pairs is presented in **Table 2.15**. It can be observed that the optimum exergetic efficiency for NH_3-N_2O pair is 35.62297% which is greater than that of NH_3-CO_2 pair. But on the other hand NH_3-CO_2 results in lower overall cost rate than NH_3-N_2O. Since the refrigerants show the solutions which are nondominated in nature, and no one can be called superior at this stage, it becomes imperative to apply TOPSIS method to assign an order of preference to them.

Table 2.15: Results of Multi-objective optimization

Refrigerant Pair	T_E (°C)	T_C (°C)	T_{MC} (°C)	ΔT_{CHX} (°C)	η_{Ex} (%)	$\dot{C}_{OA}$ (x 10^5 USD $Year^{-1}$)	Rank
NH_3-CO_2	-47.0445	45.57968	-8.7816	2.034058	34.67983	1.794756	2
NH_3-N_2O	-46.6647	45.28511	-8.7571	2.092285	35.62297	1.799291	1

After applying TOPSIS it has been found that NH_3-N_2O pair is superior to NH_3-CO_2 refrigerant pair as it has got rank 1 and later one has got rank 2 as shown in **Table 2.15**.

The corresponding optimal operational parameters are also depicted in the table which can be useful in designing an optimal system configuration using these refrigerant pairs.

2.7 Chapter Summary

In this study multi-objective optimization of an ammonia based two-stage refrigeration system and a cascade refrigeration system has been performed via simulation work in order to optimize the thermo-economic performance of the system. Exergetic efficiency and total cost are the two objective functions. The multiple regression analysis has been to formulate the objective functions with excellent R^2 values. Results of optimization show that optimal value of exergetic efficiency and total capital cost of two-stage refrigeration system is 41.76% and 223717 $ respectively. In cascade refrigeration system, NH_3-N_2O refrigerant pair show better results compared to NH_3-CO_2.

Chapter 3

Thermoeconomic and Exergoeconomic Analyses of Hybrid Cascade Refrigeration System

In this work, two stage refrigeration system and cascade refrigeration systems are combined to form a hybrid cascade refrigeration system and energetic, exergetic, economic and exergoeconomic analyses are done on it using seventeen natural refrigerant pairs. The study aims to fulfill the current need of identifying a potential eco-friendly natural refrigerant couple with the help of a comprehensive comparative thermodynamic and economic analysis by employing them in a hybrid cascade system that gives the best possible thermodynamic results.

3.1 System description

Figure 3.1(a) shows the schematic diagram of the system which consists of two thermally coupled refrigeration cycles working with two different refrigerants. First is a lower temperature cycle (LTC) which represents a two-stage compression system incorporated with a flash intercooler with indirect subcooler (FIIS) and second is called higher temperature cycle (HTC) which involves a single-stage compression system with a flash tank. Heat is extracted from cold space with the help of LTC and rejected to the environment through HTC. In LTC, the refrigerant at evaporator exit (1) gets compressed by LTC compressor I to a superheated state (2). It is then fed to FIIS, where it is de-superheated $(2-3)$, by rejecting heat to the FIIS saturated liquid refrigerant resulting in evaporation of some refrigerant. The evaporated part mixes with de-superheated stream and the combined stream (3) is fed to the LTC compressor II, where second stage compression takes place and the superheated refrigerant (4) leaving the compressor enters the cascade heat exchanger (CHX). Meanwhile, the HTC liquid

refrigerant, exiting the Flash tank (13), enters the CHX and both the fluids are allowed to interact without mixing. In CHX, the LTC refrigerant rejects heat to HTC refrigerant and gets condensed to a saturated liquid state (5). This saturated liquid refrigerant is then divided into two streams. One ($5''$) serves the FIIS as a make-up supply after expansion ($5'' - 6$) through Expansion valve II and another stream ($5'$), inside a tube, is allowed to pass through the FIIS to get subcooled ($5' - 7$) without mixing with FIIS fluid. The subcooled liquid refrigerant goes through expansion ($7 - 8$) in Expansion valve-I and enters the evaporator where it gets evaporated ($8 - 1$) to take the heat of air coming from cold space. In HTC, the liquid refrigerant converts to a saturated vapor state (9) after receiving heat in CHX. The vapor refrigerant exiting CHX mixes with another stream (14) coming from Flash tank and the combined stream (15) is then fed to HTC compressor for compression ($15 - 10$) and then allowed to condense ($10 - 11$) in the condenser by rejecting heat to the environmental air stream. The saturated condensate exiting the condenser (11) undergoes an isenthalpic expansion ($11 - 12$) in Expansion Valve III and the exit stream (12) is made to pass through the Flash tank where the flashes generated due to expansion are entrapped, and the refrigerant comes back to the saturated liquid state (13). The flash free saturated liquid refrigerant (13) advances towards the CHX for receiving the heat carried by LTC refrigerant. The flashes (saturated vapors) trapped in Flash tank get collected in its upper portion and exit it as a saturated vapor stream (14) which mixes with the exit stream (9) of CHX. Two fans, Fan I and Fan II are employed to transport heat from cold refrigerated space to the evaporator and from condenser to the environment respectively. Cold air, from the refrigerated space is sucked by Fan I at temperature $T_{ca,i}$ and thrown to the evaporator at temperature $T_{ca.i'}$ which after rejecting heat to the refrigerant cools down and leaves the evaporator at temperature $T_{ca,e}$, Similarly environmental air is sucked by

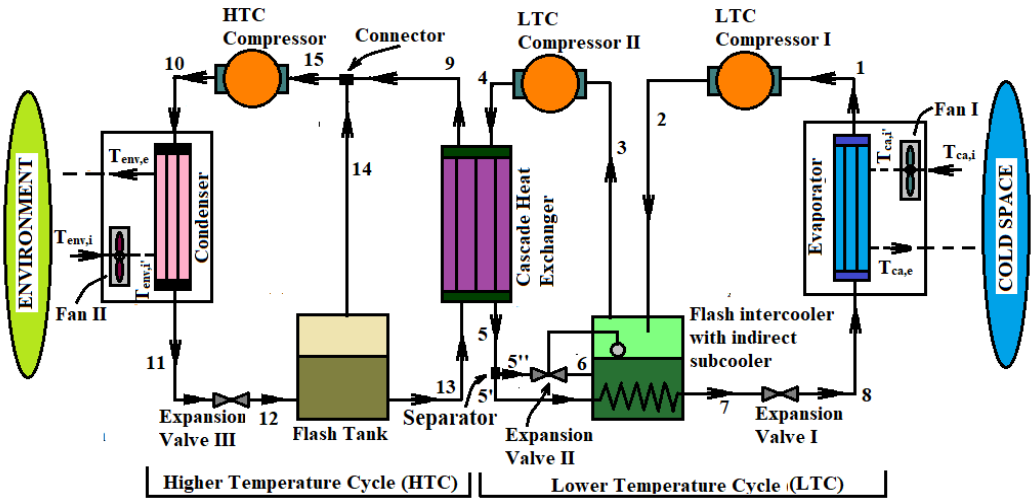

(a)

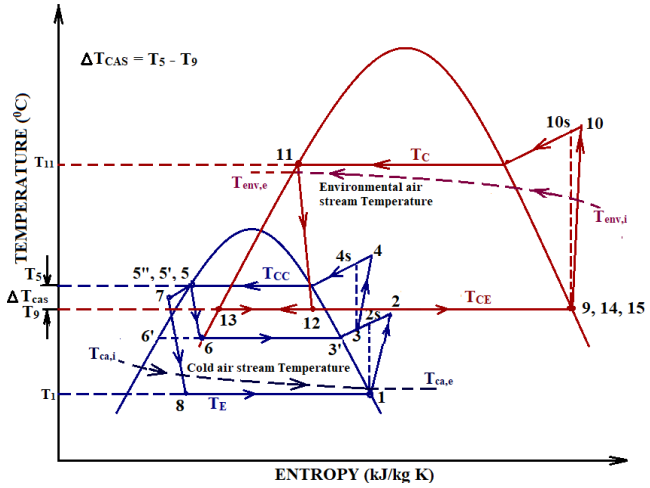

(b)

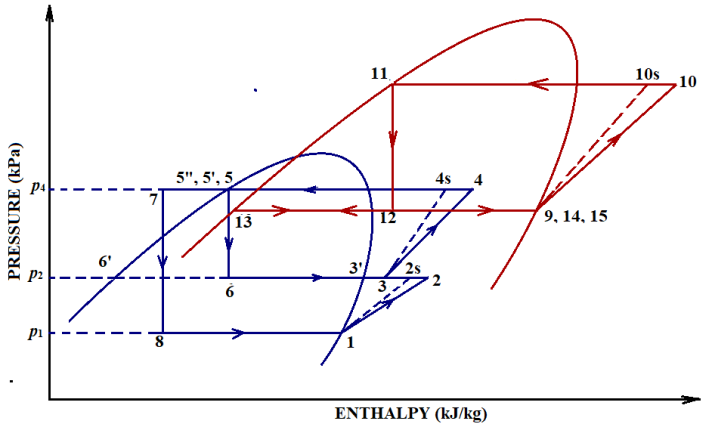

(c)

Figure 3.1: (a) Schematic cascade refrigeration system incorporated with flash tank and intercooler, **(b)** T-s diagram of the system, **(c)** P-h diagram of the system

Fan II at temperature $T_{env,i}$ and thrown to the condenser coils at temperature $T_{env,i'}$ where it takes heat of the refrigerant and leaves the condenser at a temperature $T_{env,e}$. Figure 3.1(b) and Figure 3.1(c) show the thermodynamic plots on T-s and p-h diagrams respectively.

3.2 Mathematical Modelling for thermoeconomic analysis

For comparing the thermodynamic performance of a system with respect to different refrigerant couples, an energy and exergy analysis has been carried out. For this very purpose energy, exergy and economic models are developed in EES software which is provided with built-in mathematical and thermodynamic property functions, employed to calculate the properties of refrigerants at the required thermodynamic states **[42]**. The results are obtained for different refrigerant couples and compiled in the form of different plots. The equations involved in mathematical modelling for thermodynamic and economic analysis are as follows:

3.2.1 Energy Analysis:

The energy analysis of the system is based on the first law of the thermodynamics which is applied on different components to understand their behaviour under various energy interactions, which contribute to the overall performance of the system. Before applying the first law of thermodynamics, some assumptions are taken while doing the analysis:

- Pressure and heat losses in pipes are negligible.
- Changes in kinetic and potential energy are negligible.
- All system components are operating in steady-state conditions.
- Refrigerants, at the exit of the evaporator, condenser and cascade heat exchanger are at the saturated state.

Based on the above assumptions, the mass and energy balance equations for k^{th} component are expressed in a general form as:

$$\sum_k(\dot{m})_{inlet} = \sum_k(\dot{m})_{exit} \quad (3.1)$$

$$\dot{Q}_k + \sum_k(\dot{m}h)_{inlet} = \dot{W}_k + \sum_k(\dot{m}h)_{exit} \quad (3.2)$$

Where $\dot{Q}_k$ and $\dot{W}_k$ are the rates of heat input and work output, and $\dot{m}$ and h are the mass flow rate and specific enthalpy associated with the streams at the inlet and exit of the k^{th} component. The mass and heat balance equations for each system component are presented in **Table 3.1.**

Table 3.1: Process specifications, settings and mass and heat balance equations of process equipment

Process Equipment	Mass Balance Equation	Heat Balance Equation	System Specifications
Evaporator	$\dot{m}_8 = \dot{m}_1$, $\dot{m}_{ca,i'} = \dot{m}_{ca,e}$	$\dot{Q}_{evp} = \dot{m}_{ca}(h_{ca,i'} - h_{ca,e}) = \dot{m}_1(h_1 - h_8)$	$\dot{Q}_{evp}$ = 500kW T_{evp}= -35 ^{0}C ΔT_{air} = 10 ^{0}C ΔT_{sup} = 0 ^{0}C U_{evp} = 0.03 kW/m^{2}K
Condenser	$\dot{m}_{10} = \dot{m}_{11}$, $\dot{m}_{env,i'} = \dot{m}_{env,e}$	$\dot{Q}_{cond} = \dot{m}_{env}(h_{env,e} - h_{env,i'}) = \dot{m}_{10}(h_{10} - h_{11})$	T_{cond} = 35 ^{0}C ΔT_{air} = 10 ^{0}C U_{cond} = 0.04 kW/m^{2}K
CHX	$\dot{m}_4 = \dot{m}_5$ $\dot{m}_{13} = \dot{m}_9$	$\dot{m}_4(h_4 - h_5) = \dot{m}_9(h_9 - h_{13})$	T_5 = 0 ^{0}C ΔT_{cas} = 2 ^{0}C U_{cas} = 1 kW/m^{2}K
Flash Intercooler	$\dot{m}_2 + \dot{m}_6 = \dot{m}_3$, $\dot{m}_{5'} = \dot{m}_7$	$\dot{m}_6h_6 + \dot{m}_{5'}h_{5'} + \dot{m}_2h_2 = \dot{m}_3h_3 + \dot{m}_7h_7$	a = 0.9, b = 0.9 U_{FI} = 1 kW/m^{2}K
Flash Tank	$\dot{m}_{12} = \dot{m}_{13} + \dot{m}_{14}$	$\dot{m}_{12}h_{12} = \dot{m}_{13}h_{13} + \dot{m}_{14}h_{14}$	-
LTC compressor I	$\dot{m}_1 = \dot{m}_2$	$\dot{W}_{LTC\ comp\ I} = \dot{m}_1(h_2 - h_1)$	Overall efficiency (equation 5)
LTC compressor II	$\dot{m}_3 = \dot{m}_4$	$\dot{W}_{LTC\ comp\ II} = \dot{m}_3(h_4 - h_3)$	Overall efficiency (equation 5)
HTC Compressor	$\dot{m}_9 = \dot{m}_{10}$	$\dot{W}_{HTC\ comp} = \dot{m}_{10}(h_{10} - h_{15})$	Overall efficiency (equation 4)
Expansion Valve I	$\dot{m}_7 = \dot{m}_8$	$h_7 = h_8$	-
Expansion Valve II	$\dot{m}_{5''} = \dot{m}_6$	$h_{5''} = h_6$	-
Expansion Valve III	$\dot{m}_{11} = \dot{m}_{12}$	$h_{11} = h_{12}$	-

Power input to the compressors is given by:

$$\dot{W}_{comp} = \frac{\dot{m}(h_s - h_i)}{\eta_s \eta_{el} \eta_m} = \frac{\dot{m}(h_s - h_i)}{\eta_{total}} \quad (3.3)$$

Where h_i is the specific enthalpy of compressor's inlet-stream and h_s is the specific enthalpy of compressor's exit-streams when the compression would have been done isentropically. η_s, η_{el}, and η_m are the isentropic, electrical and mechanical efficiencies of the compressor and η_{total} is the net efficiency which accounts for all the three efficiencies. η_{total} for HTC compressor can be expressed as **[15]**:

$$\eta_{total} = \begin{cases} 0.0071\lambda^5 - 0.1264\lambda^4 + 0.9023\lambda^3 - 3.2277\lambda^2 + 5.7871\lambda - 3.3429, & \lambda < 4.3 \\ -0.0261\lambda + 0.9069, & \lambda \geq 4.3 \end{cases} \quad (3.4)$$

η_{total} for LTC compressors can be expressed as **[15]**:

$$\eta_{total} = \begin{cases} -0.1234\lambda^4 + 1.1251\lambda^3 - 3.8902\lambda^2 + 6.0433\lambda - 2.8860, & \lambda < 2.7 \\ -0.0237\lambda^4 + 0.3051\lambda^3 - 1.4740\lambda^2 + 3.1348\lambda - 1.7978, & \lambda \geq 2.7 \end{cases} \quad (3.5)$$

Where λ is the pressure ratio across the compressor.

The intermediate pressure in flash intercooler (p_2) of LTC is expressed by **[14]**:

$$p_2 = \sqrt{(p_1 p_4)} \quad (3.6)$$

Where p_1 and p_4 are the operating pressures of LTC evaporator and LTC condenser.

The intercooler, in the LTC side also serves as an indirect sub-cooler. Based on mass and energy balance equations of the flash intercooler, Torella et. al. **[12]** defined two parameters for the analysis of any inter-stage configuration which govern the phenomenon of intercooling and sub-cooling. These parameters are:

- Sub-cooling parameter, $a = \frac{h_5 - h_8}{h_5 - h_{6'}}$ (3.7)

  This parameter governs the degree of subcooling in the lower temperature cycle. Its value varies from 0 to 1. *a=0* implies no sub-cooling i.e. $h_8 = h_5$, while *a=1,* implies the case of maximum sub-cooling when $h_8 = h_{6'}$. *i.e.* specific enthalpy of the refrigerant at state 7 ($h_7 = h_8$) attains its minimum possible value *i.e.* specific enthalpy of the saturated liquid ($h_{6'}$) in the intercooler.

- De-superheating parameter, $b = \frac{h_2 - h_3}{h_2 - h_{3'}}$ (3.8)

  This parameter governs the degree of intercooling or de-superheating. It varies from 0 to 1. *b=0* implies no intercooling i.e. $h_3 = h_2$, while *b=1*, implies that the intercooling is done up to the corresponding saturated state i.e. $h_3 = h_{3'}$.

The power input to the evaporator and condenser fans are estimated by **[47]**:

$$\dot{W}_{Fan\ I} = 0.075\left(\dot{Q}_{evp}\right) \quad (3.9)$$

$$\dot{W}_{Fan\ II} = 0.027\left(\dot{Q}_{evp} + \sum_j \dot{W}_{comp}\right) \quad (3.10)$$

Where $\sum_j W_{comp}$ is the sum of power inputs to all the compressors.

Gross power consumption of the system can be written as the sum of power consumed by compressors as well as the two fans:

$$\dot{W}_{total} = \dot{W}_{LTC\ comp\ I} + \dot{W}_{LTC\ comp\ II} + \dot{W}_{HTC\ comp} + \dot{W}_{Fan\ I} + \dot{W}_{Fan\ II} \quad (3.11)$$

The COP of the system can be expressed as:

$$COP = \frac{\dot{Q}_{evp}}{\dot{W}_{total}} \quad (3.12)$$

3.2.2 Exergy Analysis

Exergy is the work potential delivered by a system when it is brought to the dead state from a given state. The exergy analysis method is based on the Second law of thermodynamics. In absence of electromagnetic, electric, nuclear and surface tension effects, and neglecting the kinetic and potential energies the physical exergy flow rate associated with a refrigerant stream is expressed by **[25]**:

$$\dot{E}x_j = \dot{m}_j\left[(h - h_0)_j - T_0(s - s_0)_j\right] \quad (3.13)$$

Where T_0 is the thermodynamic averaged temperature of the ambient environment defined as follows **[48]**:

$$T_0 = \frac{(T_e - T_i)_{env}}{\ln\,(T_e/T_i)_{env}} \quad (3.14)$$

Where T_i, and T_e are the temperatures of environmental air at inlet and exit of the condenser.

Applying exergy balance equation for a k^{th} component, the exergy destruction in that component can be written as **[25]**:

$$(\dot{E}x_d)_k = \left(\sum_j \dot{E}x_j^Q\right)_k - (\dot{E}x^W)_k + (\sum_i \dot{E}x_i)_k - (\sum_e \dot{E}x_e)_k \quad (3.15)$$

Where $\dot{E}x_j^{\dot{Q}}$ and $\dot{E}x^W$ are the exergy transfer rates associated with the heat transfers and work transfers taking place across the control surface of the k^{th} component and $\dot{E}x_i$ and $\dot{E}x_e$ are the physical exergies associated with the refrigerant streams at inlet and exit of the k^{th} component. The Expressions for exergy destructions of different components is presented in **Table 3.2**.

Table 3.2: Exergy Destruction in different components of the system

Component	Exergy Destructions $(\dot{E}x_d)_k$
Evaporator + Fan I	$(\dot{E}x_d)_{evp} = \left(\dot{E}x_{ca,i} - \dot{E}x_{ca,e}\right) + (\dot{E}x_8 - \dot{E}x_1) + \dot{W}_{Fan\ I}$
Condenser + Fan II	$(\dot{E}x_d)_{cond} = \left(\dot{E}x_{env,i} - \dot{E}x_{env,e}\right) + (\dot{E}x_{10} - \dot{E}x_{11}) + \dot{W}_{Fan\ II}$
CHX	$(\dot{E}x_d)_{cas} = (\dot{E}x_4 - \dot{E}x_5) + (\dot{E}x_{13} - \dot{E}x_9)$
FIIS	$(\dot{E}x_d)_{FI} = \left(\dot{E}x_2 + \dot{E}x_{5'} + \dot{E}x_6\right) - (\dot{E}x_3 + \dot{E}x_7)$
Flash tank	$(\dot{E}x_d)_{FT} = \dot{E}x_{12} - \dot{E}x_{13} - \dot{E}x_{14}$
LTC compressor I	$(\dot{E}x_d)_{LTC\ comp\ I} = (\dot{E}x_1 - \dot{E}x_2) + \dot{W}_{LTC\ comp\ I}$
LTC compressor II	$(\dot{E}x_d)_{LTC\ comp\ II} = (\dot{E}x_3 - \dot{E}x_4) + \dot{W}_{LTC\ comp\ II}$
HTC compressor	$(\dot{E}x_d)_{HTC\ comp} = (\dot{E}x_9 - \dot{E}x_{10}) + \dot{W}_{HTC\ comp}$
Expansion valve I	$(\dot{E}x_d)_{EV\ I} = (\dot{E}x_7 - \dot{E}x_8)$
Expansion valve II	$(\dot{E}x_d)_{EV\ II} = \left(\dot{E}x_{5''} - \dot{E}x_6\right)$
Expansion valve III	$(\dot{E}x_d)_{EV\ III} = (\dot{E}x_{11} - \dot{E}x_{12})$

It should be noted that the power consumptions of Fan I and Fan II of evaporator and condenser are the parasitic loads, so they have been added to the exergy destructions of these components.

The total input exergy to the system:

$$\dot{E}x_{input} = \dot{W}_{total} \quad (3.16)$$

The output exergy of the system can be expressed as:

$$\dot{E}x_{output} = \dot{E}x_{ca,e} - \dot{E}x_{ca,i} \quad (3.17)$$

Exergy loss of system can be written as:

$$\dot{E}x_{loss} = \dot{E}x_{env,e} - \dot{E}x_{env,i} \quad (3.18)$$

Hence the total exergy destruction can be calculated as:

$$\left(\dot{E}x_d\right)_{total} = \dot{E}x_{input} - \dot{E}x_{output} - \dot{E}x_{loss} = \sum_k \left(\dot{E}x_d\right)_k \quad (3.19)$$

Where $\sum_k \left(\dot{E}x_d\right)_k$ represents the sum of exergy destructions in all the system components. The exergy efficiency of the system can be determined by:

$$\psi = \frac{\dot{E}x_{output}}{\dot{E}x_{input}} = \frac{\dot{E}x_{ca,e} - \dot{E}x_{ca,i}}{\dot{W}_{total}} = 1 - \frac{\sum_k (\dot{E}x_d)_k + \dot{E}x_{loss}}{\dot{W}_{total}} \quad (3.20)$$

3.2.3 Economic Analysis

The economic analysis is focussed on analyzing the overall cost of the system for different refrigerant couples. The overall cost is evaluated on a per year basis so it is also called total cost rate ($/yr). The total annual cost rate consists of two components, one is the annual operational cost and another is the annualized capital investment and maintenance costs of the components.

$$\dot{C}_{total} = \dot{Z}_{op} + \sum_k \dot{Z}_k \quad (3.21)$$

Where $\dot{Z}_{op}$ is the annual operational cost ($/yr) and $\dot{Z}_k$ is annualized capital and maintenance cost ($/yr) of k^{th} component.

$$\dot{Z}_{op} = N \times \dot{W}_{total} \times \alpha_{el} \quad (3.22)$$

Where N is the total working hours of the system per year and α_{el} is the cost of electricity in $/kWh. The rate of capital and maintenance costs of k^{th} system components is estimated as follows **[49]**:

$$\dot{Z}_k = Z_k \times \emptyset \times CRF \quad (3.23)$$

Where Z_k is the capital cost, $\emptyset$ is the maintenance factor and $\dot{Z}_k$ is the annualized capital and maintenance cost of k^{th} component expressed here in \$/yr. Cost functions for estimating the capital cost (Z_k) of components are presented in **Table 3.3**. CRF is the capital recovery factor defined as **[45]**:

$$CRF = \frac{i(1+i)^n}{(1+i)^n - 1} \tag{3.24}$$

Where *i* and *n* are annual cost rate and system life-time respectively.

Table 3..3: Cost functions for estimating the capital costs of the components [25, 50-52]

Component	Capital cost function ($\boldsymbol{Z_k}$)
Evaporator and condenser	$1397 \times A_{evp\ or\ cond}^{0.89}$
Cascade heat exchanger	$383.5 \times A_{cas}^{0.65}$
LTC compressors	$10167.5 \times \dot{W}_{LTC\ comp\ I\ or\ II}^{0.46}$
HTC compressor	$9624.2 \times \dot{W}_{HTC\ comp}^{0.46}$
Flash tank	$280.3 \times \dot{m}_i^{0.67}$
Flash intercooler with indirect sub-cooler	$1438.1 \times A_{FI}^{0.65}$
Expansion valves	$114.5 \times \dot{m}$
Fans	$155 \times (\dot{V} + 1.43)$
Installation of the refrigeration system	$150.2 \times \dot{Q}_{evp}$

Where $\dot{W}$ is power input to the compressors, $\dot{V}$ is the volume flow rate handle by fans, and $\dot{m}_i$ is inlet mass flow rate of flash tank and A is the surface area of heat exchangers, which can be expressed as **[53]** :

$$A = \frac{\dot{Q}}{U_0 F \Delta T_{lm}} \tag{3.25}$$

Where $\dot{Q}$ is the heat exchanged, U_0 and ΔT_{lm} are the overall heat transfer coefficient and logarithmic mean temperature difference (LMTD) of the heat exchangers respectively. F is the correction factor of LMTD which has been determined by the relationship given by Fettaka et al. **[53]**.

3.2.4 Payback Analysis

Payback period refers to the amount of time it takes to recover the cost of an investment. For a brief evaluation of feasibility of the system and the assessment of economic

accountability of refrigerant pairs, a simple payback analysis is done on the system using the three refrigerant pairs.

Since fishes need to be maintained at -18 ^{0}C to -20 ^{0}C to prevent them from decomposition **[54]** , and the cold space temperature considered in the study is taken as -20 ^{0}C, the payback analysis is based on employing the system to provide cooling to a cold storage used in fisheries. In cold storages, hiring is done on volume occupied or weight of loading on per hour basis. **Table 3.4** presents a rough estimation of heat balance of total cooling load and the volume of cold space available for fish storage.

Table 3.4: Heat balance of the cooling load [54]

Means of Heat loss/gain	Heat Transfer Rate
Heat gain through fish loading: $\dot{Q}_{FL} = \frac{\text{Fish loading per day} \times \text{Heat gain due to fish loading}}{24 \times 3600}$ (3.26) Fish loading per day: $500\ ton$ Heat gain due to fish loading: $5.5\ kcal/kg$	$\dot{Q}_{FL} = 133.10\ kW$
Heat loss through air change: $\dot{Q}_{AC} = \frac{\text{Store volume} \times \text{Average air change per day} \times \text{Heat loss rate}}{24 \times 3600}$ (3.27) Average air changes per day: 2.7 Store volume : $32075\ m^3$ Heat loss rate: $40\ kcal/m^2$	$\dot{Q}_{AC} = 167.75\ kW$
Heat gain due to Fan, Electric lamps, Men working etc.	$\dot{Q}_{OL} = 104.37\ kW$
Heat loss through walls: $\dot{Q}_{cooling} = (\dot{Q}_{evp} - \dot{Q}_{FL} - \dot{Q}_{AC} - \dot{Q}_{OL})$ $= U_{ins} \times A_{wall} \times (T_{env,i} - T_{ca,i})$ (3.28) Insulation wall material: Polyurethane Insulation wall heat transfer coefficient (U_{ins}): $0.28\ W/m^2K$ Surface area available for heat transfer (A_{wall}): $7522.37\ m^2$ Inside temperature ($T_{ca,i}$): -20 ℃ Outside temperature ($T_{env,i}$): 25 ℃ Cold space dimensions: $86m \times 24m \times 16m$ Insulation wall thickness: $0.25\ m$ Volume of the cold space: $32075\ m^3$	$\dot{Q}_{Cooling} = 94.78\ kW$

As can be seen from the heat balance sheet presented in Table 4 that, out of 500 kW of total cooling, only 94.78 kW can be used to design a space which can be kept at -20^{0}C. Taking into account heat losses through the walls, the available refrigerated space comes out to be 32075 m^3 which is the inside volume of cold space (86mx24mx16m) with insulation wall thickness of 0.25m. If average weight to volume ratio of fish is 2.4 tons/m^3 and renting charges are 0.43 $/ton/day and average occupancy of space is 60% **[54]**.

The net earning in one year from such space can be calculated by:

$$\dot{R} = \frac{(32075 \times 0.6 \times 2.4 \times 0.43) \times N}{24} = 3530264\ \$/yr \quad (3.29)$$

Considering the overall investment in cold storage in its complete life time to be 1.5 times the total investment done in refrigeration system in its complete life time (including total capital, running and maintenance cost)

Total investment in cold storage in its complete life time can be expressed as:

$$G = 1.5 \times \dot{C}_{total} \times n \quad (3.30)$$

Therefore, Payback period can be expressed as:

$$t = \frac{G}{\dot{R}} \quad (3.31)$$

3.2.5 System specifications

The operating conditions used for thermodynamic modelling of the system are specified in **Table 3.1** and other important parameters which have been used in the study are mentioned as follows:

In engineering economics capital cost along with the maintenance cost is annualized by using equation (23). The maintenance factor (ϕ) is taken as 1.06. The annual interest rate (i) and system lifetime (n) are taken to be 14% and 15 yrs. The average cost of electricity (α_{el}) is 0.12 US$ kWh^{-1} (average non-domestic cost of electricity in Delhi, India) and the average annual operational hours (N) of the system are 4266 hrs **[15]**.

3.3 Thermoeconomic results and discussions

3.3.1 Model Validation

In this study, comparative energy, exergy, and economic analysis have been done on the aforementioned system using different natural refrigerant couples. The system has been modelled on EES software and the model is validated from the results of a published work.

Table 3.5: Validation of the present model from published data [15]

	Operating Conditions -1			Operating Conditions -2		
	$Q_{evp} = 500\ kW, T_{evp} = -35.2$ ℃, $T_{cond} = 35.01$ ℃, $T_5 = -1.98$ ℃, $\Delta T_{cas} = 2.27$ ℃, $\Delta T_{sup} = 0.45$ ℃, $T_{ca,i} = -20$ ℃, $T_{env,i} = 25$ ℃ $N = 4266\ hours$			$Q_{evp} = 500\ kW, T_{evp} = -40$ ℃, $T_{cond} = 36.67$ ℃, $T_5 = 0$ ℃, $\Delta T_{cas} = 3.33$ ℃, $\Delta T_{sup} = 1.67$ ℃, $T_{ca,i} = -20$ ℃, $T_{env,i} = 25$ ℃ $N = 4266\ hours$		
	Results					
Parameters	Present Model	Mosaffa et al. **[15]**	% deviation	Present Model	Mosaffa et al. **[15]**	% deviation
$A_{evp}\ (m^2)$	1671	1671	0	1148	1148	0
$A_{cond}\ (m^2)$	625.3	627.6	0.37	607.8	612.6	0.78
$A_{cas}\ (m^2)$	61.43	59.86	-2.62	49.59	46.81	-5.94
$\dot{W}_{comp}\ (kW)$	264.6	267.37	1.04	301.7	307.93	2.02
$\dot{E}x_d\ (kW)$	220.6	223.5	1.3	258.7	264.8	2.3
COP	1.549	1.536	-0.85	1.386	1.36	-1.91
ψ (%)	31.66	31.3	-1.15	28.32	27.75	-2.05
$\dot{C}_{total}\left(\frac{\$}{yr}\right)$ [@ $0.09\$/kWh$]	554353	675530	17.94	523011	661197	20.9
$\dot{C}_{total}\left(\frac{\$}{yr}\right)$ [@ $0.12\$/kWh$]	595659			569194		

Table 3.5 presents a comparison of published values with corresponding present values of important system parameters at two different operating conditions. It can be seen that the deviation ranges from -5.94 % to 2.3% except the total system cost which results in a deviation of 20.9%. This is because of the exclusion of the penalty cost due to R744 emission in present analysis. Although the cost of electricity in the present

analysis, is taken as 0.12 $/kWh, in **Table 3.5**, the overall system cost rate has been calculated at a rate of 0.09 $/kWh (value taken in the referenced work) for validation of the economic model.

Natural refrigerant analysis

The system operates with two different refrigerants working between different temperature ranges. The refrigerants with higher NBP values are compatible in HTC and those having lower values are compatible in LTC [33]. For selecting the refrigerants for HTC and LTC, eight natural refrigerants are listed in **Table 3.6** with their basic properties and the corresponding T-s diagrams are shown in Figure 2. After comparing their properties, it is observed that R717, R290, R1270, and R600a are suitable for HTC and R744, R744a, R170, R1150 are suitable for LTC. While R290 and R1270 can be used in LTC also with R717 and R600a as HTC refrigerants. Seventeen refrigerant pairs have been formed employing R717 in HTC paired with R744, R744a, R170, R1150, R290, R1270 in LTC, R290 in HTC paired with R744, R744a, R170, R1150, R1270 in LTC, and R600a in HTC paired with R744, R744a, R170, R1150, R290, R1270 in LTC.

Table 3.6: Properties of natural refrigerants [30, 36, 55]

S. No.	Names of Refrigerants	Designations	NBP (^{0}C)	Critical Temper-ature (^{0}C)	Critical Pressure (bar)	Triple Point (^{0}C)	Specific heat ratio	Latent heat (kJ/kg)
1.	Ammonia	R717	-33.35	132.3	113	-77.7	1.346	1370
2.	Carbon Dioxide	R744	-78.4	30.98	73.77	-56.6	1.3	349.5
3.	Nitrous Oxide	R744a	-88.47	36.37	72.45	-90.82	1.7949	379.43
4.	Ethane	R170	-88.84	32.12	48.72	-182.8	1.296	489.7
5.	Ethylene	R1150	-104	9.195	50.4	-169.16	1.358	482.5
6.	Propane	R290	-42.39	96.98	42.47	-187.1	1.184	426.1
7.	Propylene	R1270	-48	92.42	46.67	-185	1.211	439.5
8.	Isobutane	R600a	-12	134.7	36.4	-159.6	1.127	366.2

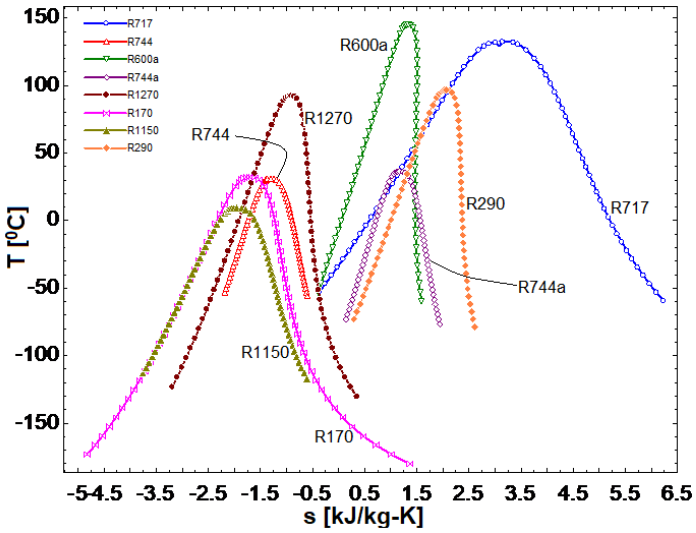

Figure 3.2: T-s diagrams of different natural refrigerants

3.3.2 Thermoeconomic Analysis

Analysis of refrigerants with Ammonia (R717) in HTC cycle

Simultaneous exergy and economic analyses are performed on six natural refrigerant couples each having R717 in HTC and R744, R744a, R290, R1270, R170 and R1150 in LTC. **Figure 3.3(a)** depicts the variations of exergy efficiency with evaporator temperature. It can be observed that exergy efficiencies of all pairs increase continuously with an increase in evaporator temperature. **Figure 3.3(b)** shows the variation of total cost rate with the evaporator temperature. Total system cost rates decrease with the increase in T_{evp}, until the T_{evp} becomes around -45^{0}C and then starts to increase. This is because, as the T_{evp} is increased while keeping T_{cond}, T_5 and ΔT_{cas} fixed, the temperature difference between the LTC evaporator and LTC condenser reduces and hence the pressure ratio also reduces which demands less compressor power and hence increases the exergy efficiency continuously. Due to the same phenomenon, the energy expenses of the compressor reduce but at the same time evaporator area increases with increase in T_{evp} which increases the capital and maintenance cost of the evaporator for the same cooling capacity. Due to these two opposite trends, the overall cost first decreases and then starts increasing after a certain

evaporator temperature. Similarly, increasing T_{cond} increases the temperature difference in HTC evaporator and condenser temperature and hence increases the power demand of HTC compressor resulting decrease in exergy efficiency. This increases the operating cost while on the other hand, with an increase in condenser temperature, the condenser area decreases, which reduces the capital and maintenance cost of the system. Due to these two conflicting events, the system cost initially decreases and then after a certain value of $T_{cond,}$ it starts to increase which can be observed in **Figure 3.3(c)**. A variation of exergy efficiency and total cost rate with LTC condenser temperature (T_5) is shown in **Figure 3.3(d).** It can be observed that exergy efficiency continuously decreases and the total cost rate continuously increases with the increase in T_5. It is attributed to the increase in temperature gap between LTC evaporator and LTC condenser temperatures which results in a rise in the power demand of LTC compressors. Although at the same time the power requirement of HTC compressor decreases due to a decrease in temperature gap between HTC evaporator and condenser temperature, this event get suppressed by the previous one and the exergy efficiency keeps on decreasing and the cost keeps on increasing. **Figure 3.3(e)** shows the variation of exergy efficiency and total cost with ΔT_{cas}. It can be observed that exergy efficiency continuously decreases and the cost rate continuously increases with ΔT_{cas}. This happens because, on increasing ΔT_{cas}, the temperature gap between HTC evaporator and condenser temperature increases while that of LTC remains constant. This increases the power demand of the HTC compressor and results in decreasing the exergy efficiency and increasing the cost. Therefore, R717-R290 and R717-R1270 refrigerant pairs show maximum exergy efficiency and minimum cost. R717-R744, R717-R744a, and R717-R170 show the moderate results and R714-R1150 shows the worst results with a minimum of exergy efficiency and maximum cost.

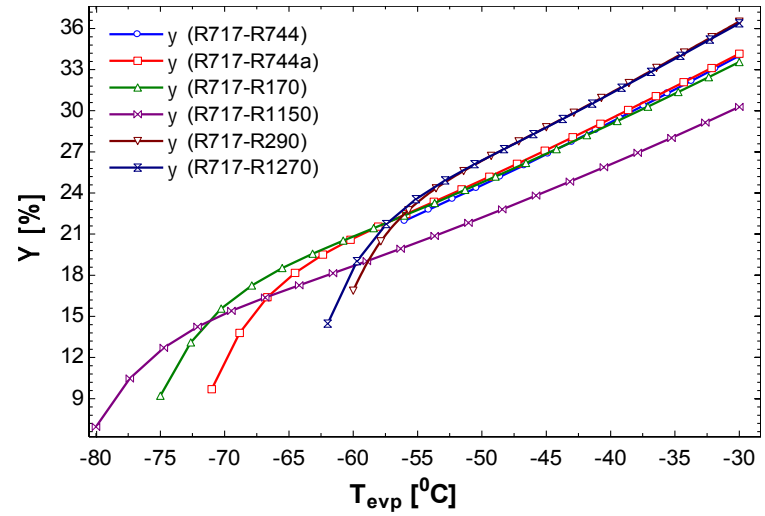
y (R717-R744)
y (R717-R744a)
y (R717-R170)
y (R717-R1150)
y (R717-R290)
y (R717-R1270)
Y [%]
T_evp [0C]

(a)

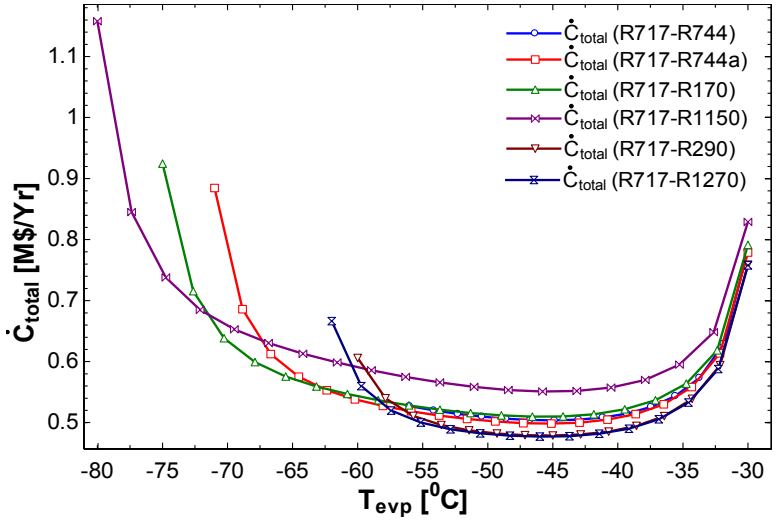
Ċtotal (R717-R744)
Ċtotal (R717-R744a)
Ċtotal (R717-R170)
Ċtotal (R717-R1150)
Ċtotal (R717-R290)
Ċtotal (R717-R1270)
Ċtotal [M$/Yr]
Tevp [0C]

(b)

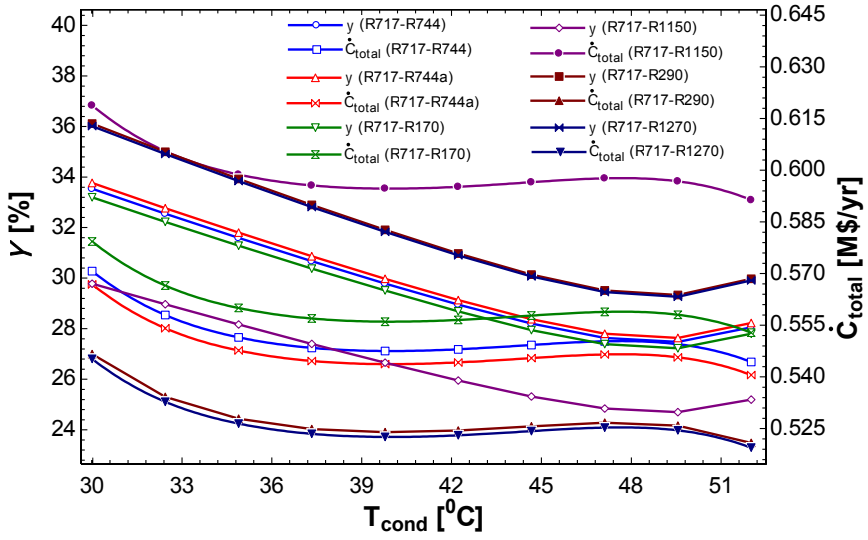
y (R717-R744)
Ċtotal (R717-R744)
y (R717-R744a)
Ċtotal (R717-R744a)
y (R717-R170)
Ċtotal (R717-R170)
y (R717-R1150)
Ċtotal (R717-R1150)
y (R717-R290)
Ċtotal (R717-R290)
y (R717-R1270)
Ċtotal (R717-R1270)
Y [%]
Ċtotal [M$/yr]
Tcond [0C]

(c)

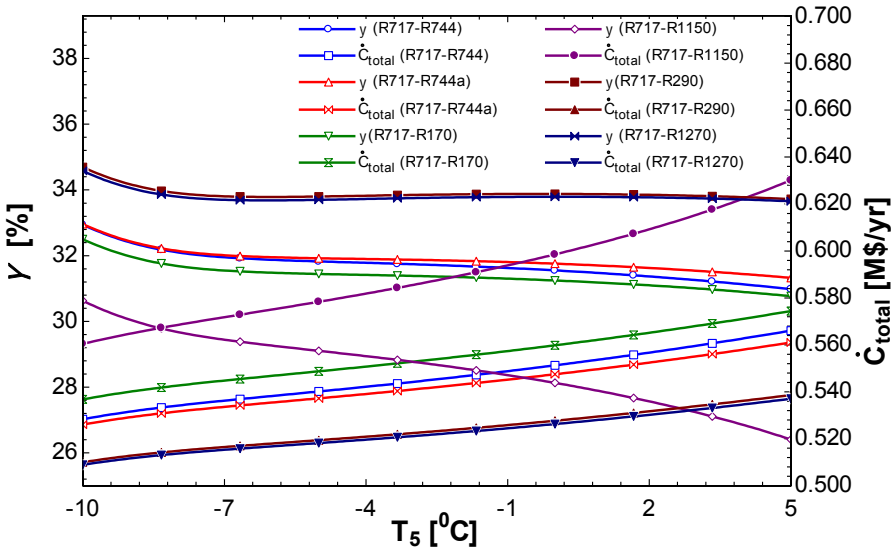

(d)

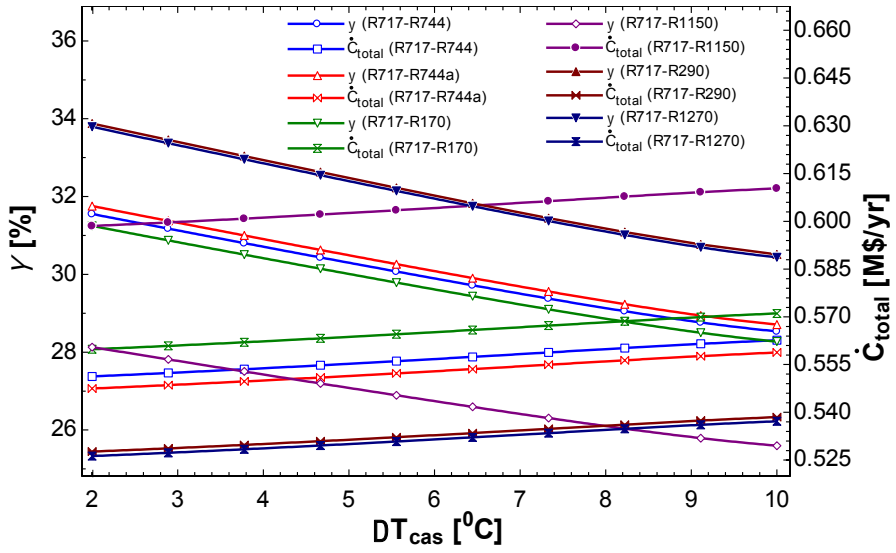

(e)

Figure 3.3: For refrigerant pairs with R717 as HTC refrigerant - **(a)** Variation of exergy efficiency with Evaporator temperature (T_{evp}), **(b)** Variation of total annualized cost of the system with Evaporator temperature (T_{evp}), **(c)** Variation of exergy efficiency and total cost rate with Condenser temperature (T_{cond})**, (d)** Variation of exergy efficiency and total cost rate with LTC condenser temperature(T_5), **(e)** Variation of exergy efficiency and total cost rate with Cascade temperature difference (ΔT_{cas})

Analysis of refrigerants with Propane (R290) in HTC cycle

Comparative exergy and economic analysis are performed on the aforementioned system using R290 as HTC refrigerant and R744, R744a, R170, R1150 and R1270 as

LTC refrigerants. In **Figure 3.4(a)**, The variation of exergy efficiency with T_{evp} is shown according to which, the exergy efficiency continuously increases because of the decrease in compressor power caused by a decrease in temperature gap in LTC with increasing T_{evp}. **Figure 3.4(b)** depicts the variation of total cost rate with T_{evp} and the total cost initially decreases and then starts to increase because of the two conflicting events, one is the decrease in LTC compressor operational charges and the second is the increase in capital and maintenance cost due to an increase in the evaporator area with T_{evp}. **Figure 3.4(c)** depicts that exergy efficiency decreases continuously with T_{cond} because the temperature gap of HTC increases with an increase in T_{cond} which increases the power requirement of the HTC compressor. The cost of the system initially decreases then starts to increase. This is because there are two major factors that affect the total cost, one is the compressor operating cost which decreases due to decline in power requirements and another is the increase in capital and maintenance cost of the condenser due to an increase in area with increasing T_{cond}. Initially, the first factor dominates while after a certain value of T_{cond} the later one dominates. **Figure 3.4(d)** displays the trend of exergy efficiency and overall cost with LTC condenser temperature (T_5) which is quite predictable. With an increase in T_5, the temperature gap of LTC increases but that of HTC decreases due to which the power consumption in LTC compressors increases and that of HTC compressors decreases due to these two opposite effects, the exergy efficiency first increases and after an optimal value of T_5, starts to decrease. But the trend of R1150 refrigerant seems to be continuously decreasing. Because the NBP of R1150 is very low and hence the optimum value of T_5 falls below the working range. Further, the cost of the system continuously increases because the increase in operating cost of the LTC compressors and cascade heat exchanger area dominates on the decrease in HTC compressor operating cost.

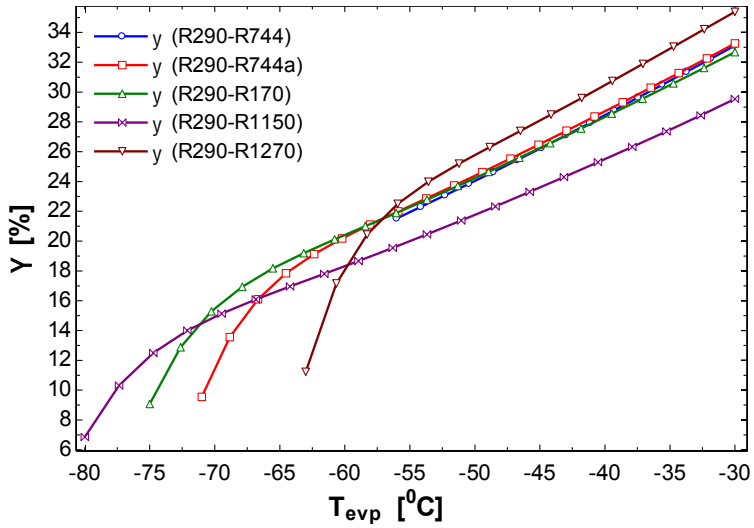
y (R290-R744)
y (R290-R744a)
y (R290-R170)
y (R290-R1150)
y (R290-R1270)
Y [%]
T_evp [0C]

(a)

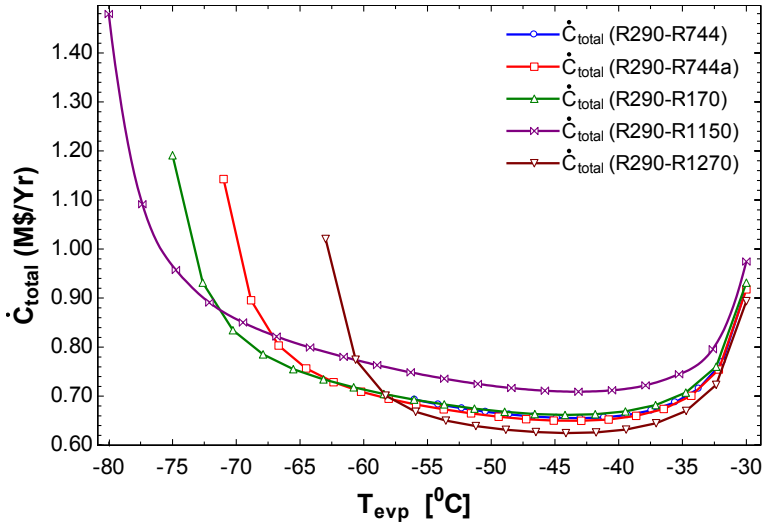
Ċtotal (R290-R744)
Ċtotal (R290-R744a)
Ċtotal (R290-R170)
Ċtotal (R290-R1150)
Ċtotal (R290-R1270)
Ċtotal (M$/Yr)
Tevp [0C]

(b)

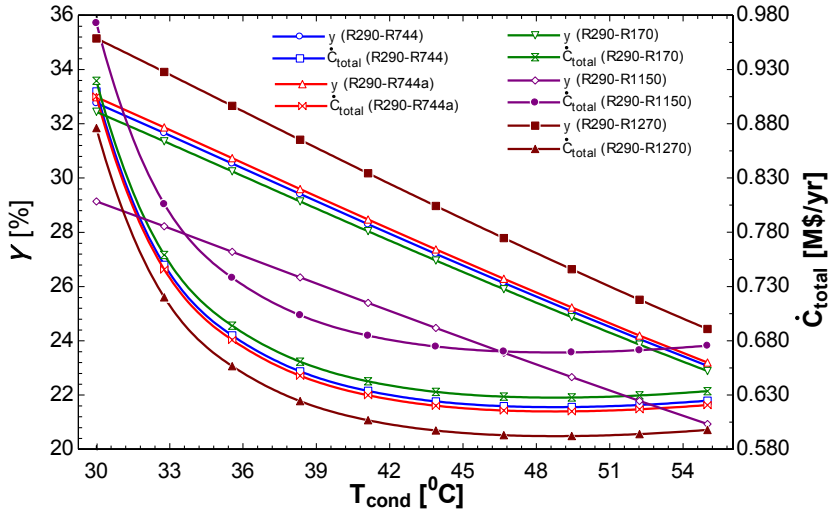
y (R290-R744)
Ċtotal (R290-R744)
y (R290-R744a)
Ċtotal (R290-R744a)
y (R290-R170)
Ċtotal (R290-R170)
y (R290-R1150)
Ċtotal (R290-R1150)
y (R290-R1270)
Ċtotal (R290-R1270)
Y [%]
Ċtotal [M$/yr]
Tcond [0C]

(c)

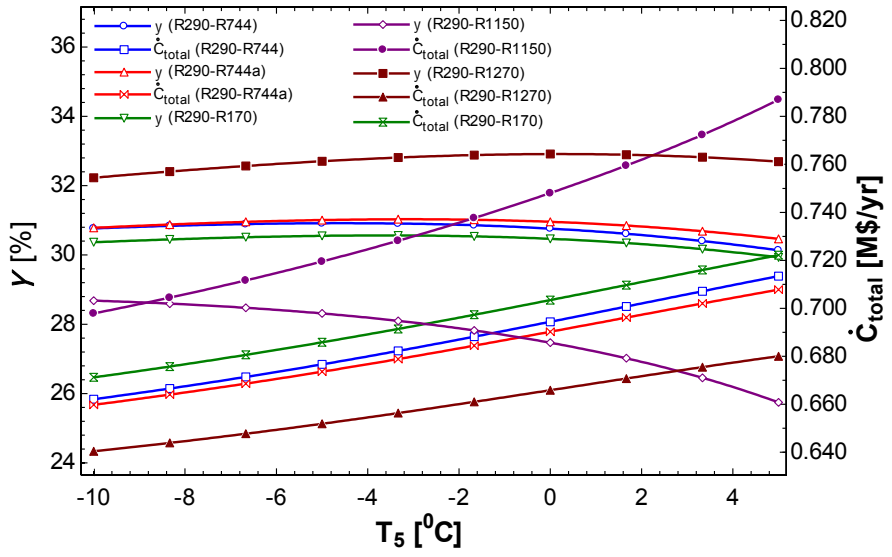

(d)

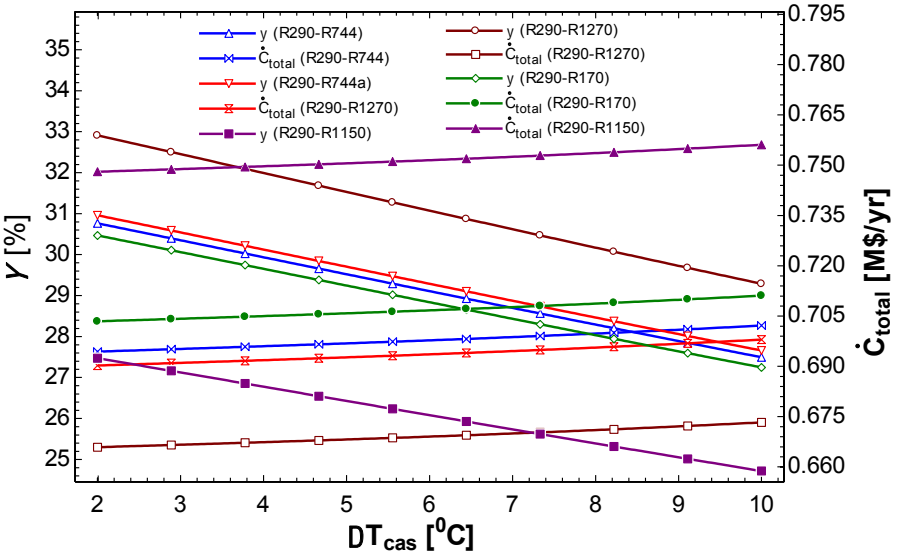

(e)

Figure 3.4: For refrigerant pairs with R290 as HTC refrigerant- **(a)** Variation of exergy efficiency with Evaporator temperature (T_{evp}), **(b)** Variation of total annualized cost of the system with Evaporator temperature (T_{evp}), **(c)** Variation of exergy efficiency and total cost rate with Condenser temperature (T_{cond})**, (d)** Variation of exergy efficiency and total cost rate with LTC condenser temperature(T_5), **(e)** Variation of exergy efficiency and total cost rate with Cascade temperature difference (ΔT_{cas})

In **Figure 3.4(e)** it can be seen that the exergy efficiency decreases and total cost increases with the increase in ΔT_{cas}. Both these trends are evident due to the fact that, with an increase in ΔT_{cas}, HTC compressor power requirement increases and that of

LTC compressor remain constant. In all the results, the exergy efficiency curve for the R290-R1270 pair is at the top and the cost curve is at the bottom. So, the comparative analysis reveals that R1270 as an LTC refrigerant is the best match for R290 as HTC refrigerant.

Analysis of refrigerants with Isobutane (R600a) in HTC cycle

In continuation with the study of natural refrigerant couples operating in the aforementioned system, R600a as HTC refrigerant has been paired with R744, R744a, R170, R1150, R290 and R1270 as LTC refrigerants and the relative exergy and economic performances are shown in **Figure 3.5**. The variation of exergy efficiency and total cost rate with T_{evp} has been investigated and the results are not different from the previous findings. Exergy efficiency continuously increases as shown in **Figure 3.5(a)** and the overall cost rate first decreases and then starts to increase as shown in **Figure 3.5(b)**. The reason is same as that has been mentioned earlier. In **Figure 3.5(c)**, a variation of exergy efficiency and total cost rate with T_{cond} is shown. The trend of system cost rate with T_{cond} for all pairs of refrigerants is similar to those shown in **Figure 3.3(c)** and **3.4(c)** but the exergy efficiencies first decrease and after T_{cond} around 53^0C, they start to increase for all refrigerant pairs. In **Figure 3.5(d)** the variation of exergy efficiency and overall cost rate with LTC condenser temperature (T_5) has been shown. The curves of exergy efficiency first increase and then decrease. This is because of the two facts affecting exergy efficiency. One is the increase in LTC compressor power and the other is the decrease in HTC compressor power with T_5. Initially, the first factor dominates over the second, while after an optimum value of T_5, the second factor overcomes the first one which results in such trends. The overall cost of the system continuously increases because the increase in LTC compressor operating cost dominates throughout the total cost rate.

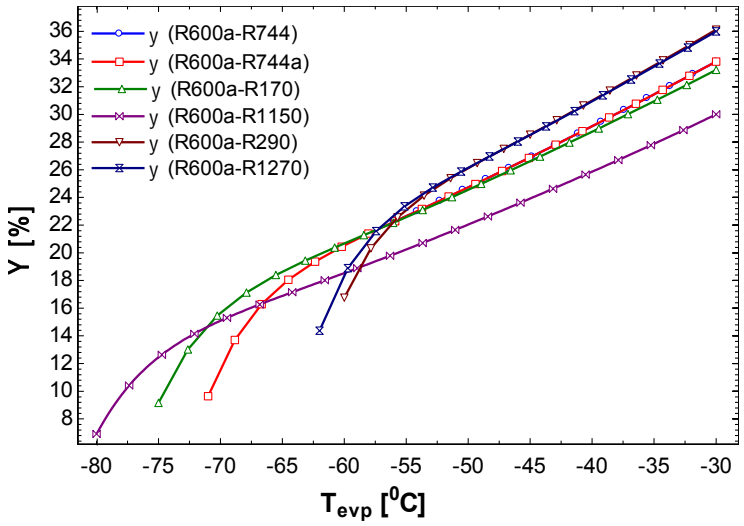
y (R600a-R744)
y (R600a-R744a)
y (R600a-R170)
y (R600a-R1150)
y (R600a-R290)
y (R600a-R1270)
Y [%]
T_evp [0C]

(a)

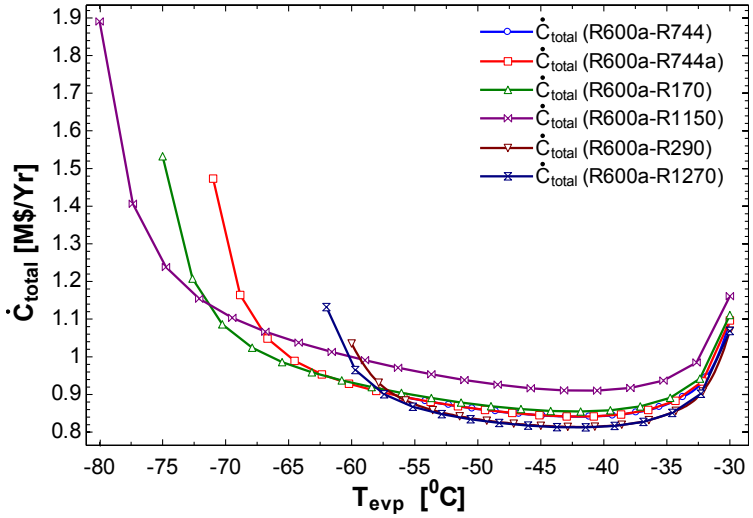
Ċtotal (R600a-R744)
Ċtotal (R600a-R744a)
Ċtotal (R600a-R170)
Ċtotal (R600a-R1150)
Ċtotal (R600a-R290)
Ċtotal (R600a-R1270)
Ċtotal [M$/Yr]
Tevp [0C]

(b)

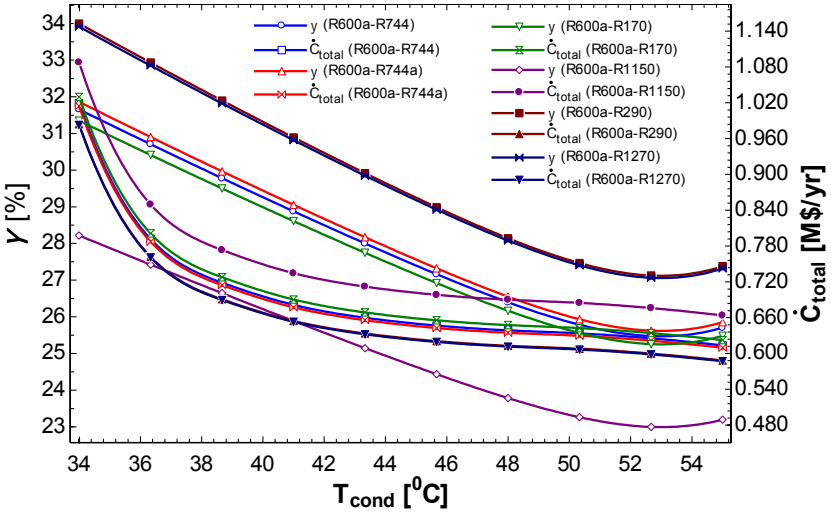
y (R600a-R744)
Ċtotal (R600a-R744)
y (R600a-R744a)
Ċtotal (R600a-R744a)
y (R600a-R170)
Ċtotal (R600a-R170)
y (R600a-R1150)
Ċtotal (R600a-R1150)
y (R600a-R290)
Ċtotal (R600a-R290)
y (R600a-R1270)
Ċtotal (R600a-R1270)
Y [%]
Ċtotal [M$/yr]
Tcond [0C]

(c)

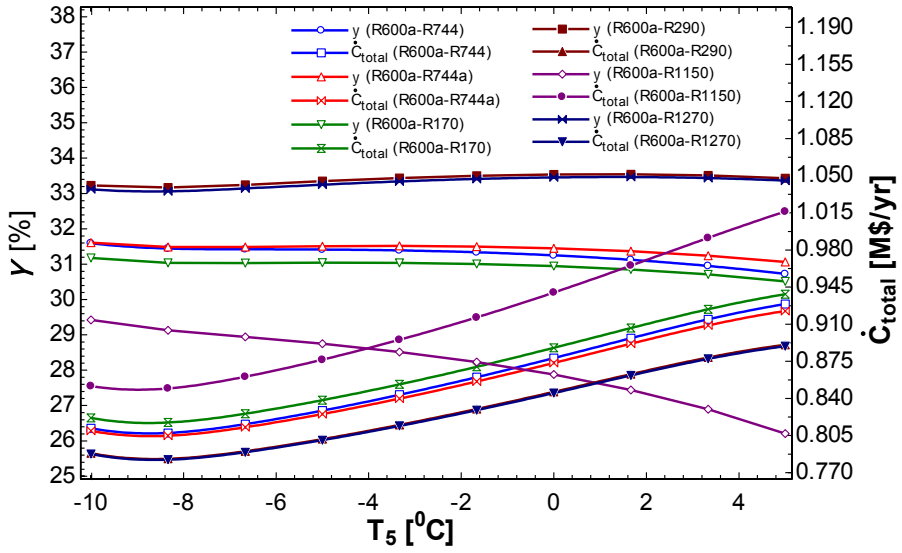

(d)

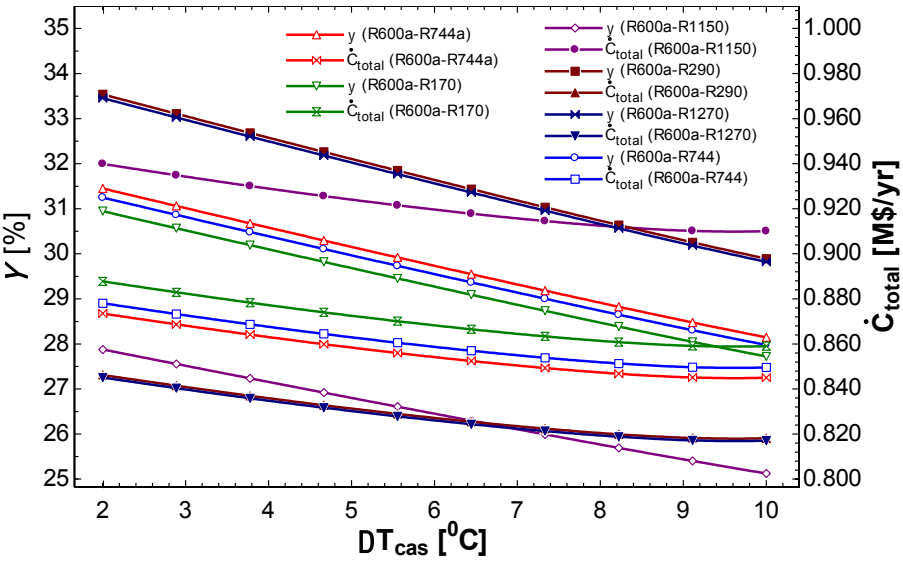

(e)

Figure 3.5: For refrigerant pairs with R600a as HTC refrigerant- **(a)** Variation of exergy efficiency with Evaporator temperature (T_{evp}), **(b)** Variation of total annualized cost of the system with Evaporator temperature (T_{evp}), **(c)** Variation of exergy efficiency and total cost rate with Condenser temperature (T_{cond})**, (d)** Variation of exergy efficiency and total cost rate with LTC condenser temperature(T_5), **(e)** Variation of exergy efficiency and total cost rate with Cascade temperature difference (ΔT_{cas})

The exergy efficiency curve of R1150 seems to be continuously decreasing, as the value of optimum T_5 falls below the operating range of T_5 considered in this study due to low NBP. The exergy efficiency and total cost rate continuously decrease with ΔT_{cas} as shown in **Figure 3.5(e)**. The reason is the hike in HTC compressor power with an

increase in ΔT_{cas} as discussed earlier. It can be noticed from all the four plots that refrigerant R290 possesses the highest exergy efficiency and minimum cost rate. So it can be concluded that R290 is the best match for LTC when paired with R600a as HTC refrigerant.

Comparative analysis of R717-R290, R290-R1270 and R600a-R290 refrigerant couples

From the above analysis, it is evident that R717-R290, R290-R1270, and R6004-R290 are the best refrigerant pairs from exergy and economic point of view. So, they are compared based on different thermodynamic performance parameters and total system cost rates to figure out the best of them. In **Figure 3.6(a)** the variation of system COP and total exergy destruction with T_{evp} has been plotted to investigate the first and second law performances of the system using these three refrigerant pairs. It can be seen that for all the three refrigerant pairs, COP continuously increases and exergy destruction decreases with T_{evp}. This is because of the decrease in LTC compressor's power demands due to the decrease in the LTC temperature gap. It can easily be seen that the refrigerant pair R717-R290 possesses the highest COP and least exergy destruction throughout the working range of T_{evp}. R290-R1270 shows the worst results and R600a-R290 shows moderate results. To compare the exergy and economic performances, the variation of exergy efficiency and total cost rate has been plotted with T_{evp} as shown in **Figure 3.6(b)**. The trends are same as in **Figures 3.3(a)**, **3.4(a)** and **3.5(a)** and the reasons behind these trends have already been discussed while explaining these figures in earlier sections. Here the purpose of introducing these plots is to compare these three refrigerant couples on the same platform and it can be seen that R717-R290 shows the highest exergy efficiency and minimum cost rate for each value of working T_{evp}. R600a-R290 is thermodynamically better but economically inferior than R290-1270.

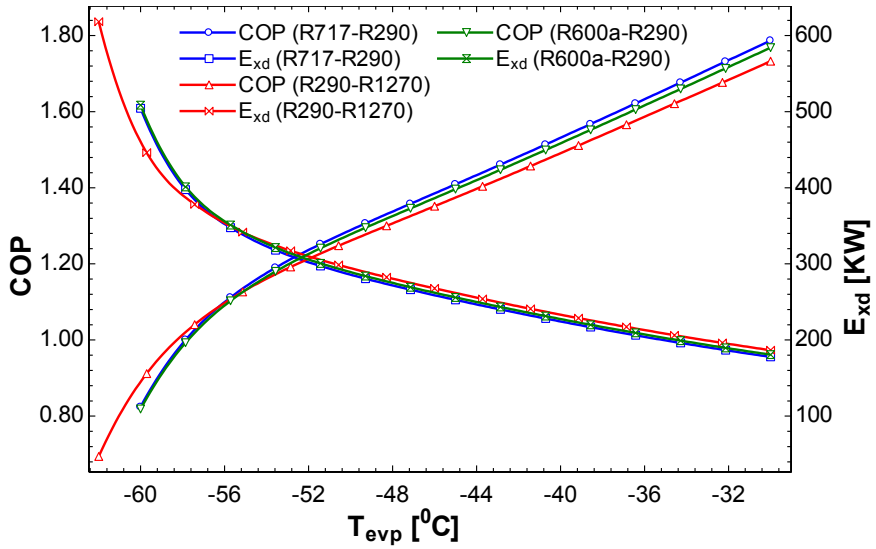

(a)

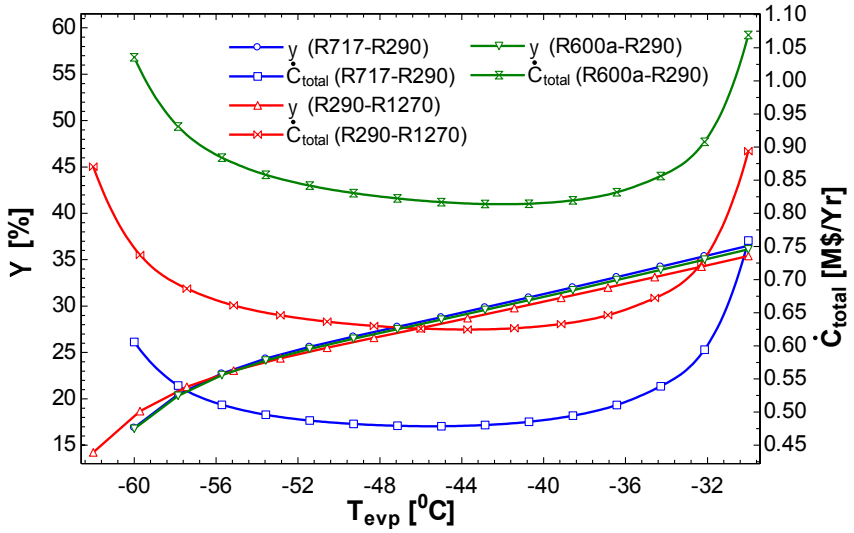

(b)

Figure 3.6: (a) Variation of COP and total exergy destruction with Evaporator temperature (T_{evp}), **(b)** Variation of exergy efficiency and total cost with Evaporator temperature (T_{evp})

LTC condenser temperature (T_5) plays an important role in the performance of the system because it affects both the cycle performances in an opposite manner. So, the exergy efficiency and COP initially increase and after an optimal value of T_5, it starts to decrease. The total cost rate continuously increases because the power requirements of LTC compressors increase more rapidly than that of a decrease in HTC compressor

power. **Figure 3.7(a)** shows the curves of exergy efficiency and total cost rates with T_5 and it can be observed that again R717-R290 refrigerant pair possesses the maximum exergy efficiency and minimum total cost rate for all specified values of T_5. While R600a-R290 is better than R290-R1270 from an exergy point of view but is worst from

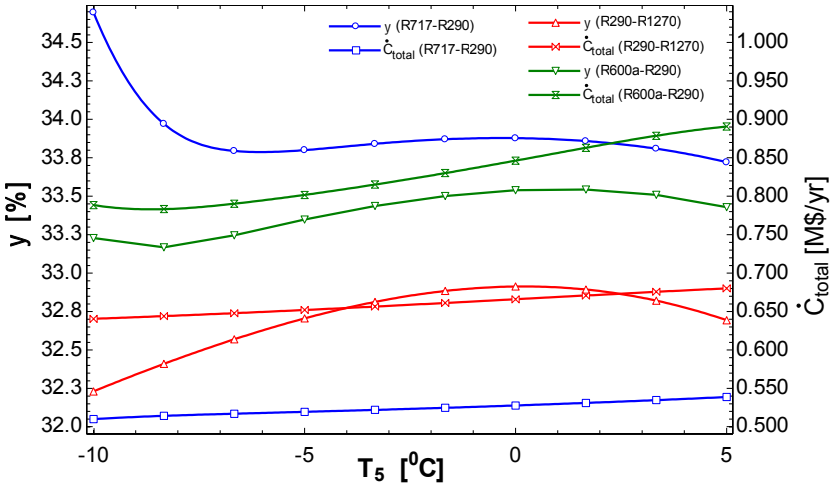

(a)

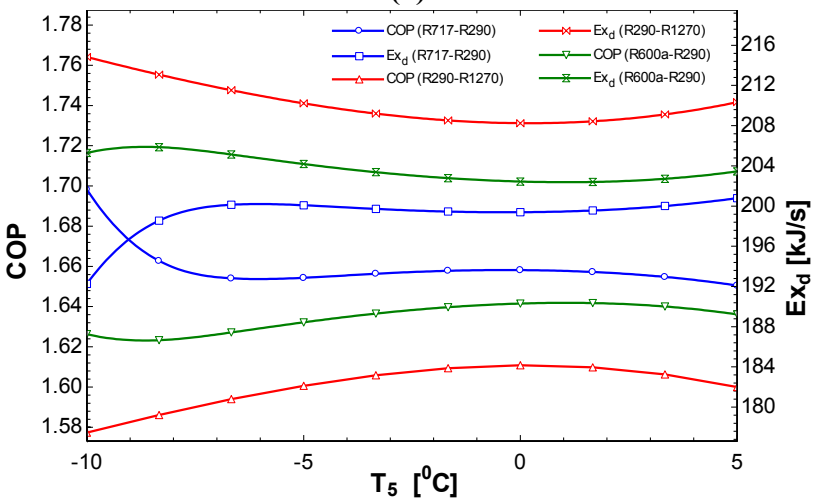

(b)

Figure 3.7: (a) Variation of exergy efficiency and total cost rate with LTC condenser Temperature (T_5) **(b)** Variation of COP and total exergy destruction with LTC condenser Temperature (T_5)

an economic point of view. Just like exergy efficiency, COP initially increases and then decreases and exergy destruction initially decreases and then increases after a certain value of the T_5 as shown in **Figure 3.7(b)**. The subcooling parameter '*a*' governs the

degree of subcooling of the refrigerant coming out from the cascade heat exchanger. The change in the value of '*a*' affects the system performance and cost significantly. The variation of exergy efficiency and total cost rate are shown in **Figure 3.8**. Both the exergy efficiency and cost increase with the subcooling parameter '*a*'. This is quite obvious because as the value of '*a*' increases subcooling at state 7 increases. Since the cooling load is fixed, more subcooling reduces the difference of specific enthalpies through the evaporator which results in a reduction of the mass flow rate through the LTC compressor I and the compressor power. So, the performance of LTC increases which results in an increase in the exergy efficiency of the system but at the same time, more amount of subcooling requires more surface area in the intercooler with indirect subcooler which increases the capital as well as maintenance cost of the LTC intercooler with indirect subcooler.

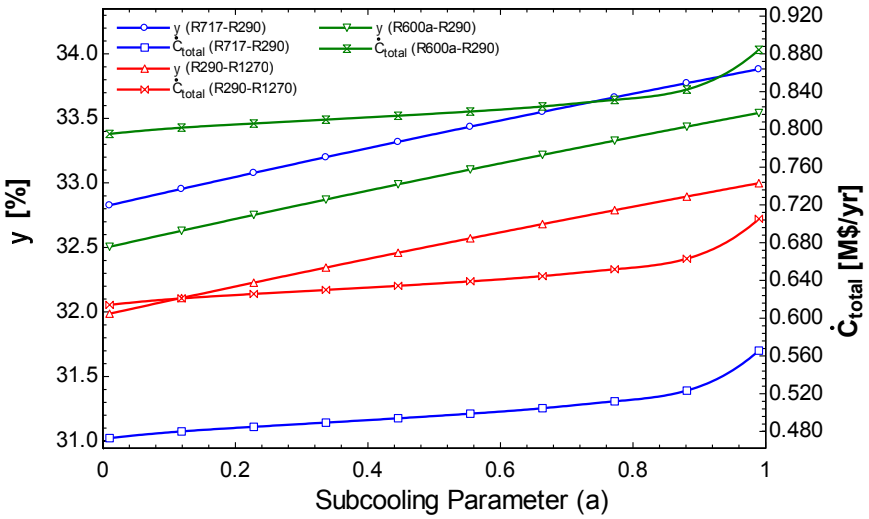

Figure 3.8: Variation of Exergetic efficiency and total cost with De-superheating parameter

The variation of COP with subcooling parameter '*a*' and de-superheating parameter '*b*' for the three refrigerants couples is shown in **Figure 3.9**. For each refrigerant couple, COP curves are shown for three different values of de-superheating parameters (*i.e.* for *b*=0, *b*=0.5, and *b*=1). Results show that COP continuously rises with subcooling

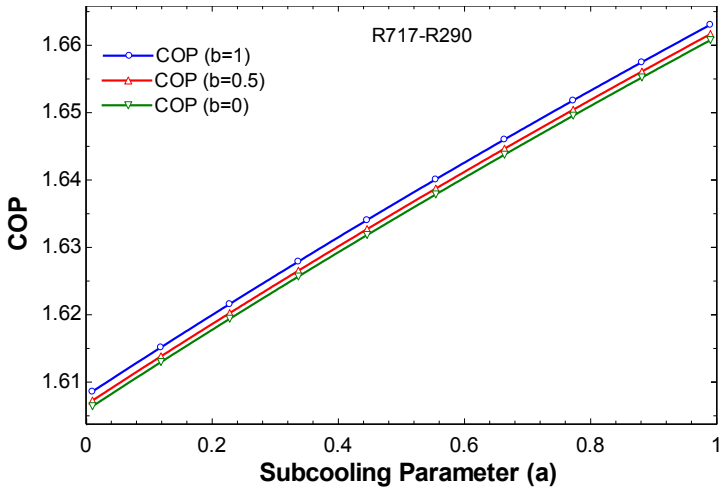

(a)

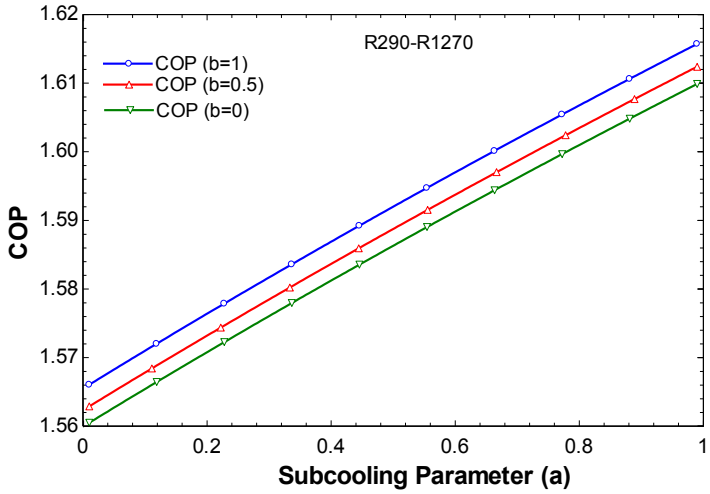

(b)

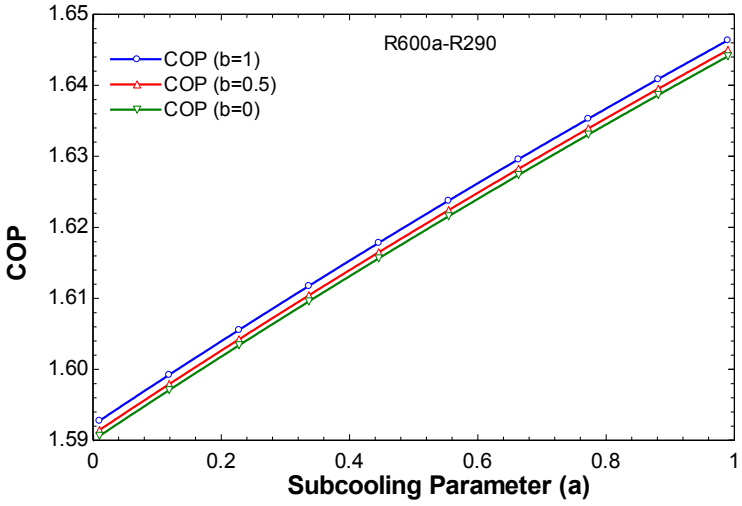

(c)

Figure 3.9: Variation of COP with De-superheating parameter at different values of subcooling parameters for **(a)** R717-R290, **(b)** R290-R1270, **(c)** R600a-R290 refrigerant pairs

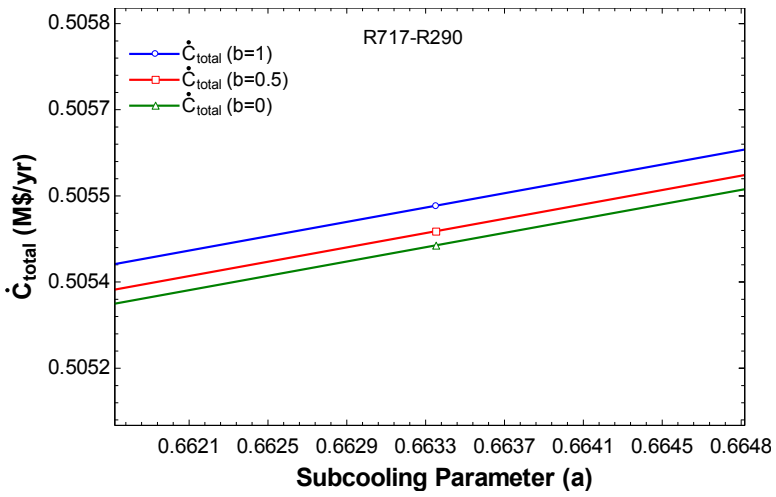

(a)

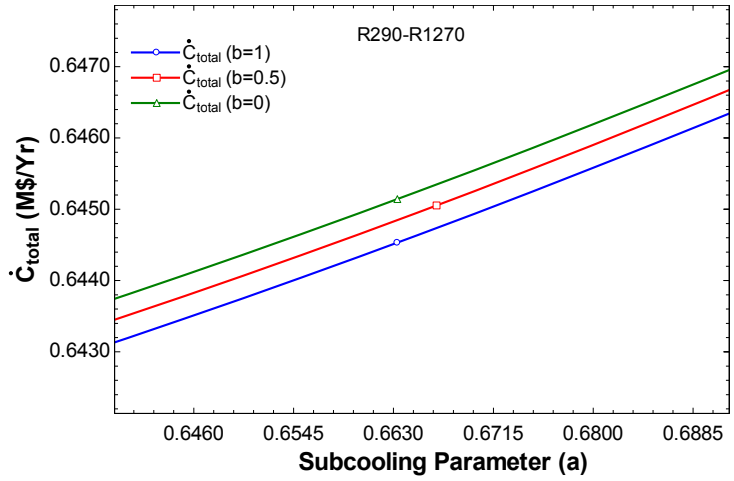

(b)

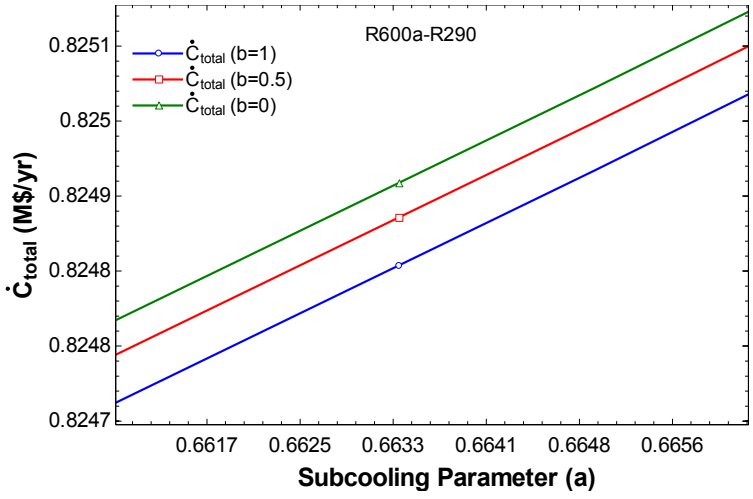

(c)

Figure 3.10: Variation of total cost rate with de-superheating parameter at different values of subcooling parameters for **(a)** R717-R290, **(b)** R290-R1270, **(c)** R600a-R290 refrigerant pairs

parameter for all the three refrigerant pairs for all the values of de-superheating parameters and, at a given value of '*a*', the value of COP for different values of '*b*' is in the order of COP(*b*=0)<COP(*b*=0.5)<COP(*b*=1) for all the three refrigerant couples. This is because subcooling with fixed cooling load reduces the demand of LTC compressor I while de-superheating reduces the power demand of LTC compressor II and both these phenomena contribute to an increase in overall system COP.

Figure 3.10 shows the variation of total cost rate with de-superheating parameter for the three refrigerant pairs for different values of subcooling parameters (*i.e.* for *b*=0, *b*=0.5 and *b*=1). Total cost rate continuously increases with '*a*' for all values of '*b*' for the three refrigerant pairs but, for R717-R290 couple, at a given value of '*a*', $C_{total}(b=0)<C_{total}\ (b=0.5)<C_{total}(b=1)$ as shown in **Figure 3.10(a)**. For R290-R1270 couple, at a given value of '*a*', $C_{total}(b=0)>C_{total}(b=0.5)>C_{total}(b=1)$ as shown in **Figure 3.10(b)** and for R600a-R290, at a given value of '*a*', $C_{total}(b=0)<C_{total}(b=0.5)<C_{total}(b=1)$ as shown in **Figure 3.10(c)**. This is because the de-superheating increases the intercooler surface area while on the other hand, it decreases the energy expenses of LTC compressor II. These opposite effects of increasing the de-superheating parameter increase the total cost rate in the case of R717-R290 decrease it in the case of R290-R1270 and keep unaffected in the case of R600a-R290 refrigerant couple.

To compare the response of optimum LTC condenser temperature (T_5) by using the three refrigerant couples, a graph showing optimum values of T_5 with T_{evp} has been plotted as shown in **Figure 3.11**. It can be seen that R600a-R290 refrigerant couple possesses the highest optimum T_5. The optimum value of T_5 for R290-R1270 refrigerant couple dominates over that of R717-R290 below T_{evp} being around -35 ^{0}C

and after this R717-R290 dominates over R290-R1270. This is because, in comparison to R717-R290, R290-R1270 refrigerant couple possesses a slower rate of increase in optimum T_5 with respect to T_{evp}.

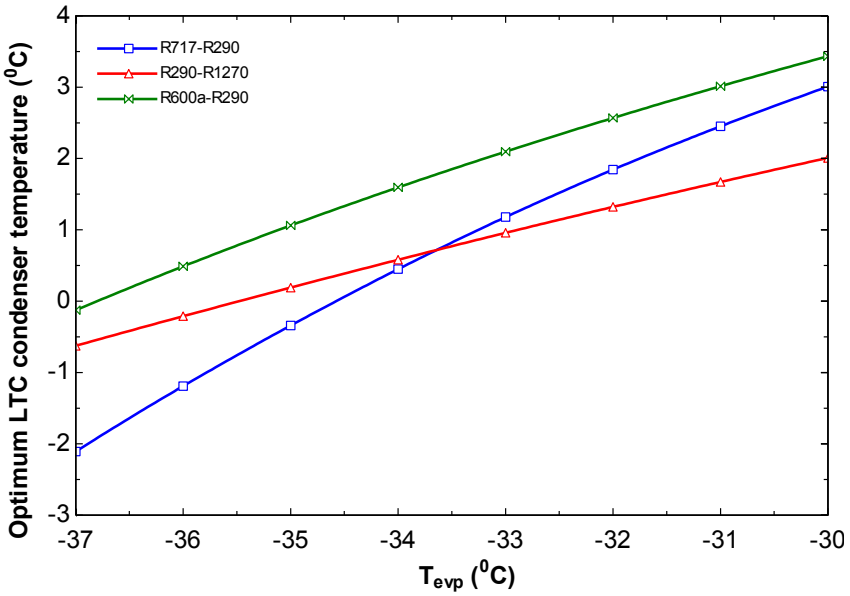

Figure 3.11: Variation Of optimum LTC condenser temperature with Evaporator temperature (T_{evp})

Figure 3.12 shows the variation of LTC compressor I discharge temperature (T_2) and compressor II discharge temperature (T_4) with T_{evp}. As can be seen that T_2 initially decreases and then starts to increase, while T_4 continuously decreases with T_{evp} for all the three refrigerant couples. This is attributed to the fact that the discharge temperature depends on refrigerant property and the compressor's compression ratio. When LTC refrigerant is fixed, the compression ratio is the only parameter on which discharge temperature depends. This compression ratio for LTC compressor I is the geometric mean of evaporator and LTC condenser pressure. Since the LTC condenser pressure is fixed, the intermediate pressure also increases with an increase in evaporator temperature. Initially, the rate of increase in intermediate pressure is less than that of the evaporator temperature and pressure and hence the compression ratio for the LTC compressor I decrease, while after a certain value of T_{evp}, this ratio increases due to a

rapid increase in intermediate pressure which results in a slight increase in T_2. Whereas the compression ratio for LTC compressor II continuously decreases because the LTC condenser temperature pressure is fixed and hence the discharge temperature of LTC compressor II continuously decreases. It can be seen that R290-R1270 possesses maximum values of T_4 and T_2 for all values of T_{evp} and R600a-R290 and R717-R290 gives the same value of T_4 and T_2 because both refrigerant pairs have R290 as LTC refrigerants.

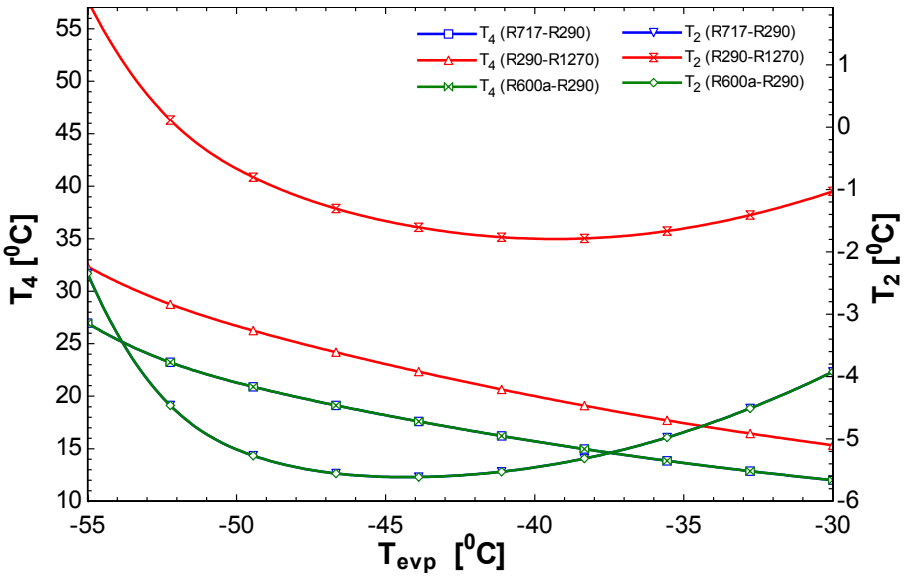

Figure 3.12: Variation of LTC compressor I discharge temperature (T_2) and LTC compressor II discharge temperature (T_4) with Evaporator Temperature (T_{evp})

Refrigerant couple R717-R290 has been proven to be the most powerful and economical refrigerant couple among all the 17 refrigerant pairs while R290-R1270 and R600a-R290 have shown mixed results.

3.3.3 Optimization:

A thermodynamics optimization has also been performed for the three pair of refrigerants which not only reveals the optimum operating conditions but also give an order of preference among the three refrigerant pairs. COP has been selected as the objective function to be maximized and T_{evp}, T_{cond}, T_5, ΔT_{cas}, a and b are six design

variables of the optimization problem. The range of design variables is presented in **Table 3.7**.

Table 3.7: Range of operating conditions for optimization

Design variables	Bounds
Evaporator Temperature $(\boldsymbol{T_{evp}})$	$-64^0C \leq T_{evp} \leq -30^0C$
Condenser Temperature $(\boldsymbol{T_{cond}})$	$30^0C \leq T_{cond} \leq 56^0C$
Temperature difference in cascade heat exchanger $(\boldsymbol{\Delta T_{cas}})$	$2^0C \leq \Delta T_{cas} \leq 4^0C$
LTC condenser temperature $(\boldsymbol{T_5})$	$-9^0C \leq T_5 \leq 1^0C$
Sub-cooling parameter $(\boldsymbol{a})$	$0 \leq a \leq 1$
De-superheating parameter $(\boldsymbol{b})$	$0 \leq b \leq 1$

Conjugate direct method which is a very efficient tool for this purpose, is used for the optimization and the results are presented in **Table 3.8**. The results reveal that optimum COP of R290-R1270 couple is 2.8% less than that of R717-R290 and the cost rate is 40.84% higher while the optimum COP of R600a-R290 is 5.37% lower than R717-R290 and the cost rate is 161.71% higher. This clearly states that R717-R290

Table 3.8: Results of thermodynamic optimization for the three refrigerant pairs:

Parameters	Optimum Values		
	R717-R290	R290-R1270	R600a-R290
T_{evp} (^{0}C)	-30	-30	-30
T_{cond} (^{0}C)	30	30	33.53
T_5 (^{0}C)	0.9256	-1.007	2.874
ΔT_{cas} (^{0}C)	2	2	2
a	0.9963	0.9961	0.9963
b	1	1	1
p_2 (kPa)	286.2	347.4	294.7
A_{evp} (m^2)	4438	4438	4438
A_{cond} (m^2)	926.1	4281	17496
A_{cas} (m^2)	104.1	91.06	104
$\dot{E}x_d(kW)$	158.8	166.4	173.5
$\dot{W}_{total}$ (kW)	260.9	268.5	275.6
COP	1.917	1.862	1.814
ψ (%)	39.14	38.03	37.06
$\dot{C}_{total}(\$/yr)$	836395	1178000	2189000

refrigerant couple not only delivers pretty good thermodynamic performances but excellent cost-effectiveness when they are used in the aforementioned system.

Since compressors and fans are the energy input devices, their total power consumption has been considered as the total power input to the system while the cooling output is taken as 500 kW for all the three refrigerant couples. The heat rejected through the condenser is considered as a loss of power at the output. The distribution of energy input and output as a percentage of the total energy supplied in different components at thermodynamic optimal conditions for the three refrigerant couples is shown in **Figure 3.13**.

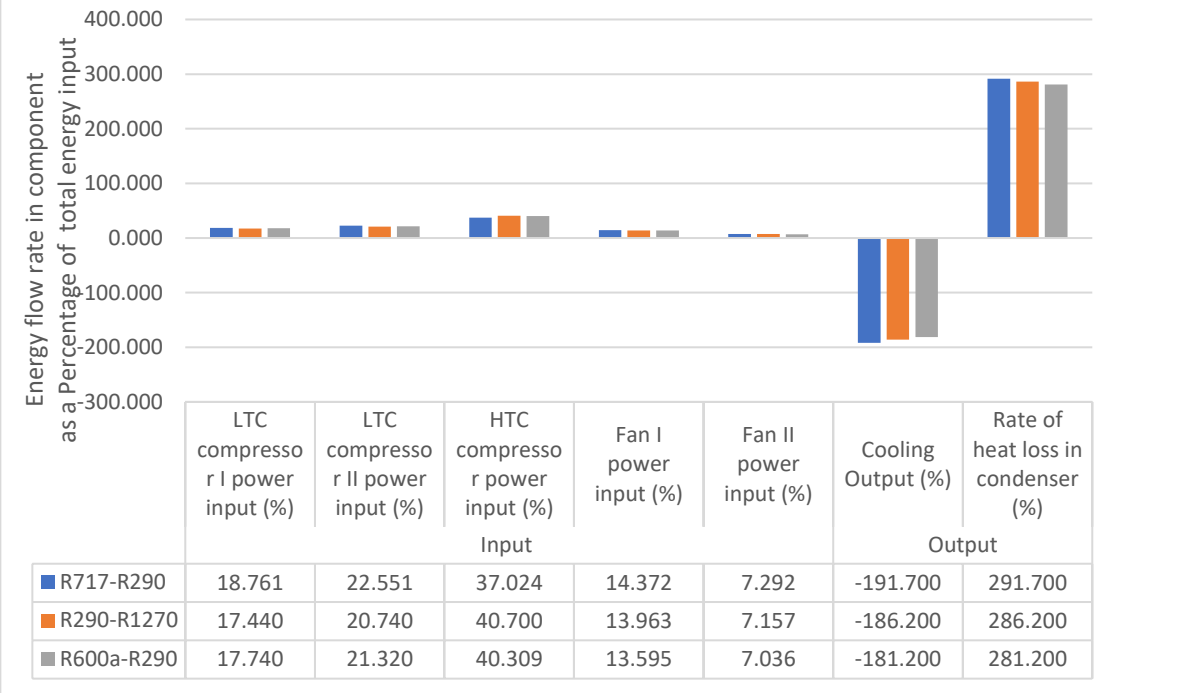

	Input					Output	
	LTC compressor I power input (%)	LTC compressor II power input (%)	HTC compressor power input (%)	Fan I power input (%)	Fan II power input (%)	Cooling Output (%)	Rate of heat loss in condenser (%)
R717-R290	18.761	22.551	37.024	14.372	7.292	-191.700	291.700
R290-R1270	17.440	20.740	40.700	13.963	7.157	-186.200	286.200
R600a-R290	17.740	21.320	40.309	13.595	7.036	-181.200	281.200

Figure 3.13: Distribution of energy input and output in different components.

It can be seen that the power consumption is relatively higher in LTC compressors and fans but lower in HTC compressor for R717-R290 refrigerant couple. This is because R717 in HTC has relatively high latent heat of vaporization which results in a mass flow rate of 0.54 kg/s after evaporation in CHX which is approximately one-fourth of the corresponding values for other two pairs (2.064 kg/s for R290-R1270 and 2.228

kg/s for R600a-R290). Due to this fact the volume handled by HTC compressor decreases and so the power demand. While R290 responds oppositely due to relatively lower latent heat and hence the power consumption of LTC compressors becomes higher. On the other hand the cooling output of R717-R290 is the highest (191.7%) which leads to highest COP of 1.917.

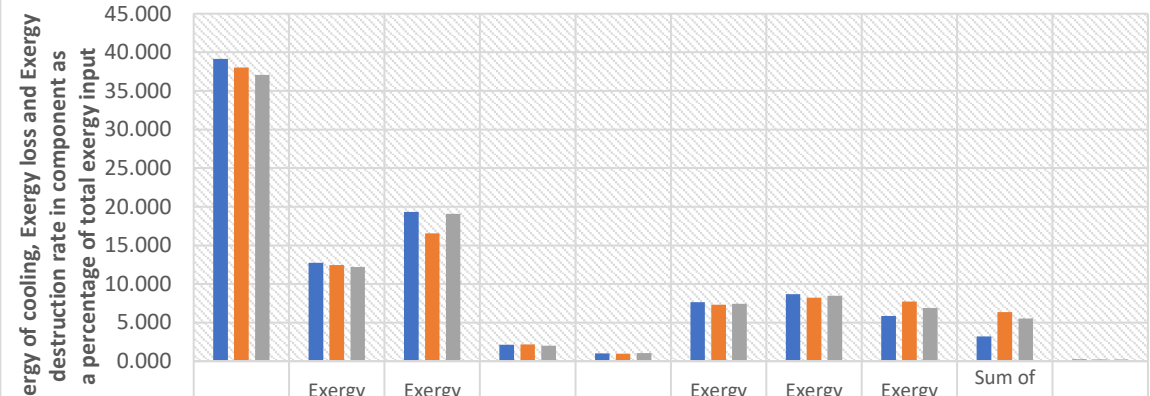

	Exergy of cooling (%)	Exergy destruction in Evaporator+Fan I (%)	Exergy destruction in Condenser+Fan II (%)	Exergy destruction in CHX (%)	Exrgy destruction in FIIS (%)	Exergy destruction in LTC comp I (%)	Exergy destruction in LTC comp II (%)	Exergy destruction in HTC comp (%)	Sum of Exergy destructions in other components (%)	Exergy loss in condenser (%)
R717-R290	39.140	12.740	19.330	2.127	1.021	7.638	8.679	5.863	3.220	0.242
R290-R1270	38.030	12.442	16.572	2.173	0.951	7.295	8.227	7.733	6.339	0.238
R600a-R290	37.060	12.208	19.092	2.025	1.056	7.431	8.468	6.901	5.532	0.227

Figure 3.14: Distribution of exergy of cooling, exergy loss and exergy destruction rates as a percentage of exergy input.

Figure 3.14 depicts that, how total exergy input is distributed in exergy of cooling output, exergy destructions in different components and exergy loss. The results correspond to thermodynamic optimal conditions and respective values are calculated as a percentage of total exergy input which is the sum of exergies added to the system in the form of rates of work input to the compressors and fans. It is evident that the maximum part of input exergy (39.14% for R717-R290, 38.030% for R290-R1270 and 37.060% for R600a-R290) is reflected as exergy of cooling which is also output exergy and hence the exergy efficiencies for three couples turn to be 39.14%, 38.03%, and 37.06% respectively. Exergy destruction is maximum in condenser and Fan II due to

the irreversibility involved with fan and temperature difference between the refrigerant and air streams in the condenser. The same is the reason with evaporator and Fan I. The exergy destructions associated with compressors are almost the similar except the HTC compressor of R717-R290. The reason is again the less mass flow rate of R717 working in HTC as discussed earlier. Exergy destructions in CHX and FIIS are very nominal due to heat transfer with low-temperature difference and insignificant in remaining components like expansion valve and flash tank.

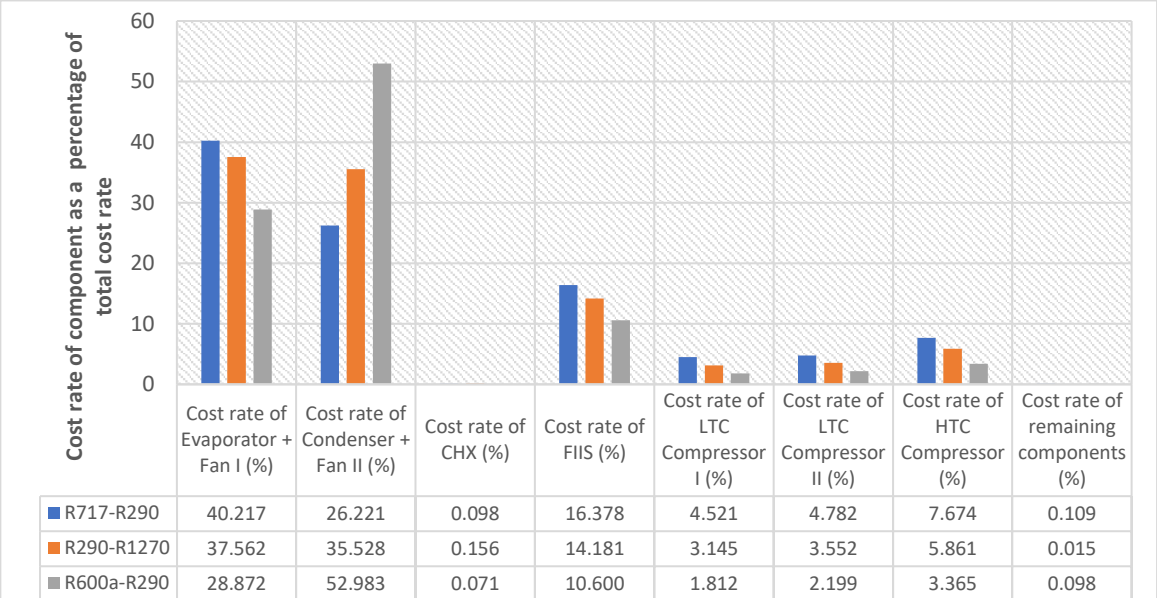

	Cost rate of Evaporator + Fan I (%)	Cost rate of Condenser + Fan II (%)	Cost rate of CHX (%)	Cost rate of FIIS (%)	Cost rate of LTC Compressor I (%)	Cost rate of LTC Compressor II (%)	Cost rate of HTC Compressor (%)	Cost rate of remaining components (%)
R717-R290	40.217	26.221	0.098	16.378	4.521	4.782	7.674	0.109
R290-R1270	37.562	35.528	0.156	14.181	3.145	3.552	5.861	0.015
R600a-R290	28.872	52.983	0.071	10.600	1.812	2.199	3.365	0.098

Figure 3.15: Cost rates of different components as a percentage of total cost rate.

Figure 3.15 shows the percentage share of components in the rate of expenditure of the overall plant. It can be seen that in all the components, maximum expenditure belongs to R717-R290 except the condenser where the trend is opposite. The maximum cost rate of condenser belongs to R600a-R290 and the minimum is possessed by R717-R290. Here the reason is the high amount of heat transferred by the condenser and the low value of LMTD in case of R600a-R290 refrigerant couple. The mass flow rate through all three compressors is maximum for this case which results in the highest power consumption of 218.72 kW by the compressors which is approximately 7% higher (204.37kW) than that of R717-R290 refrigerant couple. This energy, along with

fan's power and cooling load has to be rejected by the condenser. Further, the HTC compressor discharge temperature for R600a-R290 is 35.27 ^{0}C while it is 84.57 ^{0}C for R717-R290 refrigerant couples. Owing to this the value of LMTD of the condenser (1.098 ^{0}C) for R600a-R290 is lower than that of other couples. Due to excessive heat transfer and lower value of LMTD, the condenser surface area requirement increases and hence the cost of the condenser for R600a-R290 becomes highest. Since all the costs are expressed on a percentage basis, the cost of remaining components for the other two cases becomes higher to compensate for the cost of the condenser.

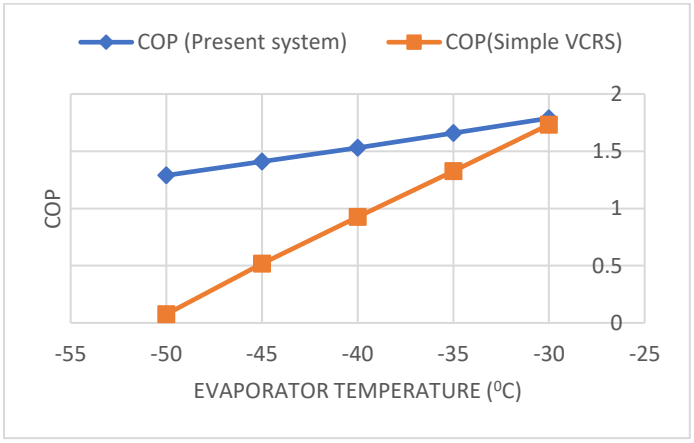

(a)

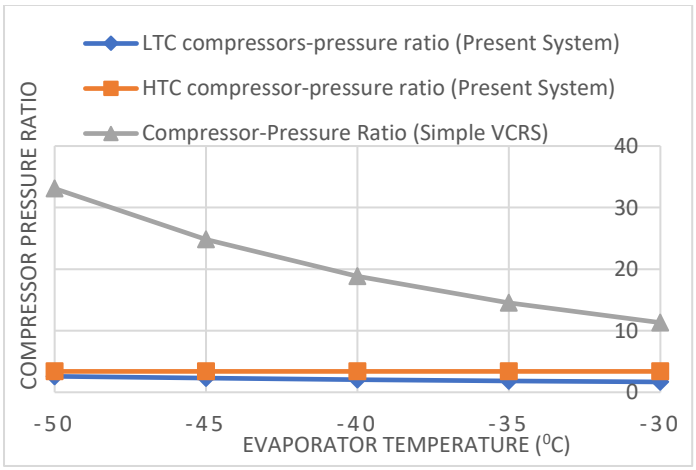

(b)

Figure 3.16 (a) Comparison of COP variations in present system with simple VCRS, **(b)** Comparison of the compressor pressure ratios in present system with simple VCRS.

Figure 3.16 presents a comparative analyis of present system with a single stage VCRS. Ammonia has been taken as refrigerant and equation 4 has been used for overall efficiency estimation of single stage VCRS compressor. It can be seen in **Figure 3.16(a)** that, as the evaporator temperature increases, COP of the single stage VCRS approaches to the COP of present system but it does not meet or exceed the present system's COP. Even at -30 ^{0}C of T_{evp}, COP of present system is more than that of single stage VCRS. In case of single stage VCRS there is a problem of high pressure ratio involved in the compression process which adversely influences the compressor's size, cost and life. At -30 ^{0}C evaporator temperature, the compression ratio of both LTC compressors of present system is 1.682 and that of HTC compressor is 3.391, while for the same operating conditions of evaporator and condenser temperatures, compression ratio of single stage VCRS is 11.31 which is 575% higher than LTC compressor and 233% higher than HTC compressor as shown in **Figure 3.16(b)**. This makes the present system more thermodynamically superior than that of a single stage VCRS.

Table 3.9 presents the total investment in a fish cold storage in its complete life time (G), the annual income ($\dot{R}$) earned from it and the payback period (t). As can be seen that the payback period of R717-R290 is minimum, therefores this is the best refrigerant couple out of the three, while R290-R1270 is better than R600a-R290.

Table 3.9: The payback period of system for the three refrigerant couples

S. No.	Refrigerant couple	G (\$)	$\dot{R}$ ($\$/yr$)	t (yrs)
1	R717-R290	18818887	3530264	5.33
2	R290-R1270	26505000	3530264	7.50
3	R600a-R290	49252500	3530264	13.95

3.2 Mathematical Modelling for exergoeconomic Analysis

An exergy aided economic analysis, also known as exergoeconomics is a significant tool to analyse and optimize the thermo-economic performance of systems. The concept of exergoeconomics is based on the principle of cost balance and has been used in many studies for getting a better system design under thermo-economic framework. In mathematical modelling for exergoeconomic analysis component wise expressions for exergy destructions are formed in terms of fuel and product exergy rates.

The product and fuel exergy for the overall system can be estimated as:

$$\dot{E}x_P = (\dot{E}x_{ca,e} - \dot{E}x_{ca,i}) \tag{3.32}$$

$$\dot{E}x_F = \dot{W}_{total} \tag{3.33}$$

From the principle of exergy balance, the exergy destructed in k^{th} component can be expressed as **[45]**:

$$\left(\dot{E}x_d\right)_k = \dot{E}x_F - \dot{E}x_P \tag{3.34}$$

Where $\dot{E}x_F$ is the fuel exergy which represents the exergy associated with the streams which act as the driving input, and $\dot{E}x_P$ is product exergy which indicates the amount of exergy flow associated with the streams which carry the desired output of the k^{th} component. The expressions of fuel exergy and product exergy for each system component are presented in **Table 3.10.**

The exergy efficiency of k^{th} component can be expressed as the ratio of product and fuel exergy flow rates in that component:

$$\psi_k = \frac{(\dot{E}x_F)_k}{(\dot{E}x_P)_k} \tag{3.35}$$

Where $(\dot{E}x_P)_k$ and $\left(\dot{E}x_F\right)_k$ are the product and fuel exergy for k^{th} component.

The exergy efficiency of overall system can be expressed as:

$$\psi = \frac{\dot{E}x_P}{\dot{E}x_F} = \frac{\dot{E}x_{ca,e} - \dot{E}x_{ca,i}}{\dot{W}_{total}} = 1 - \frac{\sum_k (\dot{E}x_d)_k}{\dot{W}_{total}} \tag{3.36}$$

Table 3.10: Component-wise basic equations involved in exergy and exergo-economic analysis

Component	Fuel Exergy Rate $(\dot{\chi}_F)_k$	Product Exergy Rate $(\dot{\chi}_P)_k$	Cost Balance Equation	Auxiliary Equation
EVP	$\dot{E}x_8 - \dot{E}x_1$	$\dot{E}x_{ca,e} - \dot{E}x_{ca,i'}$	$\dot{C}_8 + \dot{C}_{ca,i'} + \dot{Z}_{EVP} = \dot{C}_1 + \dot{C}_{ca,e}$	$\frac{\dot{C}_8}{\dot{E}x_8} = \frac{\dot{C}_1}{\dot{E}x_1}$
CD	$\dot{E}x_{10} - \dot{E}x_{11}$	$\dot{E}x_{env,e} - \dot{E}x_{env,i'}$	$\dot{C}_{10} + \dot{C}_{env,i'} + \dot{Z}_{CD} = \dot{C}_{11} + \dot{C}_{env,e}$	$\frac{\dot{C}_{env,i'}}{\dot{E}x_{env,i'}} = \frac{\dot{C}_{env,e}}{\dot{E}x_{env,e}}$
CHX	$\dot{E}x_{13} - \dot{E}x_9$	$\dot{E}x_5 - \dot{E}x_4$	$\dot{C}_4 + \dot{C}_{13} + \dot{Z}_{CHX} = \dot{C}_9 + \dot{C}_5$	$\frac{\dot{C}_9}{\dot{E}x_9} = \frac{\dot{C}_{13}}{\dot{E}x_{13}}$
FIS	$\dot{E}x_{5''} + \dot{E}x_6 - \dot{E}x_7$	$\dot{E}x_3 - \dot{E}x_2$	$\dot{C}_2 + \dot{C}_6 + \dot{C}_{5'} + \dot{Z}_{FIS} = \dot{C}_3 + \dot{C}_7$	$\frac{\dot{C}_6 + \dot{C}_{5'}}{\dot{E}x_6 + \dot{E}x_{5'}} = \frac{\dot{C}_7}{\dot{E}x_7}$
FT	$\dot{E}x_{12} - \dot{E}x_{14}$	$\dot{E}x_{13}$	$\dot{C}_{12} + \dot{Z}_{FT} = \dot{C}_{13} + \dot{C}_{14}$	
LC1	$\dot{W}_{LC_1}$	$(\dot{E}x_2 - \dot{E}x_1)$	$\dot{C}_1 + \dot{C}_{w,LC1} + \dot{Z}_{LC1} = \dot{C}_2$	
LC2	$\dot{W}_{LC_2}$	$(\dot{E}x_4 - \dot{E}x_3)$	$\dot{C}_3 + \dot{C}_{w,LC2} + \dot{Z}_{LC2} = \dot{C}_4$	
LC3	$\dot{W}_{HC}$	$(\dot{E}x_{10} - \dot{E}x_9)$	$\dot{C}_{15} + \dot{C}_{w,LC3} + \dot{Z}_{LC3} = \dot{C}_{10}$	
F1	$\dot{E}x_7$	$\dot{E}x_8$	$\dot{C}_{ca,i} + \dot{C}_{w,F1} + \dot{Z}_{F1} = \dot{C}_{ca,i'}$	
F2	$\dot{E}x_{5''}$	$\dot{E}x_6$	$\dot{C}_{env,i} + \dot{C}_{w,F2} + \dot{Z}_{F2} = \dot{C}_{env,i'}$	$\frac{\dot{C}_{env,i}}{\dot{E}x_{env,i}} = 0$
EV1	$\dot{E}x_{11}$	$\dot{E}x_{12}$	$\dot{C}_7 + \dot{Z}_{EV1} = \dot{C}_8$	
EV2	$\dot{W}_{F_1}$	$\dot{E}x_{ca,i'} - \dot{\chi}_{ca,i}$	$\dot{C}_{5''} + \dot{Z}_{EV2} = \dot{C}_6$	
EV3	$\dot{W}_{F_2}$	$\dot{E}x_{env,i'} - \dot{E}x_{env,i}$	$\dot{C}_{11} + \dot{Z}_{EV3} = \dot{C}_{12}$	

In exergo-economic analysis, each exergy stream carry some economic value. The economic value of an exergy stream entering to a component is added to the capital, maintenance and operational costs of the component while evaluating the total investment. Similarly the exergy loss and destruction in a component is treated as economic loss of the whole system contributed by that particular component. An exergo-economic factor of a component signifies the relative importance of the particular component. The exergo-economic factor can be calculated by **Bejan et al. [45]**:

$$f_k = \frac{\dot{Z}_k}{\dot{Z}_k + c_{F,k}(\dot{E}x_{d,k})} \tag{3.37}$$

Where $c_{F,k}$ is the unit cost of fuel exergy for the k^{th} component and can be calculated by solving the exergy cost rate balance for k^{th} component, which can be expressed in general form as **[45]:**

$$\sum_e \left(c\dot{E}x\right)_k = \sum_i \left(c\dot{E}x\right)_k + \dot{Z}_k + \dot{Z}_{op_k} \quad (3.38)$$

Where c is the unit cost of exergy associated with the exergy stream. In the present study exergy losses are considered to be negligible and exergy destructions are due to thermodynamic inefficiencies present in the system. A component having lower value of f_k, should be given more attention to increase its efficiency. Although the capital cost of the whole system increases in doing that, but that will lead to a reasonable improvement in the overall performance of the system. However the components with higher values of exergoeconomic factor should be given less importance while investing in it to improve its performance. The exergoeconomic equations for different system components are listed in **Table 3.10**.

Irreversibility analysis

Figure 3.17 presents a relative comparison of exergy destructions in different components due to the three refrigerant couples. The exergy destruction is almost equal for all refrigerant couples in evaporator, CHX, FIS, Flash tank, LTC compressor I, Fan I, Fan II, Expansion valve I and Expansion valve II but it is insignificant in condenser for propane-propylene refrigerant couple. This is because the exergy loss of propane is almost equal to the exergy gain of air in the condenser. It can be seen that although the LTC compressor efficiencies are same, but exergy destruction in LTC compressor II is higher than that of LTC compressor I. This is because of more mass flow rate handle by LTC compressor II than that of LTC compressor I. Exergy destruction in HTC compressor is less than that in LTC compressors because the overall efficiency estimation of HTC copressor (e.g. 0.8058 for propylene-propane) is greater than that of

LTC compressors (e.g. 0.6312 each for propylene-propane). Flash tank contributes zero destruction in exergy because the temperature of inlet stream, exit stream and that of flash tank are same therefore all the interactions associated with flash tank are at zero temperature difference making the process almost reversible. The difference in exergy distructions in other components for different refrigerant pairs is due to the difference in thermophysical properties of the refrigerants which respond in different manner in the same component.

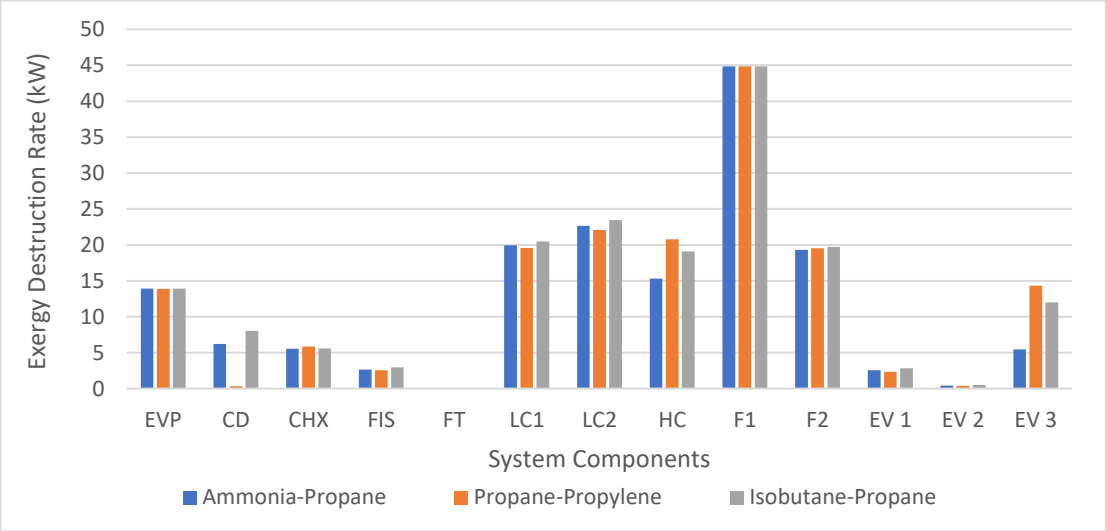

Figure 3.17: Comparison of exergy destructions in different system components for the three different refrigerants

Figure 3.18 (a), Fig. 3.18 (b) and Figure 3.18 (c) shows the percentage share of individual components in contributing the total exergy destruction of system for Ammonia-propane, Propane propylene and isobutane-propane refrigerant pairs respectively. It can be seen that a major part of the pi chart is covered by Fan 1 with 28.23%, 26.93% and 26% of total exergy destruction for Ammonia-propane, Propane-propylene and Isobutane-propane pairs respectively. This is because the optimal evaporator temperature comes out to be -30 ^{0}C which is its maximum value whereas the cold space temperature is fixed to -20 ^{0}C. In this case the temperature gap between cold space and evaporator is minimum. Due to minimum temperature gap between

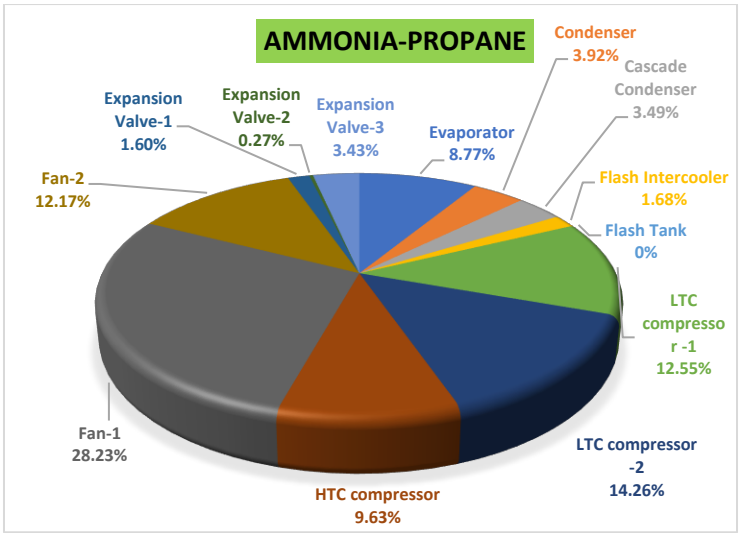

(a)

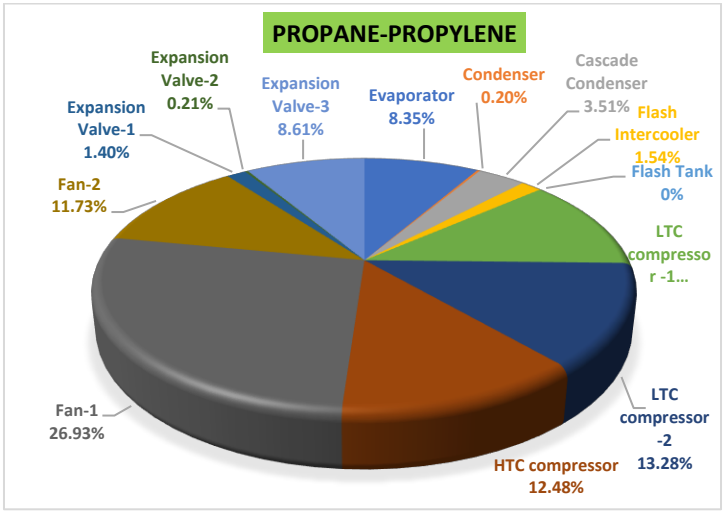

(b)

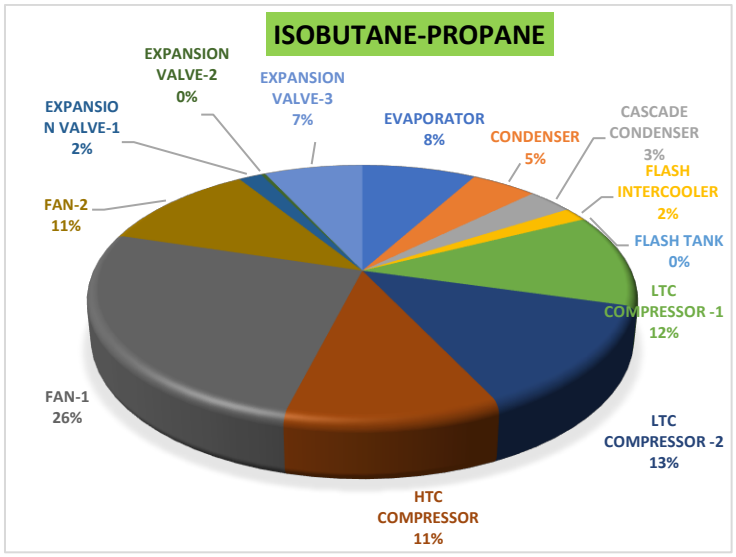

(c)

Figure 3.18: Percentage share of system components in total Exergy destruction at thermodynamic optimal conditions for: **(a)** Ammonia-Propane, **(b)** Propane-Propylene, **(c)** Isobutane-Propane refrigerant couples

evaporator and cold space the exergy destruction of evaporator (heat exchanger) reduces but on the other hand this demands a high amount of air flow (e.g. 49.7 kg/s for propylene-propane) to produce cooling (transfer of heat) of 500kW. This drastic increases in air handled by fan 1 results in high entropy generation and hence a highest exergy destruction. The second highest exergy destruction is shown by LTC compressor II (22.64 kJ/s, 22.09 kJ/s and 23.41 kJ/s for ammonia-propane, propane-propylene and isobutane-propane refrigerant couples respectively) due to nonisentropic compression (e.g. $\eta_{Total} = 0.6312$ for propane-propylene) with heavy mass flow rate (1.547 kg/s, 1.5 kg/s and 1.572 kg/s for ammonia-propane, propane-propylene and isobutane-propane respectively). LTC compressor I has the same isentropic efficiency but less mass flow rate (1.322 kg/s, 1.291 kg/s and 1.329kg/s for ammonia-propane, propane-propylene and Isobutane-propane respectively), so it possesses the third highest exergy destruction rate. Flash tank has zero exergy destruction due to zero heat loss and the other least exergy destruction components are flash intercooler and expansion valve II because of minimum heat loss in intercooler and low pressure throttling process respectively. Exergy loss in evaporator is approximatly same because of similar properties of propane and propylene working as LTC refrigerants. The exergy loss in condenser for propane-propylene is significantly lower than ammonia-propane and Isobutane-propane refrigerant pairs. This is because of lower descharge temperature (38.9 ^{0}C) of HTC compressor which leads to lower condenser LMTD for propane as HTC refrigerant.

Exergoeconomic Analysis

To investigate the performance and importance of individual components, an exergoeconomic analysis for the three refrigerant couples at optimum operating conditions has been done and results are presented in **Table 3.11**. It can be seen that

The exergy efficiency of flash tank is maximum (100%) which verifies zero exergy destruction due to heat interaction between streams at zero temperature difference as discussed earlier. The exergy efficiency of flash intercooler is 88.91% which is lesser than flash tank because the flash intercooler also serves as a subcooler and a heat transfer (of 47.27 kW for propane-propylene) occures with LMTD of 1.4 ^{0}C which results in some destruction in exergy. Exergy efficiency of evaporator is 88.65%. This is because the heat transfer of 500kW occures at LMTD value of 3.756 ^{0}C exergy of 13.89 kW is distroyed in this irreverible process. Since the heat rejection (711.8 kW/s) in condenser is higher than that of evaporator and the LMTD is also greater (4.157 ^{0}C) therfore relatively more exergy is destroyed in condenser resulting in lesser efficiency (74.39%). The exergy efficiency of condenser is 74.39 % for propane-propylene which is greater than 13.03% and 10.57 % for ammonia-propane and Isobutane-propane refrigerant couples. This is because of different amounts of exergy destructions due to difference in thermophysical properties of HTC refrigerants being used. Rest of the components show almost similar exergy efficiencies for all the three refrigerant couples. The low value of exergoeconomic factor for expansion valves (0.07%, 0.042% and 0.01%), Fan I (4.141%) and the cascade heat exchangers (8.659%, 3.069% and 1.08%) indicate that investing in these components to reduce their exergy destructions will be profitable for the whole system. In flash tank having 100% exergoeconomic factor and the other components like evaporator and condenser having relatively higher values of *f*, the capital, operating and maintenance cost dominate. Cost of fuel for all compressors and fans is same (33.33×10^{-6} \$/kJ) for all refrigerant pairs bcause of the fixed energy (fuel) charges. Cost of fuel exergy is same for FIS and evaporator for each refrigerant pair. This is because the fuel exergy stream for both the components is same and carry equal cost rates.

Table 3.11: Results of Exergoeconomic analysis at optimal operating conditions of the three natural refrigerant pairs

Component	Ammonia-Propane			Propane-Propylene			Isobutane-Propane		
	ψ (%)	$c_{F\,k}$ (x10^{-6} \$/kJ)	f_k(%)	ψ (%)	$c_{F\,k}$ (x10^{-6} \$/kJ)	f_k(%)	ψ (%)	$c_{F\,k}$ (x10^{-6} \$/kJ)	f_k(%)
EVP	88.65	216.6	90.17	88.68	389	83.66	88.65	890.3	69.04
CD	13.03	301.2	78.54	74.39	301.2	99.64	10.57	301.2	97.33
CHX	91.92	167.8	8.659	92	437.9	3.069	91.36	1445	1.08
FIS	87.32	213.4	94.59	88.91	384.3	91.73	86.97	876	80.22
FT	100	167.8	100	100	437.9	100	100	1445	100
LC_1	59.29	33.33	50.74	58.17	33.33	50.66	60.21	33.33	50.63
LC_2	61.51	33.33	49.66	60.33	33.33	49.64	62.5	33.33	49.48
HC	84.16	33.33	63.46	81	33.33	57.52	81.76	33.33	59.07
F_1	19.52	33.33	4.141	19.52	33.33	4.14	19.52	33.33	4.141
F_2	1.578	33.33	14.07	1.578	33.33	14.07	1.578	33.33	14.07
EV_1	96.7	213.4	0.313	96.77	384.3	0.185	96.52	876	0.068
EV_2	93.37	213	0.31	93.8	383.7	0.195	92.9	873.8	0.068
EV_3	92.89	167.8	0.07	84.78	437.9	0.042	85.33	1445	0.01

Similary cost of fuel exergy is same for EV III and CHX is also same for all the three refrigerant pairs because the fuel exergy stream of EV III also serves as a fuel exergy to CHX in order to produce a cooling effect to the HTC refrigerant in CHX. The only component between CHX and EV III is flash tank which shows zero exergy destruction therfore the equality of c_F values for these components is in conformity with the concept of exergo-economics.

Comparison of present study with available literature

It is evident that R717-R290 is the most powerful refrigerant couple to be used in the aforementioned system. To understand the potential of R717-R290, a comparison of COP, exergy efficiency and total cost of the system using R717-R744 refrigerant couple has been shown in **Table 3.12**. It can be seen that after replacing R744 with R290 in LTC, COP and exergy efficiency of the system increase by 7.91% and 7.73% respectively while the total cost rate reduces by 5.32% while working under the same operating conditions ($\dot{Q}_{evp}$= 500kW, T_{evp} = -35.20 ^{0}C, T_{cond}= 35.01 ^{0}C, T_5= -1.98 ^{0}C, $\Delta\, T_{cas}$ =2.27 ^{0}C, N= 4266 h, α_{el} = 0.09 \$/kWh).

Table 3.12: Comparison of R717-R290 with R717-R744 results [15]

Results			
Parameter	Reference **[15]** (R717-R744)	Present work (R717-R290)	% deviation
COP	1.53	1.651	+7.91
ψ (%)	31.3	33.72	+7.73
$\dot{C}_{total}$ (\$/yr)	554523	525022	-5.32

3.4 Chapter Summary

Comparative energy, exergy, and economic and exergoeconomic analysis have been performed on cascade refrigeration system incorporated with a flash tank in its higher temperature cycle and a flash intercooler with an indirect subcooler in its lower temperature cycle using different natural refrigerant couples (Hybrid Cascade Refrigeration System). A comparative analysis of seventeen natural refrigerant couples is also presented in the thermoeconomic framework. It is found that R717-R290 is found to be the best refrigerant pair from exergetic point of view whereas R717-R1270 is the best refrigerant pair from economic point of view. The exergoeconomic analysis reveals maximum exergoeconomic factor corresponds to flsh tank with 100% whereas the second highest value is found for FIIS for all the refrigerant couples studied.

Chapter 4

Multi-objective optimization of Hybrid Cascade Refrigeration system

In this work, thermodynamic and economic optimization of hybrid cascade refrigeration system is done using twenty two natural refrigerant pairs and seven best pairs are selected on the basis of these results. Further a multi-objective optimization is performed on the system using seven refrigerant pairs and TOPSIS decision-making technique has been employed to select the most efficient solution from pareto optimal front and assign the order of preference for different refrigerant pairs. Best natural refrigerant pair suitable for the system is identified. This study is an endeavour towards seeking alternative environment-friendly natural refrigerants for low-temperature applications through a comprehensive comparative analysis based on thermo-economic optimization.

4.1 Optimization Procedure:

The system description of hybrid cascade refrigeration system has been discussed in section 3.1. In present study, Twenty-two refrigerant pairs with four HTC refrigerant groups are compared based on results obtained from two single-objective optimizations including thermodynamic optimization (maximization of exergetic efficiency) and economic optimization (minimization of total cost rate) respectively. Best LTC refrigerant has been selected for each of the four HTC refrigerants resulting in four most compatible refrigerant pairs from thermodynamic optimization. Similarly, four refrigerant pairs are selected from the results of economic optimization. Therefore a total of eight refrigerant pairs are obtained out of twenty-two pairs which are either most efficient or most economical. After taking the union of these eight members,

seven most compatible refrigerant pairs are obtained. Multi-objective optimization is performed on these seven refrigerant pairs to carry out further comparative analysis and identify the best refrigerant pair.

4.1.1 Conjugate Direct Method

The Thermodynamic and economic optimizations are done by the conjugate direct method using minmax tool provided with EES software wherein the hybrid cascade refrigeration system was modelled using basic energy, exergy and economic equations discussed in section 3.2. Exergetic efficiency and total cost rate are the objective functions to be maximized and minimized respectively and the operating conditions $a, b, T_{evap}, T_{cond}, T_{cc}$ and ΔT_{cas} are the six design variables. In the conjugate direct method, a series of one-dimensional searches are used to find an optimal point which is a function of design variable X_1, X_2, … X_n. Thereafter this process is repeated to confirm the optimum point. These one-dimensional searches do not essentially require numerical derivatives which is an advantage of this algorithm because it makes this algorithm capable of dealing with functions that are not easily differentiable **[14]**.

4.1.2 Multi-objective Genetic Algorithm

Multi-objective optimization is a realistic approach to optimize more than one objective functions (commonly conflicting in nature) simultaneously. Model **[*M*]** shows the formulation of a general multi-objective optimization problem mathematically **[44]**.

$$minimize\ F(\vec{x}) = \left[f_1\ (x), f_2\ (x)\ \ldots\ldots f_p\ (x)\right]^T$$

$$Subject\ to:$$

$$\vec{g}(\vec{x}) \leq 0 \qquad \textbf{[}\boldsymbol{M}\textbf{]}$$

$$\vec{h}(\vec{x}) = 0$$

$$\vec{x} \in R^n, \vec{f}(\vec{x}) \in R^p, \vec{g}(\vec{x}) \in R^m\ and\ \vec{h}(\vec{x}) \in\ R^q$$

Where integers p, n, m and q are the number of objective functions, independent variables, inequality and equality constraints respectively and $\vec{x} \in R^n$ and $\vec{f}(\vec{x}) \in R^p$ are decision variable vector and objective function vector respectively.

Multi-objective Genetic algorithm (MOGA) tool provided with MATLAB software is used in present work which is one of the most efficient and frequently used tools based on an artificial neural network to search the solutions of real-world multi-objective problems. Genetic algorithm is a method of optimization involving iterative search procedures in a binary search space based on an analogy with the process of natural selection (Darwinism) and evolutionary genetics. The search procedure does not result in a global solution which maximizes or minimizes all the objective functions concurrently, however, the attention is focussed on the use of Pareto optimal solutions that are not dominated by other solutions and can not be enhanced for any objective without worsening at least one objective. The set of all non-dominated solutions is represented as Pareto optimal set, and the relevant objective function values are called the Pareto optimal front **[23]**.

Exergetic efficiency and total cost rate are the two conflicting objective functions whereas the operating parameters $a, b, T_{evap}, T_{cond}, T_{cc}$ and ΔT_{cas} are the six design variables considered in the formulation of the multi-objective optimization problem. Expressions for the objective functions in terms of six design variables are developed through multiple linear regression analysis with the help of linear regression tool provided in EES software wherein the system was simulated using basic energy, exergy and economic equations presented in Section 3.2**.** Since all the possible constraints related to practical and theoretical issues have been taken care of while setting the variable limits and formulating the thermodynamic and economic equations, there are no equality or inequality constraints involved in formulation of multi-objective

optimization problem. The upper and lower bounds of design variables along with the other system settings are mentioned in **Table 4.1**.

Table 4.1. Lower and upper bounds of design variables for different refrigerant pairs

Parameter	Refrigerant pair	Lower Bound	Upper Bound
$\boldsymbol{a}$	For all pairs	0	1
$\boldsymbol{b}$	For all pairs	0	1
$\boldsymbol{T_{evap}}$ (℃)	For pairs having R744 as LTC refrigerant	-56	-40
	For pairs having R744a as LTC refrigerant	-88.47	-40
	For pairs having R290 as LTC refrigerant	-42.39	-40
	For pairs having R1270 as LTC refrigerant	-48	-40
	For pairs having R170 as LTC refrigerant	-88.84	-40
	For pairs having R1150 as LTC refrigerant	-104	-40
$\boldsymbol{T_{cond}}$ (℃)	For all pairs	35	55
$\boldsymbol{T_{cc}}$ (℃)	For all pairs	-9	1
$\Delta\boldsymbol{T_{cas}}$ (℃)	For all pairs	2	4

4.1.3 Non-dominated Shorting Genetic Algorith-II (NSGA-II):

NSGA-II is implemented to validate and prove the accuracy of final results obtained via MOGA. It is an enhanced version of Non-dominated shorting genetic algorithm (NSGA) and works on a principle, that allows the elites of population to be carried to the next generation. It is a fast shorting algorithm which explicitly preserves the diversity of population through a mechanism based on crowding distance and emphasizes on non-dominance and optimality **[24]**. A MATLAB code for NSGA-II is run using the same objective functions obtained through multiple linear regression analysis and same boundry conditions as tabulated in **Table 4.1**.Pareto frontier obtained via NSGA-II is subjected to TOPSIS method for getting the best optimal solution.

4.1.4 TOPSIS decision making

MOGA provides a set of non-dominated solutions which is represented by Pareto optimal front. Although all the solutions are potentially optimum and desired but due to practical reasons, only one solution has to be opted for design considerations. That unique solution is selected by TOPSIS (Technique for Order of Preference by

Similarity to Ideal Solution) method which is based on the concept that the best solution is always farthest to the nonideal solution (worst solution) from the single-objective optimization criterion of an objective function. In this procedure, A $u \times v$ weighted normalised decision matrix (WNDM) is formed where u is the number of solutions and v is the number of objective functions. Euclidian distances of all the solutions from ideal and non-ideal solutions are calculated which can be expressed as **[46]**:

Euclidian distance of a solution from an ideal solution,

$$S_i^+ = \sqrt{\sum_{j=1}^{v}(V_{ij} - V^{ideal})^2} \tag{4.1}$$

Euclidian distance of a solution from non-ideal solution,

$$S_i^- = \sqrt{\sum_{j=1}^{v}(V_{ij} - V^{non-ideal})^2} \tag{4.2}$$

Where V_{ij} is the weighted normalised value (WNV) of j^{th} objective function for i^{th} solution and V^{ideal} and $V^{non-ideal}$ are the best and worst values of WNVs of objective functions respectively. Based on $S_i^+$and S_i^- a performance score of each solution is calculated which can be expressed for i^{th} solution as:

$$C_i = \frac{S_i^-}{S_i^- + S_i^+} \tag{4.3}$$

In the TOPSIS method, a solution with the highest value of performance score is selected.

$$i_{choice} = i \in \max(C_i) \tag{4.4}$$

4.2 Results and discussions

Model Validation

The thermodynamic and economic models are validated from the results of Mosaffa et al.**[15]. Table 4.2** displays the values of some important system parameters obtained through the present model and the reference data at the similar operating conditions. A

deviation of -1.3% to +2.62% in corresponding values is observed to the published data whereas the total cost rate obtained from the present model comes out to be 17.94% lower than that of the reference value. This is because the cost of penalty due to emission of carbon dioxide has not been included in total cost estimation in present work.

Table 4.2: Validation of thermodynamic and economic models

Parameters	Operational Conditions		
	$Q_{evap} = 500\ kW, T_{evap} = -35.2$ ℃, $T_{cond} = 35.01$ ℃, $T_5 = -1.98$ ℃, $\Delta T_{cas} = 2.27$ ℃, $\Delta T_{sup} = 0.45$ ℃, $T_{cs} = -20$ ℃, $T_{env} = 25$ ℃, $N = 4266\ hours, \alpha = 0.09\ \$\ kWh^{-1}$		
	Results		
	Present Model	Reference**[15]**	% deviation
$\boldsymbol{A_{evp}}$ $(\boldsymbol{m^2})$	1671	1671	0
$\boldsymbol{A_{cond}}$ $(\boldsymbol{m^2})$	625.3	627.6	-0.37
$\boldsymbol{A_{cas}}$ $(\boldsymbol{m^2})$	61.43	59.86	+2.62
$\boldsymbol{\dot{W}_{comp}}$ *(kW)*	264.6	267.37	-1.04
$\boldsymbol{\dot{E}x_d}$ *(kW)*	220.6	223.5	-1.3
$\boldsymbol{COP}$	1.549	1.536	+0.85
$\boldsymbol{\psi}$ (%)	31.66	31.3	+1.15
$\boldsymbol{\dot{C}_{total}}$ ($/yr)	554353	675530	-17.94

Natural refrigerant pair formation

The system requires two different refrigerants to be used in two different cycles (*i.e* HTC and LTC). For HTC, a refrigerant with higher NBP is suitable whereas, for LTC, a refrigerant with lower NBP is suitable. Keeping this in view, out of eight natural refrigerants twenty-two possible refrigerant pairs are formed which are arranged in four groups and each group is named after the HTC refrigerant being used in the refrigerant pairs falling in the group. **Table 4.3** shows the four refrigerant groups.

Table 4.4 presents the values of operational parameters and settings used to model different system components. Other important parameters regarding economic model are the maintenance factor (ϕ), the annual interest rate (i), system lifetime (n), the

average cost of electricity (α_{el}) and average annual operational hours (N) which are taken as 1.06, 14%, 15 yrs, 0.12 \$ kWh^{-1} and 4266 hrs respectively **[25]**.

Table 4.3: Natural refrigerant pairs (HTC-LTC)

R717 refrigerant group	R290 refrigerant group	R1270 refrigerant group	R600a refrigerant group
R717-R744	R290-R744	R1270-R744	R600a-R744
R717-R744a	R290-R744a	R1270-R744a	R600a-R744a
R717-R290	R290-R1270	R1270-R290	R600a-R290
R717-R1270	R290-R170	R1270-R170	R600a-R1270
R717-R170	R290-R1150	R1270-R1150	R600a-R170
R717-R1150			R600a-R1150

Table 4.4. Values of operational parameters used in thermodynamic modelling of the system

Parameter	Value
Cooling capacity $(\dot{\boldsymbol{Q}}_{\boldsymbol{evap}})$	$500\ kW$
Environment temperature $(\boldsymbol{T}_{\boldsymbol{env}})$	25 ℃
Temperature of cold air at the evaporator inlet $(\boldsymbol{T}_{\boldsymbol{cs}})$	−30 ℃
Ambient pressure $(\boldsymbol{p}_{\boldsymbol{0}})$	$101.3\ kPa$
Overall heat transfer coefficient of the evaporator $(\boldsymbol{U}_{\boldsymbol{evap}})$	$0.03\ kW/m^2K^1$
Overall heat transfer coefficient of the condenser $(\boldsymbol{U}_{\boldsymbol{cond}})$	$0.04\ kW/m^2K^1$
Overall heat transfer coefficient of the cascade heat exchanger $(\boldsymbol{U}_{\boldsymbol{cas}})$	$1\ kW/m^2K^1$
Overall heat transfer coefficient of the flash intercooler $(\boldsymbol{U}_{\boldsymbol{FIIS}})$	$1\ kW/m^2K^1$
Temperature difference of the air in evaporator and condenser	10 ℃

Single-objective optimization

Here twenty-two refrigerant pairs have been studied based on two single objective optimizations subjected to maximization of exergetic efficiency (thermodynamic optimization) and minimization of total cost rate (economic optimization) respectively out of which seven pairs have been chosen for multi-objective optimization based on their performance obtained via thermodynamic and economic optimizations.

Table 4.5 presents the results of thermodynamic optimization which aims to maximize the exergetic efficiency and find a set of thermodynamic optimal values of six operational parameters. The presented results build an understanding of tuning these parameters to achieve best thermodynamic performance of cascade refrigeration

system working with these pairs. It can be noticed that the subcooling (a) and de-superheating parameters (b) approach towards their maximum values (*i.e.* 1) for all the refrigerant pairs which signify that the flash intercooler is configured to deliver maximum subcooling and de-superheating to achieve maximum lower temperature cycle performance.

Table 4.5: Results of Thermodynamic optimization

Refrigerant Pair		Thermodynamic optimal operating condition						Maximum Exergetic Efficiency
HTC	LTC	a	b	T_1 (℃)	T_{11}(℃)	T_5 (℃)	ΔT_{cas}(℃)	ψ_{max} (%)
R717	R744	1	1	-40	36.09	-9	4	38.63
	R744a	1	1	-40	37.84	-7.809	4	37.92
	R290	0.9967	1	-40	36.09	-9	4	40.71
	R1270	0.9963	1	-40	36.09	-9	4	40.61
	R170	1	1	-40	36.09	-9	4	38.2
	R1150	1	1	-40	36.09	-9	4	35.82
R290	R744	1	1	-40	35	-6.455	2	35.63
	R744a	1	1	-40	35	-4.745	2	35.78
	R1270	0.9963	1	-40	35	-1.534	2	37.69
	R170	1	1	-40	35	-4.993	2	35.31
	R1150	1	1	-40	35	-8.421	2	33.07
R1270	R744	1	1	-40	35	-6.901	2	35.63
	R744a	1	1	-40	35	-5.228	2	35.77
	R290	0.9964	1	-40	35	-2.372	2	37.72
	R170	1	1	-40	35	-4.994	2	35.31
	R1150	1	1	-40	35	-9	2	33.12
R600a	R744	1	1	-40	35	-9	2	36.33
	R744a	0.9997	1	-40	35	-9	2	36.41
	R290	0.9965	1	-40	35	-1.562	2	38.34
	R1270	0.996	1	-40	35	-1.159	2	38.27
	R170	1	1	-40	35	-9	2	35.94
	R1150	1	1	-40	35	-9	2	33.77

The thermodynamic optimal evaporator temperature (T_1) is its maximum value whereas the condenser temperature (T_{11}) approaches towards its lowest possible value of provided operational range for all the pairs to minimize the temperature lift of the overall cycle which further leads to maximization of overall cycle performance. The

cascade condenser temperature (T_5) and cascade temperature gap (ΔT_{cas}) attain different optimal values depending upon properties of different refrigerant pairs to maximize the exergetic efficiency which is presented in **Table 4.5**. After a comparative analysis, it can be observed that, out of six refrigerant pairs of R717 group, R717-R290 pair shows the maximum optimum exergetic efficiency of 40.71% whereas R717-1150 gives the minimum value of 35.82%. Similarly, from R290, R1270 and R600a groups R290-R1270, R1270-R290 and R600a-R290 show maximum optimum exergetic efficiencies as 37.69%, 37.72% and 38.32% respectively whereas R290-1150, R1270-R1150 and R600a-R1150 result in minimum optimum exergetic efficiencies of 33.07%, 33.12% and 33.77% respectively. As a result of comparative analysis based on thermodynamic optimization it is clear that, out of twenty-two refrigerant pairs categorized in four different groups, R717-R290, R290-R1270, R1270-R290 and R600a-R290 pairs are the best candidates (one pair from each group).

Thermodynamic optimization often lead to excessive cost therefore an economic optimization is required to look into the economic side of the behaviour of natural refrigerant pairs. In this regard, **Table 4.6** depicts the results of economic optimization which is subjected to the minimization of the total cost rate of the system. The values of economic optimal operational parameters and resulting minimum total cost rate for twenty refrigerant pairs have been tabulated here. It can be noticed that the subcooling parameter (a) attains zero value for each refrigerant pair to configure the flash intercooler for zero indirect subcooling through minimization of sub-cooler coil area which further leads to minimization of the capital cost of the flash intercooler. De-superheating parameter (b) attains maximum value for all pairs which signifies that the superheated LTC refrigerant coming out of LTC compressor I is completely intercooled to the corresponding saturated vapor state which results in minimization of gross LTC

compressor work causing minimization of the overall running cost of the system. Other parameters are also tuned to different economic optimal values depending upon the thermophysical properties of different refrigerant pairs being used which can be seen in **Table 4.6**.

Table 4.6: Results of Economic optimization

Refrigerant Pair		Economic optimal operating condition						Minimum Total cost rate
HTC	LTC	a	b	T_1 (°C)	T_{11}(°C)	T_5(°C)	ΔT_{cas}(°C)	$\dot{C}_{Total,min}$ $(M\$/yr)$
R717	R744	0	1	-53.93	38.61	-9	2.286	0.4568
	R744a	0	1	-54.24	38.61	-9	2.286	0.4534
	R290	0	1	-42.39	38.61	-9	2.286	0.5358
	R1270	0	1	-48	38.61	-9	2.286	0.4529
	R170	0	1	-54.47	38.61	-9	2.286	0.4586
	R1150	0	1	-54.05	38.61	-9	2.286	0.4849
R290	R744	0	1	-52.46	53.94	-8.132	2	0.546
	R744a	0	1	-53.11	53.94	-8.132	2	0.5424
	R1270	0	1	-48	53.94	-8.132	2	0.5361
	R170	0	1	-53.31	53.94	-8.132	2	0.5485
	R1150	0	1	-52.89	53.94	-8.129	2	0.5795
R1270	R744	0	1	-52.02	54.32	-9	2	0.5326
	R744a	0	1	-53.31	54.32	-9	2	0.5295
	R290	0	1	-42.39	54.32	-9	2	0.6048
	R170	0	1	-53.53	54.32	-9	2	0.5353
	R1150	0	1	-53.12	54.32	-9	2	0.5642
R600a	R744	0	1	-52.11	54.32	-1.098	2	0.5653
	R744a	0	1	-51.37	54.32	-1.099	2	0.5588
	R290	0	1	-42.39	54.32	-1.099	2	0.6229
	R1270	0	1	-48	54.32	-1.099	2	0.5457
	R170	0	1	-52.59	54.32	-1.098	2	0.5677
	R1150	0	1	-51.88	54.32	-1.098	2	0.6188

After comparing the optimum total cost rates for six refrigerant pairs of R717 group, it can be found that R717-R1270 yields the minimum optimum cost rate of 0.4529 M$/yr whereas R717-R290 shows the maximum optimum cost rate of 0.5358 M$/yr. Similarly in R290, R1270 and R600a groups, R290-R1270, R1270-R744a and R600a-R1270 give minimum optimum cost rates of 0.5361 M$ yr^{-1}, 0.5295 M$ yr^{-1} and 0.5457 M$ yr^{-1} respectively whereas R290-R1150, R1270-R290 and R600a-R290 pairs result

in maximum optimum cost rates of 0.5795 M$ yr^{-1}, 0.6048 M$ yr^{-1} and 0.6229 M$ yr^{-1} respectively. Based on comparative analysis based on economic optimization, it can be drawn that, out of twenty-two refrigerant pairs categorized in four different groups, R717-R1270, R290-R1270, R1270-R744a, and R600a-R1270 are the most economical refrigerant pairs (one pair from each group).

Twenty-two refrigerant pairs were studied through two single objective optimizations and a group-wise comparative analysis revealed that R717-R290, R290-R1270, R1270-R290, and R600a-R-290 are the best pairs from a thermodynamic point of view whereas R717-R1270, R290-R1270, R1270-R744a, and R600a-R1270 are the best pairs from an economic point of view. In these eight pairs, R290-R1270 refrigerant pair is common in both the results therefore there is a total of seven unique pairs which are either thermodynamically most efficient or economically most reasonable. Hence out of twenty-two refrigerant pairs, R717-R290, R290-R1270, R1270-R290, R600a-R290, R717-R1270, R1270-R744a and R600a-R1270 may be selected as seven best refrigerant pairs from either of the criteria. Now it is imperative to perform a thermo-economic multi-objective optimization on these refrigerant pairs to investigate their potential on both thermodynamic as well as economic criteria concurrently.

Multi-objective optimization

Thermodynamic and economic trends are generally divergent in nature, therefore a bi-criteria optimization is required to reveal new insights to thermo-economic behaviour of these refrigerant pairs and compare them on a mediated level plateform. Here, multi-objective optimization is performed on seven best refrigerant pairs selected via single-objective optimization. The functions of exergetic efficiency and total cost rate along with lower and upper bounds of design variables are fed to multi-objective genetic algorithm (MOGA) tool of MATLAB software to perform the multi-objective

optimization procedure which aims to minimize the total cost rate and maximize the exergetic efficiency. MOGA ends up providing a set of seventy nondominated optimal solutions for each refrigerant pair which are represented in the form of Pareto optimal fronts.

Pareto optimal front

Figure 4.1(a)-(g) show pareto optimal fronts for the seven refrigerant pairs. All the solutions shown in Pareto optimal fronts are non-dominated solutions and any one of them can be used to design an optimal system configuration. But the designer has to opt for any one solution which depends on the importance or weightage given to the objective functions as per his constraints. When exergetic efficiency is important, it has to be given more weightage while the selection of the final solution and when the cost is the major constraint, it has to be given more weightage than exergetic efficiency while selecting the final solution. Here, for each refrigerant pair, TOPSIS decision-making technique has been used for selection of final solutions considering five different weightages of exergetic efficiencies taken as 1, 0.75, 0.50, 0.25 and 0 which are shown in each figure by five larger bullets ‘A’, ‘B’, ‘C’, ‘D’ and ‘E’ respectively. Solution ‘A’ is called an ideal solution for exergetic efficiency because the weightage of exergetic efficiency involved in this solution is 1 (weightage of the total cost as 0) which signifies that exergetic efficiency is the utmost priority and there are no concerns about the cost while selecting the solution and so the value of exergetic efficiency in this solution is highest. Similarly, solution ‘E’ is called an ideal solution for total cost rate with a weightage of exergetic efficiency as 0 (weightage of the total cost as 1) resulting in a solution with a minimum total cost even though the exergetic efficiency is compromised. **Table 4.7** shows the ideal solutions of exergetic efficiency and total cost rate for each refrigerant pair.

Table 4.7: Ideal solutions for exergetic efficiency and total cost rates.

Refrigerant pair	Ideal solution for Exergetic efficiency		Ideal solution for total cost rate		% increase in Exergetic efficiency	% increase in total cost rate
	ψ (%)	$\dot{C}_{Total}$ $(M\$/yr)$	ψ (%)	$\dot{C}_{Total}$ $(M\$/yr)$		
R717-R290	40.4119	0.646909	37.6865	0.559401	7.23	15.64
R717-R1270	40.4208	0.63948	34.2118	0.437928	18.14	46.02
R290-R1270	37.4801	0.773281	29.0868	0.515331	28.85	50.05
R1270-R290	37.3287	0.743141	33.0643	0.629709	12.89	18.01
R1270-R744a	35.4964	0.799432	24.9715	0.47551	42.14	68.12
R600a-R290	38.3884	0.867401	34.2190	0.634739	12.09	36.65
R600a-R1270	38.8588	0.885587	30.7423	0.510982	26.40	73.31

It can be observed from **Fig. 4.1(a)-(g)** that as the weightage of exergetic efficiency is increased, the TOPSIS selection shifts towards a solution of higher cost rate. This shows a clear conflict between the two objective functions for each of the refrigerant pair. **Fig. 4.1(a)** is the Pareto optimal front of R717-R290 refrigerant pair which shows that as the exergetic efficiency increases from 37.68% to 40.41% which is an increase of 7.23%, the total cost rate also increases from 0.559401 M$ yr^{-1} to 0.646909 M$ yr^{-1} which is a hike of 15.64%. Similarly **Fig. 4.1(b), Fig. 4.1(c), Fig. 4.1(d), Fig. 4.1(e), Fig. 4.1(f)** and **Fig. 4.1(g)** show the Pareto optimal fronts for R717-R1270, R290-R1270, R1270-R290, R1270-R744a, R600a-R290 and R600a-R1270 in which a hike in total cost rate of 46.02%, 50.05%, 18.01%, 68.12%, 36.65% and 73.31% are recorded with 18.14%, 28.85%, 12.89%, 42.14%, 12.09%, and 26.40% increase in exergetic efficiency respectively which has been tabulated in **Table 4.7**.

It is the sole choice of decision-maker to take the value of weightage for different objective functions depending upon their relative importance. However, following a common practice here, equal weightage (both 0.50) has been given to both the objective functions while selecting the final solution (which is point 'C' in this case) for each refrigerant pair. **Table 4.8** presents the optimum values of operational parameters and objective functions for each refrigerant pair.

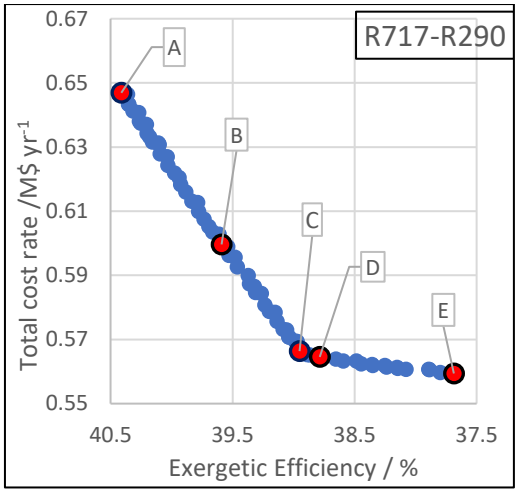
R717-R290
A
B
C
D
E
0.67
0.65
0.63
0.61
0.59
0.57
0.55
Total cost rate /M$ yr-1
40.5
39.5
38.5
37.5
Exergetic Efficiency / %

(a)

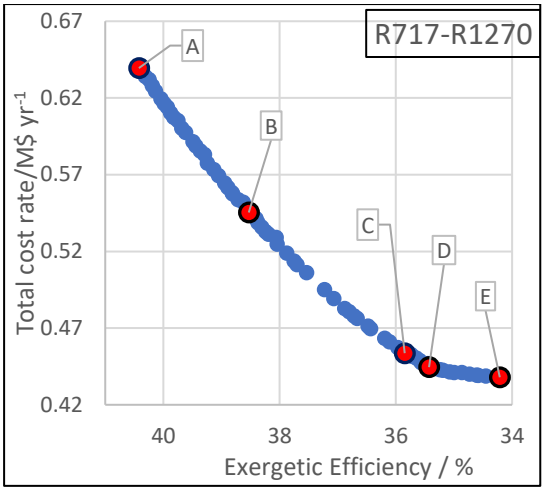
R717-R1270
A
B
C
D
E
0.67
0.62
0.57
0.52
0.47
0.42
Total cost rate/M$ yr-1
40
38
36
34
Exergetic Efficiency / %

(b)

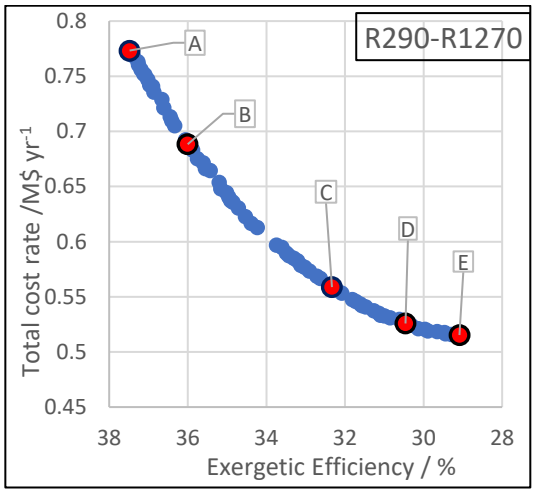
R290-R1270
A
B
C
D
E
0.8
0.75
0.7
0.65
0.6
0.55
0.5
0.45
Total cost rate /M$ yr-1
38
36
34
32
30
28
Exergetic Efficiency / %

(c)

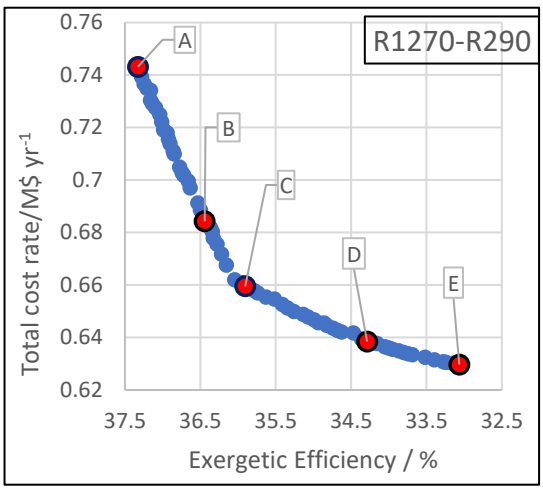
R1270-R290
A
B
C
D
E
0.76
0.74
0.72
0.7
0.68
0.66
0.64
0.62
Total cost rate/M$ yr-1
37.5
36.5
35.5
34.5
33.5
32.5
Exergetic Efficiency / %

(d)

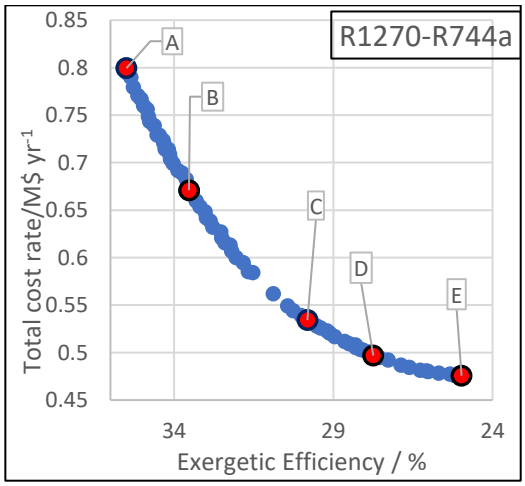
R1270-R744a
A
B
C
D
E
0.85
0.8
0.75
0.7
0.65
0.6
0.55
0.5
0.45
Total cost rate/M$ yr-1
34
29
24
Exergetic Efficiency / %

(e)

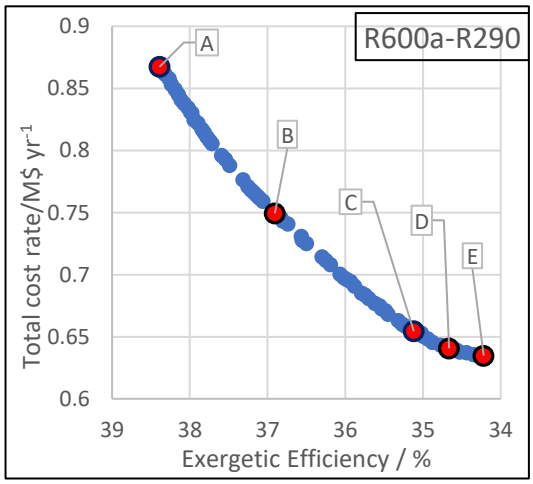
R600a-R290
A
B
C
D
E
0.9
0.85
0.8
0.75
0.7
0.65
0.6
Total cost rate/M$ yr-1
39
38
37
36
35
34
Exergetic Efficiency / %

(f)

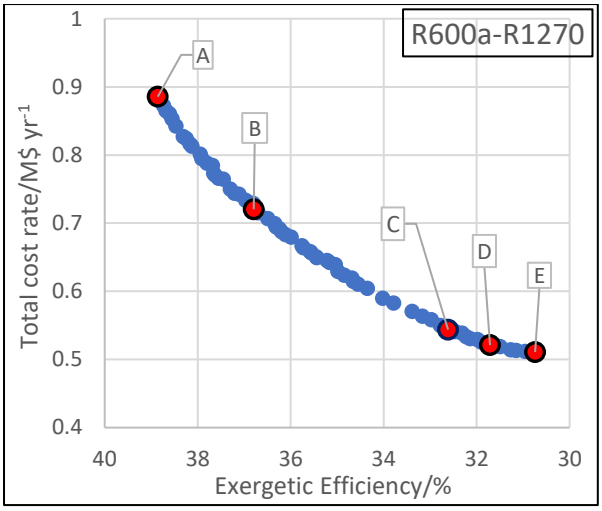

(g)

Fig. 4.1 Pareto optimal fronts for **(a)** R717-R290, **(b)** R717-R1270, **(c)** R290-R1270, **(d)** R1270-R290**, (e)** R1270-R744a, **(f)** R600a-R290 and **(g)** R600a-R1270

It can be seen that R717-R290 gives maximum exergetic efficiency of 38.95% with a cost of 0.566361 M$ yr^{-1} and R717-R1270 gives the minimum cost rate of 0.453638 M$ yr^{-1} with an exergetic efficiency of 35.84%. These two pairs show nondominated results *i.e.* R717-R290 gives more exergetic efficiency but demands more cost than R717-R1270 whereas R717-R1270 is economical but gives lesser exergetic efficiency. In such a case, no clear decision can be made about which refrigerant pair is superior. A Similar conflict can be observed in other refrigerant pairs also. In this situation, it is imperative to apply a decision making procedure to assign an order of preference or rank to different refrigerant pairs based on thermo-economic performance data. Therefore, TOPSIS decision-making technique is applied to the seven alternative pairs with exergetic efficiency and total cost rate being the two selection criteria with equal weights. The ranks assigned to different refrigerant pairs by TOPSIS method are indicated in **Table 4.8**. It can be seen that R717-R1270 is the best refrigerant pair as it has been assigned rank 1. Since the top two ranked pairs involve R717 as HTC refrigerant, it can be drawn that R717 is the best HTC refrigerant. R600a-R290 pair

should be the last choice and other refrigerant pairs may be chosen according to their ranks based on thermo-economic optimization results.

Table 4.8. Order of preferences of refrigerant pairs based on TOPSIS results

Refrigerant Pair (HTC-LTC)	Thermo-economic optimal Operating Conditions						Optimum Performance Parameters		Rank
	a	b	T_1 (℃)	T_{11} (℃)	T_5 (℃)	ΔT_{cas} (℃)	ψ (%)	$\dot{C}_{Total}$ (M$/yr)	
R717-R290	0.9999	0.9999	-42.365	35	-8.9993	2.0004	38.9512	0.566361	2
R290-R1270	0.9983	0.8677	-47.7023	38.1676	-8.8424	2.0542	32.3312	0.558809	5
R1270-R290	0.9996	0.8579	-42.3803	35.6519	-8.8834	2.1045	35.904	0.659494	6
R600a-R290	0.9982	0.613	-42.3418	46.2399	-8.6105	2.2516	35.1177	0.654438	7
R717-R1270	0.9995	0.8918	-47.311	35.1369	-8.9328	2.1262	35.8479	0.453638	1
R1270-R744a	0.9912	0.9833	-50.5672	37.5787	-8.9464	2.1571	29.8155	0.534131	4
R600a-R1270	0.9972	0.9817	-46.4284	48.0651	-8.8999	2.0568	32.6153	0.543655	3

NSGA- II

Fig. 4.2 shows the pareto frontier for R717-R290 pair obtained via NSGA-II. TOPSIS method is applied to identify solutions 'A', 'B', 'C', 'D' and 'F' corresponding to different weightages of exergetic efficiency as 1, 0.75, 0.50, 0.25 and 0 respectively. It can be seen that pareto frontier obtained from NSGA-II technique is broader with 1327 optimal solutions compared to Multi-objective Genetic Algorith (MOGA) technique with 70 optimal solutions.

Table 4.9 presents comparison of multi-objective optimization results of R717-R1270 pair obtained via MOGA and NSGA-II techniques for different exergetic efficiency weightages (*i.e.* solutions A, B, C, D and E). It can be seen that in solution 'C' optimal exergetic efficiency obtained by NSGA-II is 0.1861% greater and optimum total cost rate is 0.1959% lower than that of MOGA. So NSGA-II gives slightly better results as compared to MOGA. Similar is the case with solution 'D' where NSGA-II gives

0.2134% higher exergetic efficiency and 0.2536% lower cost. But the other solutions (A, B and E) given by MOGA are non-dominated by those of NSGA-II. Overall no significant difference in results from both the technique is observed which validates and proves the accuracy of MOGA results.

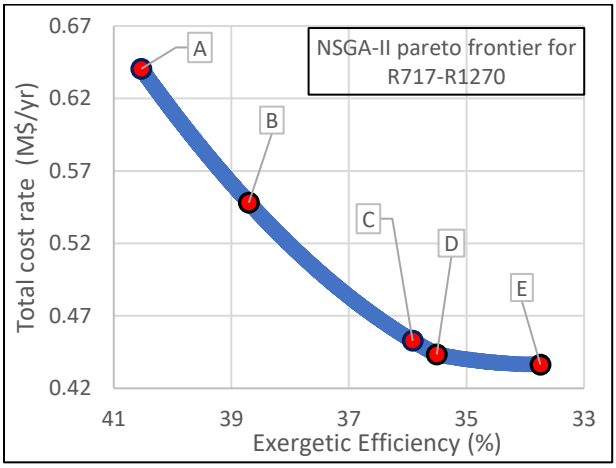

Fig. 4.2 Pareto prontier obtained via NSGA-II for R717-R1270 refrigerant pair.

Table 4.9. Comparison of NSGA-II and MOGA results for R717-R1270 refrigerant pair.

TOPSIS Selections	NSGA II		MOGA		% deviation in ψ	% deviation in $\dot{C}_{Total}$
	ψ (%)	$\dot{C}_{Total}$ (M$/yr)	ψ (%)	$\dot{C}_{Total}$ (M$/yr)		
A (Weightage of ψ=1)	40.5323	0.640443	40.4208	0.639480	+0.2752	+0.1506
B (Weightage of ψ=0.75)	38.7027	0.548077	38.5303	0.545328	+0.4452	+0.5041
C (Weightage of ψ=0.5)	35.9147	0.452749	35.8478	0.453638	+0.1861	-0.1959
D (Weightage of ψ=0.25)	35.5048	0.443390	35.4290	0.444517	+0.2134	-0.2536
E (Weightage of ψ=0)	33.7419	0.436388	34.2118	0.437928	-1.3926	-0.3515

Comparison of the present work with the existing literature

Mosaffa et al.**[15]** worked on the aforementioned system using NH_3-CO_2 refrigerant pair. In **Table 4.10** some important parameters obtained by using R717-R1270 refrigerant pair have been compared with the results reported in the reference study. It is evident that COP of the system improves by 7.77% whereas the exergetic efficiency increases by 7.72%, while the compressor work and total system cost rate reduces by 8.10% and 5.32% respectively when R717-R744 is replaced with R717-R1270 and the

system operates under similar operating conditions ($\dot{Q}_{evap}$= 500kW, T_{evap} = -35.20 ^{0}C, T_{cond}= 35.01 ^{0}C, T_5= -1.98 ^{0}C, ΔT_{cas} =2.27 ^{0}C, N= 4266 h, α_{el} = 0.09 \$ kWh^{-1}). This implies that R717-R1270 can be an effective replacement of NH_3-CO_2 pair for the system under study.

Table 4.10. Comparison of performance parameters using R717-R744 and R717-R1270 refrigerant pairs.

Parameter	Reference**[15]** (R717-R744)	Present work (R717-R1270)	% deviation
$\boldsymbol{COP}$	1.530	1.649	+7.77
$\boldsymbol{\psi}$ (%)	31.300	33.719	+7.72
$\dot{\boldsymbol{W}}_{\boldsymbol{comp}}$ $(\boldsymbol{kW})$	267.37	245.70	-8.10
$\dot{\boldsymbol{C}}_{\boldsymbol{total}}$ (\$/yr)	554523	525022	-5.32

4.3 Chapter Summary

A comparative analysis based on single and multi-objective optimization of on a 500kW cascade refrigeration system with flash gas removal in HTC and intercooling with indirect subcooling in it's LTC using twenty-two natural refrigerant pairs has been done in this study. The study gives new insights to the behaviour of natural refrigerants in a thermodynamic and economic optimization framework which can be useful in future endeavours of selection and implementations of natural refrigerants to the cascade refrigeration systems. It is found from the comparative analysis of twenty two natural refrigerant couples that R717-R1270 is the best refrigerant pair with optimum exergetic efficiency and total cost rate as 40.71% and 0.4529 M\$ yr^{-1} respectively.

Chapter 5
Conclusion and Future Scope

5.1 Conclusion

In the present work, results of performance analysis and multiobjective optimization of basic and hybrid multi-stage refrigeration system are presented. Performance of the systems are analyzed on the basis of energy, exergy, economic and exergoeconomic criteria whereas multi-objective optimization is done for maximizing exergetic efficiency and minimizing the total cost. Concurrently a comprehensive comparative analysis of various natural refrigerant/ refrigerant pairs is also presented. During progression of present work, it was felt that, in view of scarcity of energy efficient and environment-friendly refrigerants, natural refrigerants can be good alternatives of synthetic refrigerants if their performances are worked upon. Analysis, optimization and combining different refrigeration systems to make hybrid systems may be a solution for achieving higher thermodynamic performances of natural refrigerants. A comprehensive comparative thermodynamic and economic analysis is an efficient approach to identify the best alternative natural refrigerant for different refrigeration systems. Apart from the evaporator and condenser temperatures, de-superheating and subcooling parameters play important roles in improving the thermodynamic and economic performances of the systems. Following conclusions can be drawn from the different parts of work presented in this thesis.

Multi-objective optimization of Two-stage refrigeration system

In this work, multi-objective optimization of an ammonia based two-stage refrigeration system with flash intercooler has been performed via simulation work. Following conclusions may be drawn from the study:

- The multiple regression models of COP, exergetic efficiency and total capital cost give excellent predictions with R^2 value of 98.98%, 99.37% and 99.31% for one degree polynomials of COP and exergetic efficiency and two degree polynomials of capital cost meaning that these are the best possible fits for these parameters.
- Optimum evaporator and condenser temperatures are -20.02 ^{0}C and 36.03 ^{0}C respectively. These values are close to their maximum and minimum limits in order to minimize the temperature gap between evaporator and condenser which in turn minimizes the power input to the compressors.
- The optimum subcooling and de-superheating parameters are 0.9981 and 0.9957 which show that maximum subcooling and de-superheating favours both the objective functions concurrently.
- At thermo-economic optimal conditions, maximum exergy destruction rate is observed in compressor II with 66.56 kW and minimum in expansion valve I with 2.21 kW.

Multi-objectiev optimization of Cascade refrigeration system

A comparative analysis based on the performances obtained via multi-objective optimization of 50 kW cascade refrigeration system using NH_3-CO_2 and NH_3-N_2O refrigerant pairs has been in this study. The key conclusions drawn from the study are as follows:

- NH_3-CO_2 refrigerant pair shows an increase in optimal exergetic efficiency by 44.63% at an expense of increase in overall cost rate by 25.75%.
- NH_3-N_2O refrigerant pair gives an increase in exergetic efficiency by 49.11% at an increase in overall cost by 25.07%.

- NH_3-CO_2 gives an optimal exergetic efficiency of 34.67% and overall cost rate of 1.794756×10^5 USD $year^{-1}$ whereas NH_3-N_2O yields in optimal exergetic efficiency and overall cost rate values of 1.799291×10^5 USD $year^{-1}$.
- NH_3-N_2O refrigerant pair is better than NH_3-CO_2 refrigerant pair from multi-objective optimization view point.

Thermoeconomic analysis of Hybrid Cascade refrigeration system

Comparative energy, exergy, and economic analysis have been performed on a cascade refrigeration system incorporated with a flash tank in its higher temperature cycle and a flash intercooler with an indirect subcooler in its lower temperature cycle using different natural refrigerant couples. The following conclusions have been drawn from the study.

- The first and second law efficiencies increase with T_{evp} and decrease with T_{cond} for all the natural refrigerant couples but the total cost rate initially decrease and after a certain value of T_{evp} or T_{cond} it starts to increase.
- R717-R290 refrigerant couple results in a minimum overall system cost when operated with minimum de-superheating (b=0) while R290-R1270 and R600a-R290 refrigerant couples are economical with maximum de-superheating (b=1).
- LTC compressor I discharge temperature (T_2) first decreases and then starts to increase with T_{evp}. While the LTC compressor II discharge temperature continuously decreases with T_{evp}.
- R717-R290 is the most powerful and cost-effective refrigerant couple for the given system under the given range of working temperatures.
- Ammonia-propane is the best refrigerant pair for hybrid cascade refrigeration system from exergoeconomic point of view whereas Ammonia-propylene is the

best refrigerant pair for hybrid cascade refrigeration system from multi-objective optimization criteria.

- For maximization of the exergetic efficiency the subcooling parameter (a), de-superheating parameter (b) and evaporator temperature (T_{evap}) approach towards their highest possible values whereas the condenser temperature (T_{cond}) comes closer to its lowest possible value for each refrigerant pair.
- For minimization of cost, the flash intercooler is configured for maximum de-superheating and zero subcooling.
- R717 is the best HTC refrigerant among R717, R290, R1270 and R600a from multi-objective optimization criteria.
- The COP and exergetic efficiency of system improve by 7.77% and 7.72% respectively whereas the compressor work and total cost rate reduces by 8.10% and 5.32% respectively when R717-R744 is replaced by R717-R1270 refrigerant pair.

Exergoeconomic analysis of Hybrid Cascade Refrigeration System

The 500kW hybrid cascade refrigeration system is simulated and analysed through irreversibility, economic and exergo-economic point of view using Ammonia-propane, Propane-propylene and Isobutane-propane refrigerant pairs. The study is carried out on thermodynamic optimal operating conditions and component wise exergy efficiencies, and exergo-economic factors are found. Following conclusions are drawn from the study:

- Ammonia-propane is thermodynamically best refrigerant pair which possesses the lowest exergy destruction of 158.8 kW and highest exergy efficiency of 39.14% whereas Isobutane-propane shows the worst results of 173.5 kW of exergy destruction and 37.06% of exergy efficiency. Propane-propylene gives

moderate results with 166.4 kW exergy destruction and 38.03% exergy efficiency.

- Ammonia-propane is most reasonable, Isobutane-propane is most expensive and Propane-propylene is the moderate refrigerant pairs with overall annual cost of 83639 $/yr, 2189000 $/yr and 1178000 $/yr respectively at thermodynamic optimal conditions.
- Fan I contributes the maximum share in total exergy destruction showing 28.23%, 26.93% and 26% of total exergy destructions for ammonia-propane, propane-propylene and Isobutane-propane pairs respectively. Whereas flash tank shows zero destruction in exergy.
- Total exergy destruction is minimum in EV II (except the flash tank which shows zero exergy destruction) for ammonia-propane and Isobutane-propane showing 0.4292 kW and 0.5205 kW respectively, whereas for propane-propylene it is minimum in condenser with 0.3245 kW.
- The total cost rate first decreases to a certain value and thereafter it increases with the increase in evaporator temperature. The minimum cost is obtained at -47 ^{0}C, -40 ^{0}C and -44 ^{0}C (approx.) of evaporator temperature for ammonia-propane, Propane-propylene and Isobutane-propane respectively.
- Exergo-economic factor is minimum for EV III showing 0.07% for ammonia-propane, 0.042% for propane-propylene and 0.01% for Isobutane-propane pairs. For Ammonia -propane exergo-economic factor is maximum in FIS with 94.59%, for Propane-propylene and Isobutane-propane, it is maximum in condenser showing 99.64% and 97.33% respectively.

Multi-objectiev optimization of Cascade refrigeration system

A comparative analysis based on single and multi-objective optimization of on a 500kW cascade refrigeration system with flash gas removal in HTC and intercooling with indirect subcooling in it's LTC using twenty-two natural refrigerant pairs has been done in this study. The study gives new insights to the behaviour of natural refrigerants in a thermodynamic and economic optimization framework which can be useful in future endeavours of selection and implementations of natural refrigerants to the cascade refrigeration systems. Following conclusions are drawn from the work presented:

- For maximization of the exergetic efficiency the subcooling parameter (a), de-superheating parameter (b) and evaporator temperature (T_{evap}) approach towards their highest possible values whereas the condenser temperature (T_{cond}) comes closer to its lowest possible value for each refrigerant pair.
- For minimization of cost, the flash intercooler is configured for maximum de-superheating and zero subcooling.
- R717-R290 is thermodynamically the best refrigerant pair with an optimum exergetic efficiency of 40.71% whereas R290-R1150 is the worst refrigerant pair with optimum exergetic efficiency of 33.07%.
- R717-R1270 is the most economical refrigerant pair with an optimum total cost rate of 0.4529 M\$ yr^{-1} and R600a-R290 is the worst pair with optimum cost rate of 0.6229 M\$ yr^{-1}.
- Comparative analysis of seven potential refrigerant pairs based on their performances obtained via multi-objective optimization reveal that R717-R1270 is the most suitable refrigerant pair from thermo-economic point of view

and R717-R290 is the second-best pair whereas R600a-R290 is the worst refrigerant pair.

- As both the top-performing refrigerant pairs (*i.e* R717-R290 and R717-R1270) involve R717 as the HTC refrigerant, it can be concluded that R717 is the best HTC refrigerant among the four HTC refrigerants from multi-objective optimization criteria.
- As the weightage of exergetic efficiency is increased in TOPSIS method, it chooses a solution with higher cost rate for each refrigerant pair.
- The COP and exergetic efficiency of system improve by 7.77% and 7.72% respectively whereas the compressor work and total cost rate reduces by 8.10% and 5.32% respectively when R717-R744 is replaced by R717-R1270 refrigerant pair.

5.1 Future scope of the work:

Present research work is based on theoretical models of different multi-stage refrigeration systems and focussed on analysis and optimization of energy and exergy efficiencies as well as total cost of different systems using different natural refrigerant pairs. However the analysis can be carried out from different viewpoints of some other important performance parameters like cooling load, cold space temperature, irreversibility analysis, total equal warming index, payback period and environmental cost etc. The research may also be pursued through different methodologies and tools like REFPROP and MATLAB for analysis by using different system configurations. Other optimization algorithms like particle swarm intelligence (PSA), Strength Pareto Evolutionary Algorithm - II (SPEA2) may give new insights to the thermoeconomic

performance of the systems. Further research that can be of interest in succession to the present research work may include:

- Exergo-environmental performance analysis of hybrid cascade refrigeration system using low GWP synthetic refrigerant pairs.
- Comparative analysis of different HTC refrigerants paired with CO_2 (as LTC refrigerant) on the basis of their Total Equal Warming Index (TEWI).
- Thermo-economic analysis of different hybrid multi-stage systems using combination of other two-stage configurations.
- Comparative thermoeconomic analysis of different basic and hybrid multi-stage refrigeration systems.
- Implementation of two phase ejector in hybrid multi-stage refrigeration systems.
- Single-objective and Multi-objective optimization of multi-stage refrigeration systems using other objective functions like cooling load, total exergy destruction, overall exergoeconomic factor, exergoenvironmental factor, total equal warming index etc.
- Single-objective and Multi-objective optimization of different multi-stage refrigeration systems using suitable working range of design parameters as compressor efficiencies, overall heat transfer coefficient of heat exchangers, temperature drop/rise of evaporator/condenser air, heat exchanger effectiveness etc.
- Analysis and optimization may also carried out using multiple tools like Simulink PS Converter, TRYNSYS, ASPEN, REFPROP, EES Macro and HOMER etc.

REFERENCES

1. ICMR-IBS Centre for management Research 2003, *A Note on the refrigerator industry in India*, accessed 06th August, 2021. <https://icmrindia.org/casestudies/catalogue/Business%20Reports/BREP017.htm.>
2. Ratts EB, Brown JS. A generalized analysis for cascading single fluid vapor compression refrigeration cycles using an entropy generation minimization method. Int J Refrig 2000;23:353-65.
3. Bingming W, Huagen W, Jianfeng L, Ziwen X. Experimental investigation on the performance of NH_3/CO_2 cascade refrigeration system with twin-screw compressor. Int J Refrig 2009;32:1358–65.
4. Park H., Dong H. K., Min S. K., Thermodynamic analysis of optimal intermediate temperature in R134a-R410A cascade refrigeration systems and its experimental verification, Appl. Therm. Eng., 54 (2013) 319-327
5. Lee TS, Liu CH, Chen TW. Thermodynamic analysis of optimal condensing temperature of cascade-condenser in CO_2/NH_3 cascade refrigeration systems. Int J Refrig 2006;29:1100–8.
6. Bhattacharyya S, Garai A, Sarkar J. Thermodynamic analysis and optimization of a novel N_2O-CO_2 cascade system for refrigeration and heating, Int. J. Refrig. 32 (2009) 77–84.
7. Bhattacharyya S, Bose S, Sarkar J. Exergy maximization of cascade refrigeration cycles and its numerical verification for transcritical CO_2-C_3H_8 system. Int J Refrig 2007;30:624–32.
8. Getu HM, Bansal PK. Thermodynamic analysis of an R744–R717 cascade refrigeration system. Int J Refrig 2008;31:45–54.

9. Zubair SM, Yakub M, Kan SH. Second-law-based thermodynamic analysis of two stage and mechanical-subcooling refrigeration cycles. Int J Refrig 1996;19:506-516.

10. Dopazo, J., Fernández-Seara, J., Sieres, J., Uhía, F.J.: Theoretical analysis of a CO_2–NH_3 cascade refrigeration system for cooling applications at low temperatures. Appl. Therm. Eng. 29, 1577–1583 (2009).

11. Dopazo, J., Fernández-Seara, J.: Experimental evaluation of a cascade refrigeration system prototype with CO_2 and NH_3 for freezing process applications. Int. J. Refrig. 34, 257–267 (2011)

12. Torrella E, Larumbe JA, Cabello R, Llopis R, Sanchez D. A general methodology for energy comparison of intermediate configurations in two-stage vapour compression refrigeration systems. Energy 2011;36:4119–24.

13. Rezayan O, Behbahaninia A. Thermoeconomic optimization and exergy analysis of CO2/NH3 cascade refrigeration systems. Energy 2011;36:888–95.

14. Baakeem SS, Orfi J, Alabdulkarem A. Optimization of a multistage vapor-compression refrigeration system for various refrigerants. Appl Therm Eng 2018;136:84-96

15. Mosaffa AH, Farshi LG, Infante Ferreira CA, Rosen MA. Exergoeconomic and environmental analyses of CO2/NH3 cascade refrigeration systems equipped with different types of flash tank intercoolers. Energ Convers Manage 2016;117:442-53.

16. Shishov VV, Talyzin MS. Improving the energy efficiency of refrigeration plants by decreasing the temperature difference in air-cooled condensers. Therm Eng 2015;62:652-655.

17. Vincent CE and Heun MK, Thermoeconomic analysis and design of domestic refrigeration systems. *In: Proceedings of International Conference of Domestic Use of Energy.* South Africa 2006

18. Asgari S, Noopor AR and Boyaghchi, FA. Parametric assessment and multi-objetive optimization of an internal auto-cascade refrigeration cycle based on advanced exergy and exergoeconomic concepts. Energy 2017;125:576–90.

19. Nemati A, Nami H and Yari M. A comparison of refrigerants in a two-stage ejector-expansion transcritical refrigeration cycle based on exergoeconomic and environmental analysis. International Journal of Refrigeration 2017; 84:139–50.

20. Erol GO, Acikkalp E and Hepbasli A. Performance assessment of an ice rink re-frigeration system through advanced exergoeconomic analyses method. Energy Building 2017;138:118–26

21. Asgharian H, Baniasadi E, and Coplan CO. Energy, exergy and exergoeconomic analyses of a solar refrigeration cycle using nanofluid. International journal of exergy 2019:30(1):63-85

22. Sharifi MAR and Kalilarya. Exergoeconomic evaluation and optimisation of a novel combined power and absorption-ejector refrigeration cycle driven by natural gas. International journal of exergy 2016;19(2):232-58.

23. Knowles J, Corne D. The Pareto archived evolution strategy: a new baseline algorithm for Multiobjective optimization, in Proc. of the 1999 Cong. on Evolutionary Computation., Washington: IEEE Service Centre 1999.

24. Deb K., Pratap A., Agarwal S., Meyarivan T., A fast and elitist multiobjective genetic algorithm: NSGA-II, IEEE Trans. Evol. Comput. 6 (2002) 182–197.

25. Aminyavari M, Naja B, Shirazi A, Rinaldi F. Exergetic, economic and environmental (3E) analyses, and multi-objective optimization of a CO_2/NH_3 cascade refrigeration system. Appl Therm Eng 2014;65:42–50.

26. Eini S, Shahhosseini H, Delgarm N, Lee M, Bahadori A. Multi-objective optimization of a cascade refrigeration system: Exergetic, economic, environmental, and inherent safety analysis. Appl Therm Eng 2016;107:804-17.

27. Nasruddin, Sholahudin, S, Giannetti N., Arnas. Optimization of a cascade refrigeration system using C_3H_8 in high temperature circuit (HTC) and a mixture of C_2H_6/CO_2 in low temperature circuit (LTC). Appl Therm Eng 2016;104:96-103.

28. Yarmohammadi S, Mohammadzadeh K, Farhadi M, Hajimiri H, Modir A. Multi-objective optimization of thermal and flow characteristics of R-404A evaporation through corrugated tubes. J Energy Storage 2020;27:101137.

29. Roy R, Mandal BK. Thermo-economic analysis and multi-objective optimization of vapour cascade refrigeration system using different refrigerant combination. J Therm Anal calorim 2020;139:3247-61

30. Sarkar J, Bhattacharyya S and Lal A. Selection of suitable natural refrigerants pairs for cascade refrigeration system. Proc IMechE Part A: J Power and energy 2013;227(5):612-22

31. Parmar GG, Kapadia RG. Thermodynamic Analysis of Cascade refrigeration system using a natural refrigerants for supermarket application, Int J Innovative research in science, eng and tech 2015;4:1839-46.

32. Sarbu I, Sebarchievici C. Substitution strategy of non-ecological refrigerants In: Zanol R, editor. Ground-Source Heat Pumps, Oxford: Academic press; 2016, p.27-45

33. Paradeshi, L., Srinivas, M., Jayaraj, S.: Thermodynamic analysis of a direct expansion solar-assisted heat pump system working with R290 as a drop-in substitute for R22. J Therm Anal Calorim 2019;136(1):63–78.

34. Kilicarslan A, Hosoz M. Energy and irreversibility analysis of a cascade refrigeration system for various refrigerant couples. Energy Convers Manage 2010;51:2947–54.

35. Sun, Z., Liang, Y., Liu, S., Ji, W., Zang, R., Liang, R.: Comparative analysis of thermodynamic performance of a cascade refrigeration system for refrigerant couples R41/404A and R23/R404A. Appl Energy. 184, 19-25 (2016)

36. Sun, Z., Wang, Q., Xie, Z., Liu, S., Su, D., Cui, Q.: Energy and exergy analysis of low GWP refrigerants in cascade refrigeration system. Energy. 170, 1170-1180 (2019)

37. Sun, Z., Wang, Q., Dai, B., Wang, M., Xie, Z.: Options of low global warming potential refrigerant group for a three-stage cascade refrigeration system. Int. J. Refrig. 100, 471–83 (2019)

38. Shovon, M.K.B., Raman, S.K., Suryam, A., Kim, T.H., Kim, H.D.: Performance of ejector refrigeration cycle based on solar energy working with various refrigerants. J Therm Anal Calorim. 141, 301-312 (2020)

39. Saleh, S., Pirouzfar, V., Alihosseini, A.: Performance analysis and development of a refrigeration cycle through various environmentally friendly refrigerants. J Therm Anal Calorim. 136, 1817-1830 (2019)

40. Turgut, M.S., Turgut, O.E.: Comparative investigation and multi objective design optimization of a cascaded vapor compression absorption refrigeration system operating with different refrigerants in the vapor compression cycle. Heat and Mass Transfer. 55, 467-488 (2019)

41. Sun, X., Liu, L., Dong, Y., Zhuang, Y., Li, J., Du, J., Yin, H.C.: Multi-objective optimization and thermo-economic analysis of an enhanced compression-absorption cascade refrigeration system and ORC integrated system for cooling and power cogeneration. Energy Convers Manage. 236, 114068 (2021)

42. Klein SA, Alvarado FL. EES: Engineering equation solver for the Microsoft Windows operating system. F-Chart software 1992.

43. Sayyaadi, H., and Nejatolahi, M., Multi-objective optimization of a cooling tower assisted vapor compression refrigeration system, Int. J. Refrig.-Revue Internationale Du Froid, vol. 34, pp. 243–256, 2011.

44. Srinivas N, Deb K. Multiobjective optimization using nondominated sorting in genetic algorithms. Evol Comput 1994;2:221–48.

45. Bejan A, Tsatsaronis G, Moran MJ. Thermal design and optimization. Wiley; 1996.

46. Diyaley S, Shilal P, Shivakoti I, Ghadai RK, Kalita K. PSI and TOPSIS based selection of process parameters in WEDM. Periodica Polytechnica Mechanical Eng. 2017;61(4):255–60.

47. Wijbenga H, Van Der Hoff M, Janssen M, Infante Ferreira CA. Life cycle performance of refrigeration systems in the Dutch food and beverages sector. In: 4th IIR conf thermophys prop transf process refrig, Delft, The Netherlands.

48. Infante Ferreira CA. Refrigeration and heat pumping in food processing plants. In: Stougie L, editor. Energy effic qual energy food process ind. Delft, The Netherlands: Interduct: Delft University of Technology; 2002. p. 57–79.

49. Navidbakhsh M, Shirazi A, Sanaye S. Four E analysis and multi-objective optimization of an ice storage system incorporating PCM as the partial cold storage for air-conditioning applications. Appl Therm Eng 2013;58:30–41.

50. Sanaye S, Shirazi A. Four E analysis and multi-objective optimization of an ice thermal energy storage for air-conditioning applications. Int J Refrig 2012;36:1–14.

51. Mosaffa AH, Farshi L Garousi. Exergoeconomic and environmental analyses of an air conditioning system using thermal energy storage. Appl Energy 2016;162:515–26.

52. Xu G, Liang F, Yang Y, Hu Y, Zhang K, Liu W. An improved CO2 separation and purification system based on cryogenic separation and distillation theory. Energies 2014;7:3484–502.

53. Fettaka S, Thibault J, Gupta Y. Design of shell-and-tube heat exchangers using multiobjective optimization. Int J Heat Mass Transfer 2013;60:343–54.

54. Johnson WA, Nicholson FJ, Roger A, Stroud GD. Freezing and refrigeration storage in fisheries, CSL food science laboratory Torry, Aberdeen Scotland, UK; 1994

55. Tooru A, Hideaki C. A new condensed gas calorimeter. Thermodynamic properties of solid and liquid dinitrogen oxide. Bull. Chem. Soc. Jpn 1974.;47(9):2126-36